NASA Contractor Report 3280

Development of Advanced Avionics Systems Applicable to Terminal-Configured Vehicles

R. L. Heimbold, H. P. Lee,
and M. F. Leffler

CONTRACT NAS1-15546
SEPTEMBER 1980

NASA

NASA Contractor Report 3280

Development of Advanced Avionics Systems Applicable to Terminal-Configured Vehicles

R. L. Heimbold, H. P. Lee,
and M. F. Leffler
Lockheed-California Company
Burbank, California

Prepared for
Langley Research Center
under Contract NAS1-15546

National Aeronautics
and Space Administration

**Scientific and Technical
Information Branch**

1980

TABLE OF CONTENTS

Section		Page
	LIST OF FIGURES	v
	LIST OF TABLES	vi
	SUMMARY	1
	INTRODUCTION	3
	LIST OF SYMBOLS	4
1.0	DISCUSSION OF TECHNICAL APPROACH	6
1.1	The L-1011 Flight Management System	7
1.1.1	Basic operation	7
1.1.2	System interface	7
1.2	Descent Profile Modeling	9
1.2.1	Descent model verification	9
1.2.2	Computation of the 3-D descent profile	11
1.2.3	Computation of time-in-descent	11
1.2.4	Descent profile sensitivities and error sources	13
1.3	Wind Study	17
1.3.1	Statistical wind data	17
1.3.2	Linear wind model development	17
1.3.3	Simulation wind model development	20
1.3.4	The effect of wind estimation error on open loop performance	20
1.4	4-D Control Law Development	24
1.4.1	Altitude and range errors as feedback variables	24
1.4.1.1	Altitude error feedback	26
1.4.1.2	Range error feedback	28
1.4.2	Descent simulation errors	28
1.5	FMS Software Development	28
1.5.1	Computer organization	30
1.5.2	Emulator development	30
1.5.3	Data bank preparation	31
1.5.4	Hot mock-up checkout	31

TABLE OF CONTENTS (Continued)

Section		Page
2.0	FLIGHT TESTING.	32
2.1	Local Area Flight Testing.	32
2.2	Dallas/Ft. Worth Demonstration Flights	32
2.3	Flight Test Results.	38
2.3.1	Wind modeling	42
2.3.2	Effects of wind modeling errors on 4-D descent. . . .	47
2.4	Air Traffic Control Integration.	47
2.4.1	Metering and spacing.	48
2.5	Future 4-D Flight Management	50
3.0	CONCLUSIONS AND RECOMMENDATIONS	50
3.1	Conclusions.	50
3.2	Recommendations.	51
APPENDIX A	TIME-IN-DESCENT ALGORITHMS.	52
APPENDIX B	OPEN LOOP DESCENT SIMULATIONS	64
APPENDIX C	CLOSED LOOP DESCENT SIMULATIONS	75
APPENDIX D	L-1011 FLIGHT MANAGEMENT SYSTEM DATA BANK INFORMATION FOR THE DALLAS/FT. WORTH DEMONSTRATION FLIGHTS.	91

LIST OF FIGURES

Figure		Page
1	Descent profile	1
2	Flight management system block diagram.	8
3	FMS/Aircraft interface.	10
4	Computation of 4-D descent profile.	12
5	Incremental segment relationship.	12
6	The effects of speed, weight, temperature and E*D altitude on descent trajectory range (42000 to 9000 ft descent)	14
7	The effects of speed, weight, temperature and E*D altitude on time-in-descent (42000 to 9000 ft descent).	15
8	Descent profile, 8/6/79, test no. 216	16
9	Interlevel wind velocities.	19
10	Wind statistics, Tripoli, Libya, February	21
11	Derived wind profiles, Tripoli, Libya, February	22
12	Simulation wind models.	23
13	Effect of wind estimation error	25
14	Feedback variables.	26
15	Altitude error feedback	27
16	Range error feedback.	29
17	Software development.	31
18	Lockheed L-1011 advanced TriStar, S/N 1001.	33
19	Dallas/Ft. Worth south flow	34
20	Acton arrival Wink transition	35
21	Dallas/Ft. Worth scenario	37
22	E*D time error histogram (final estimate)	39
23	Comparison of navigation with inertial and radio references	40
24	Wind persistence, 7/30/79	43
25	Wind persistence, 8/1/79.	43
26	Segment fit to 7/30/79 wind profile, first descent.	44
27	Segment fit to 8/1/79 wind profile, first descent	44
28	Comparison of linear and segmented wind models, 7/30/79 flight tests, L-1011, S/N 1001.	45
29	Comparison of linear and segmented wind models, 8/1/79 flight tests, L-1011, S/N 1001.	46
30	Metering and spacing.	49

LIST OF TABLES

Table		Page
1	Flight Test Results and Future Protection	2
2	NASA Wind Data.	18
3	Descent Simulation Errors	28
4	Flight Test Initial Conditions.	36
5	Flight Test Results	39
6	Flight Test Terminal Errors at E*D.	41
7	Arrival Time Error Comparison	41
8	Wind Model Error.	47

SUMMARY

The main objective of this program was to develop and flight test a high profile 4-D descent. A profile descent is an aircraft's descent from cruise altitude to the terminal area at or near flight idle, as shown in figure 1. The high profile descent is the upper part of the descent, between cruise and a metering fix, the remainder of the descent from the metering fix to the runway is called the runway profile descent. A 4-D high profile descent is one in which an aircraft begins its descent at a specific point such that it arrives above a point on the earth at a desired altitude - and at a specific time.

Software in the existing production L-1011 Flight Management System, which has a 3-D capability, was modified to perform 4-D descents in flight. Eleven descents were performed — eight on flights off the coast of California between June 25 and July 30, 1979, and three on a demonstration flight to the Dallas/Ft. Worth Regional Airport on August 1, 1979. This last flight was undertaken to demonstrate the 4-D descent capability in the arrival airspace of a major hub airport. It was desired to exercise the system in conjunction

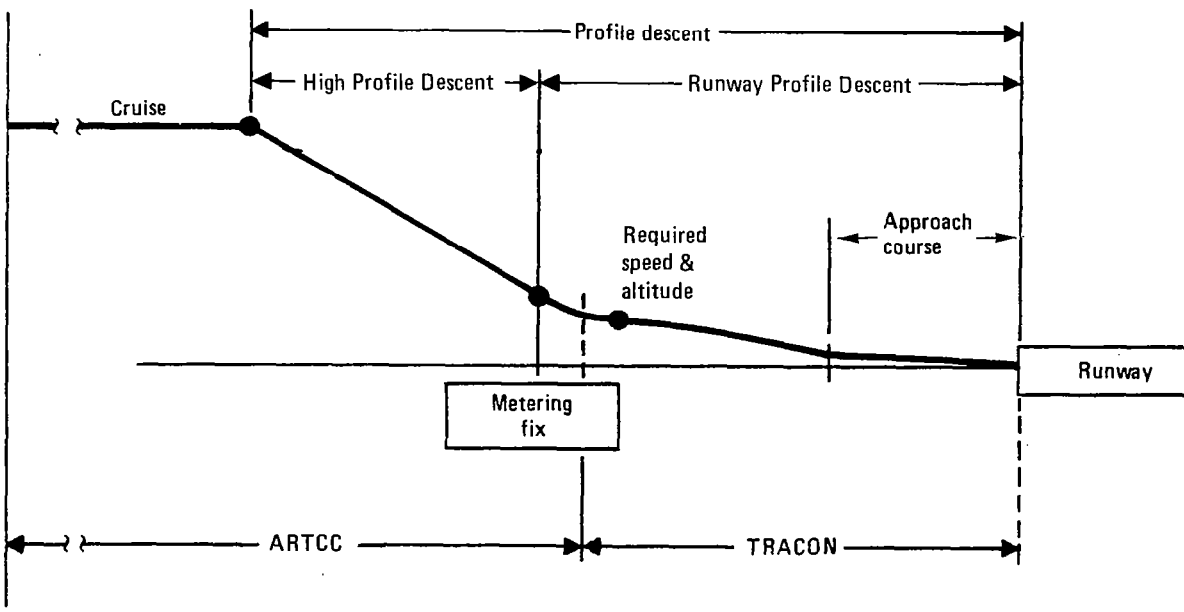

Figure 1. - Descent profile.

with the computerized time-based metering system that is used in the Ft. Worth Air Route Traffic Control Center to control flow to the Dallas/Ft. Worth Regional Airport. This system was mainly developed at the Ft. Worth Center and is now also used at the Denver Center. It is planned to make it available to all FAA centers in 1980.

Early in the program an agreement was reached between NASA and Lockheed that the end-of-descent arrival time accuracy goal would be ±30 seconds. Other goals were: airspeed 250 ±5 kts, position ±1 n.mi., and altitude ±150 ft. As shown in table 1 the 2σ (95 percent) arrival time error dispersion of nine of the eleven 4-D descents was within 19 seconds. Results of two descents were excluded because of defects in the experimental procedures; their arrival time errors were 25 and 41 seconds. It is expected that, in the future, the 2σ dispersion can be reduced to about eight seconds by means of improvements in wind modeling, aircraft/engine modeling, navigation procedures and improved automation. These topics will be discussed more fully in the body of the report. Position and altitude errors, as shown in table 1, are well within the criteria for the flight tests. Airspeed errors at the end of descent were a little high, however, incorporation of the above four improvements is expected to maintain airspeed within ±5 knots at the end of descents.

Preliminary analysis indicated that a linear wind model in which wind velocity is assumed to decrease linearly with altitude would be adequate for achieving end-of-descent arrival times within the ±30 second criteria for the worst expected wind conditions. Present thinking is that 4-D time control accuracy should be better than 30 seconds; this would indicate that a more exact wind model than the linear model is in order.

Flight test wind velocity data were analyzed for two sets of tests wherein the aircraft performed descents over the same course between the altitudes of 33000 and 11000 ft. In the first set of descents the wind velocity profiles remained relatively unchanged for over five hours. In the second set there was considerable variation of profile caused by frontal

TABLE 1. - FLIGHT TEST RESULTS AND FUTURE PROJECTION

Error		4-D Test Goals	Summary (9 Descents)	Future Projection
End of Descent Arrival Time	Mean	Not specified	−2s	0s
	2 σ	<30 s	19s	8s
Airspeed		±5 kts	±15 kts	±5 kts
Position		±1 n.mi.	±0.2 n.mi..	±0.2 n.mi.
Altitude		±150 ft	±50 ft	±50 ft

activity in the area. These two sets of data provided useful insights in the comparison of a linear wind model and a more complex segmented model based on actual measurements. The segmented model improved wind model fidelity in the stable wind velocity situation but actually degraded fidelity in the situation where the wind velocity profile was disturbed by the changing weather conditions. These two examples are not meant to provide a quantitative basis for wind modeling, however, the need to consider the effects of weather conditions on wind persistence is indicated, especially if actual wind measurements are the basis of wind profile modeling.

Control laws for the 4-D descent were synthesized using a highly accurate non-linear model of the L-1011 on an interactive computer graphics terminal. Software development was carried out on an IBM 370 emulation of the ARMA flight management computer. Prior to flight the flight management computer was connected to a hot mockup in which the computer and its software were checked out with simulated aircraft system inputs. The flight tests were conducted without any serious complications, although, as mentioned above, two of the eleven descents were degraded by procedural problems. Remedies have been found that will be incorporated on downstream 4-D flight tests.

The 4-D descent technique used in this study was a prototype technique that was tested to demonstrate the capability of achieving accurate arrival time control. The flight tests at the Dallas/Ft. Worth Regional Airport (DFW) were very instructive in learning how to refine the 4-D technique for the future so that it will fit smoothly into the air traffic control system and contribute to the solution of the air traffic congestion problem. A number of meetings were held with ATC personnel before and after the flight test demonstration at DFW; these sessions pointed out the need for the aircraft system developer to work toward the solution of flow control problems in cooperation with the ground controllers and the airlines in order to develop new procedures that are practical and that will be accepted by those who have to use them.

INTRODUCTION

This report documents the analysis performed and flight test results obtained by the Lockheed-California Company under contract (NAS1-15546) to the National Aeronautics and Space Administration Langley Research Center at Hampton, Virginia. This effort was started in October 1978 with an analytical study of time-controlled (4-D) profile descent techniques and a review of wind modeling for the descent computation. The study was subsequently expanded to include flight tests on the Lockheed L-1011 which verified the feasibility of the 4-D high-profile descent.

A motion film supplement is available on loan. A request card form and a description of the film are found at the back of this report. This film describes the flight to the Dallas/Ft. Worth Regional Airport which was the culmination of the L-1011 testing performed in the program.

Use of trade names or names of manufacturers in this report does not constitute an official endorsement of such products or manufacturers, either expressed or implied, by the National Aeronautics and Space Administration.

The authors wish to acknowledge the contributions of: Lockheed employees who participated in the Terminal-Configured Vehicle project including Dr. B.M. Sindermann, K.M. Subramanyam, W.R. Beckman, D.A. Moor, E.L. Harris, and L.V. Glouner; the Federal Aviation Administration personnel whose efforts were coordinated by R. Paclik of the Dallas-Fort Worth Tower and by G.E. Brammer of the Ft. Worth ARTCC; J. Dam, Dallas/Ft. Worth Airport Manager; and members of the NASA Langley Research Center TCV Program Office which is headed by J.P. Reeder.

LIST OF SYMBOLS

Values are presented in both SI and U.S. Customary Units. Calculations were made in U.S. Customary Units. Altimeter readings are given in feet to correspond to the instrument reading. To convert from feet to meters multiply the value of feet by 0.3048.

AC	Alternating Current
ACC	Accessory
ADI	Attitude Direction Indicator
AFCS	Automatic Flight Control System
A/L	Autoland
ARTCC	Air Route Traffic Control Center
ATC	Air Traffic Control
ATS	Auto Throttle System
B*D	Beginning-of-Descent
CADC	Central Air Data Computer
CAS	Calibrated Air Speed
CDU	Control and Display Unit
CMD	Command
CPU	Central Processor Unit
CRT	Cathode Ray Tube
DA	Drift Angle
DC	Direct Current
DCAS	Direct Computing Access System
DFW	Dallas/Fort Worth Airport

DME	Distance Measuring Equipment
ECS	Environmental Control System
E*D	End-of-Descent
EPR	Engine Pressure Ratio
ETA	Estimated Time of Arrival
FAA	Federal Aviation Administration
FD	Flight Director
FMC	Flight Management Computer
FMS	Flight Management System
GMT	Greenwich Mean Time
HSI	Horizontal Situation Indicator
HW	Head Wind
IAS	Indicated Air Speed
INAV	Inertial Navigation
INS	Inertial Navigation System
I/O	Input/Output
M	Mach Number
NASA	National Aeronautics and Space Administration
NAV	Navigation
NCU	Navigation Computer Unit
PMD	Palmdale Airport (California)
RAD/RNAV	Radio/Area Navigation
RNAV	Area Navigation
S	Laplace Operator
SAT	Static Air Temperature
STAR	Standard Terminal Arrival Route
S/N	Serial Number
TACAN	Tactical Air Navigation
TAS	True Air Speed
TCV	Terminal-Configured Vehicle
TGT	Turbine Gas Temperature
TH	True Heading
TKE	Track Error
TRACON	Terminal Radar Approach Control

TW	Tail Wind
V	Velocity
Ve	East Velocity
VGS	Ground Speed
VHF	Very High Frequency
Vn	North Velocity
V-NAV	Vertical Navigation
VOR	VHF Omnidirectional Range
VORTAC	Co-located VOR and TACAN
VT	True-air-speed
VW	Wind velocity
h	Altitude
h_{CMD}	Altitude Command
h_e	Altitude Error
R_{CMD}	Range Command
r	Range
t	Time
α	Angle of Attack
β	Regression Coefficient
ρ	Correlation Coefficient
σ	Standard Deviation
γ	Flight Path Angle
θ	Pitch Angle
θ_{CMD}	Pitch Angle Command
Σ	Summation
Δh	Incremental Altitude
Δr	Incremental Range
Δt	Incremental Time
$\Delta temp$	Deviation from Standard Air Temperature
δ_{sp}	Incremental Spoiler Command
δ_{thr}	Incremental Throttle Command

1.0 DISCUSSION OF TECHNICAL APPROACH

This section describes the development of a time-controlled (4-D) high profile descent capability and its mechanization using existing L-1011 flight

management system (FMS) hardware and software. The production configuration FMS computes an optimum descent trajectory for the L-1011 and provides automatic control capability to guide the aircraft from cruise to an end-of-descent point (E*D), arriving at a desired altitude and speed. To provide a 4-D capability a time constraint was added to the E*D arrival requirements by means of software changes to the existing computer program.

1.1 The L-1011 Flight Management System

1.1.1 Basic operation. - The FMS is an extension of the area navigation (or RNAV) capability originally certified with the aircraft in 1971. It performs the basic RNAV functions of waypoint navigation and coupled guidance as well as the automatic selection of VORTAC stations, tuning of the aircraft's VOR/DME receivers, and the mixing of inertial, radio, heading and air data sensor inputs to provide optimal navigation accuracy and reversionary mode operation in the event of degradation. The system is comprised of a computer, a CRT control and display unit (CDU), and a CRT map display.

The flight management capabilities, mainly related to automatic control of engine performance for all phases of flight, are as follows:

- selection and performance of fixed or calculated optimum climb speed schedules
- selection and performance of desired engine pressure ratio (EPR) with automatic or manual derating
- calculation of optimum cruise conditions (i.e., altitude, speed, step-climb determinations) with automatic transitioning from climb to optimum or manually-specified cruise flight
- calculation of the descent trajectory required for optimum or manually-specified descent speed schedules with automatic initiation and termination of descent at a prescribed end-of-descent point, at the desired altitude and speed
- other capabilities such as estimated time enroute to waypoints, engine-out drift down modes, calculation of flap holding speeds, reversionary airport fuel and point-of-no-return calculations based on the effects of current and forecast winds which can be entered into the system by the crew.

A description of the L-1011 FMS optimization algorithms is given in reference 1.

1.1.2 System interface. - The typical aircraft configuration is a dual system installation with the electronic map accepting inputs from either system as desired.

The functional interface of each system with the aircraft is summarized in figure 2. The major aircraft systems involved are the:

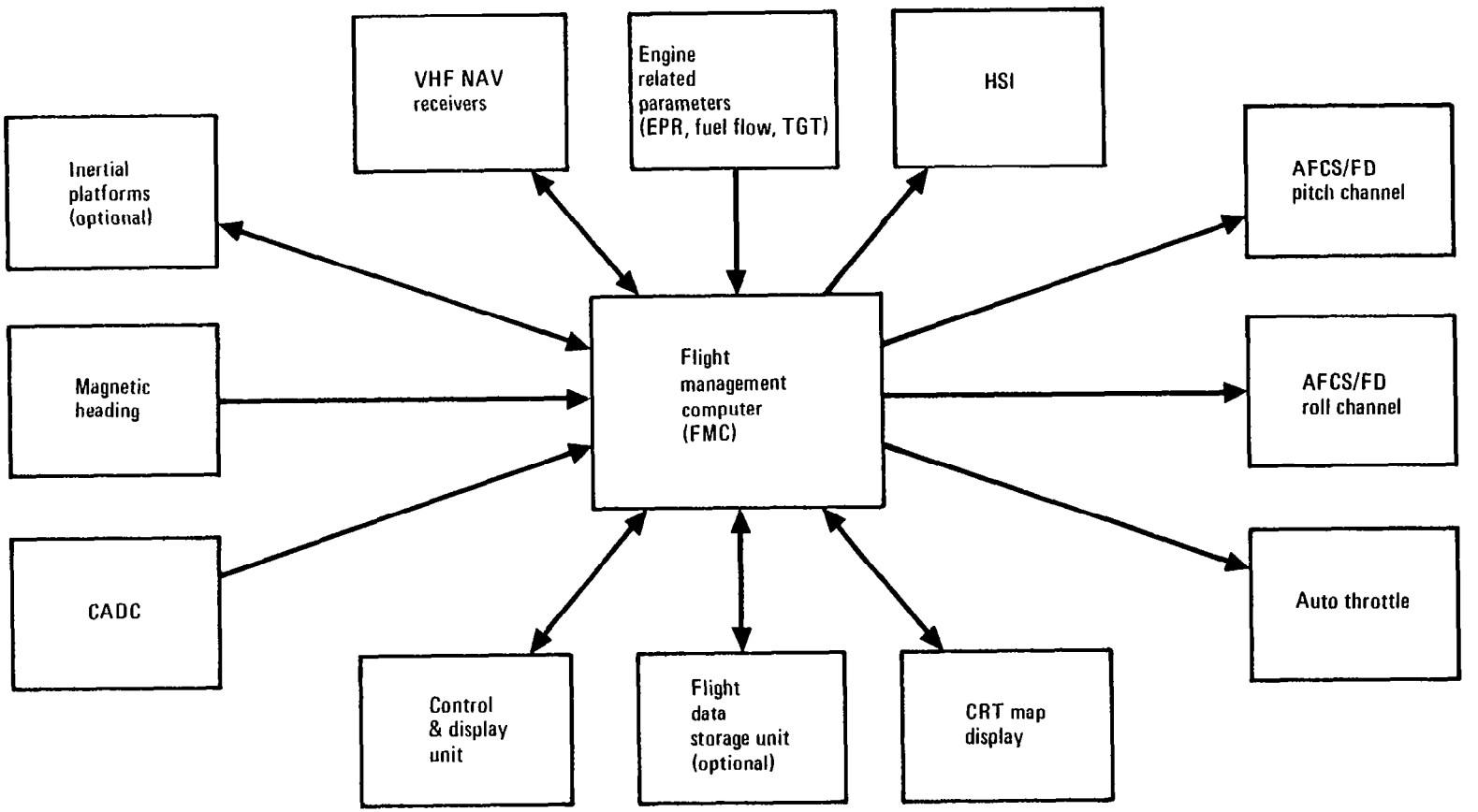

Figure 2. - Flight management system block diagram.

- inertial and radio navigation sensors
- heading reference system
- air data systems
- automatic flight control and flight director system pitch and roll channels
- automatic throttle
- related flight instruments.

The detailed interface, shown in figure 3, illustrates that considerable redundancy exists for the air data and navigation functions. Single system failures are automatically dealt with and the most optimum operational mechanization is configured for the sensors available at any given time. The available navigation modes are:

- inertial/radio mix with up to three inertial system and two each VOR/DME receivers
- inertial only (one to three inertial systems)
- radio only with sub modes of
  - DME/DME
  - VOR/DME
- heading/air data

1.2 Descent Profile Modeling

A precomputed descent profile is the basis of the 4-D control system synthesized in this study. This 3-D descent profile is computed by the FMS prior to descent using latest aircraft weight, wind and temperature data. It is based on descending at near idle power according to one of several available fixed Mach/IAS speed schedules. In the 4-D system designed for this program feedback loops are added to the 3-D system so that variations in range and altitude from the precomputed trajectory are corrected by activating the stabilizer, throttles, or speed brakes. The 3-D profile is stored in the FMS computer as a function of time. At each point in time during the descent the spatial position of the aircraft is compared with the stored trajectory to evaluate the altitude and range errors. The paragraphs which follow describe the steps taken in the development of this capability.

1.2.1 Descent model verification. - At the outset of the study the fidelity of the 3-D descent computation made by the actual airborne FMS was compared with actual flight test data of the L-1011 in descent. Thirty-six descents were simulated in the Palmdale hot mock-up lab facility using the latest production FMS hardware and software. Altitude vs. range data were taken for various combinations of initial conditions such as descent speed

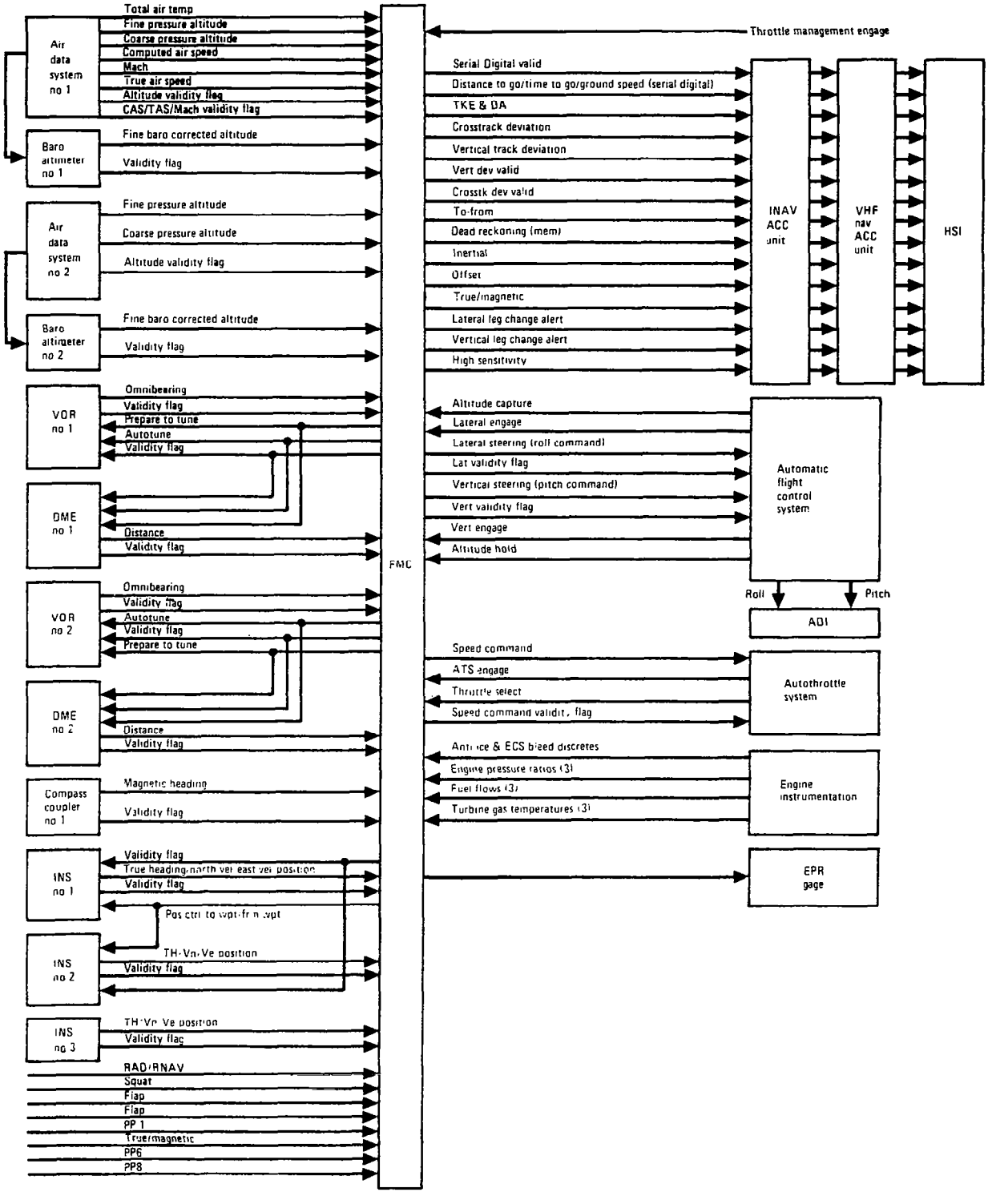

Figure 3. - FMS/Aircraft interface.

schedule, aircraft weight, temperature, and end-of-descent point altitude. These data were then entered into the interactive graphic computer simulation program at Burbank and compared with the latest L-1011 flight test data. Refinements to the FMS 3-D algorithms were then specified for the airborne computer program.

1.2.2 Computation of the 3-D descent profile. - The FMS 3-D descent profile is generated in six segments, back-computed from the specified end-of-descent point (E*D), as shown in figure 4. The profile is established by sequential build-up of incremental ranges (Δr_i) and altitudes (Δh_i) for each of the six segments. Δh is set to a constant value of 500 feet except for the level flight segments, and for segments transitioning to or from level flight. The corresponding Δr's are then computed as a function of Δh using pre-stored polynomials determined from L-1011 aerodynamic data. The point at which the back-computed profile intersects cruise altitude is the beginning-of-descent point, or B*D. The calculated position of B*D is then automatically entered as a waypoint by the FMS computer program into the flight plan previously selected by the crew. The descent profile and the position of B*D are continually updated in flight to reflect current predictions of the descent entry initial conditions. The definition of B*D as a waypoint allows the program to calculate and display other desirable flight plan-related information, such as estimated time-of-arrival (ETA), course, distance, and time enroute to B*D.

1.2.3 Computation of time-in-descent. - In order to predict the time of arrival at E*D, the total time-in-descent is computed. Then the ETA at E*D can be computed by simply adding the calculated total time-in-descent to the estimated time of arrival at B*D:

$$\text{E*D ETA} = \text{B*D ETA} + \text{calculated total time-in-descent}$$

Total time-in-descent is determined by first calculating an incremental time (Δt_i) required to descend through each $\Delta h_i / \Delta r_i$ segment of the trajectory; the total time-in-descent is then the summation of these incremental times or

$$\text{Time-in-descent} = \Sigma \Delta t_i$$

The basic relationships used in the Δt_i computation are as depicted in figure 5.

With wind velocity (VW_i), true-air speed (VT_i), Δh_i and Δr_i given at the i-th altitude level, ground speed (VGS_i) and Δt_i are then computed:

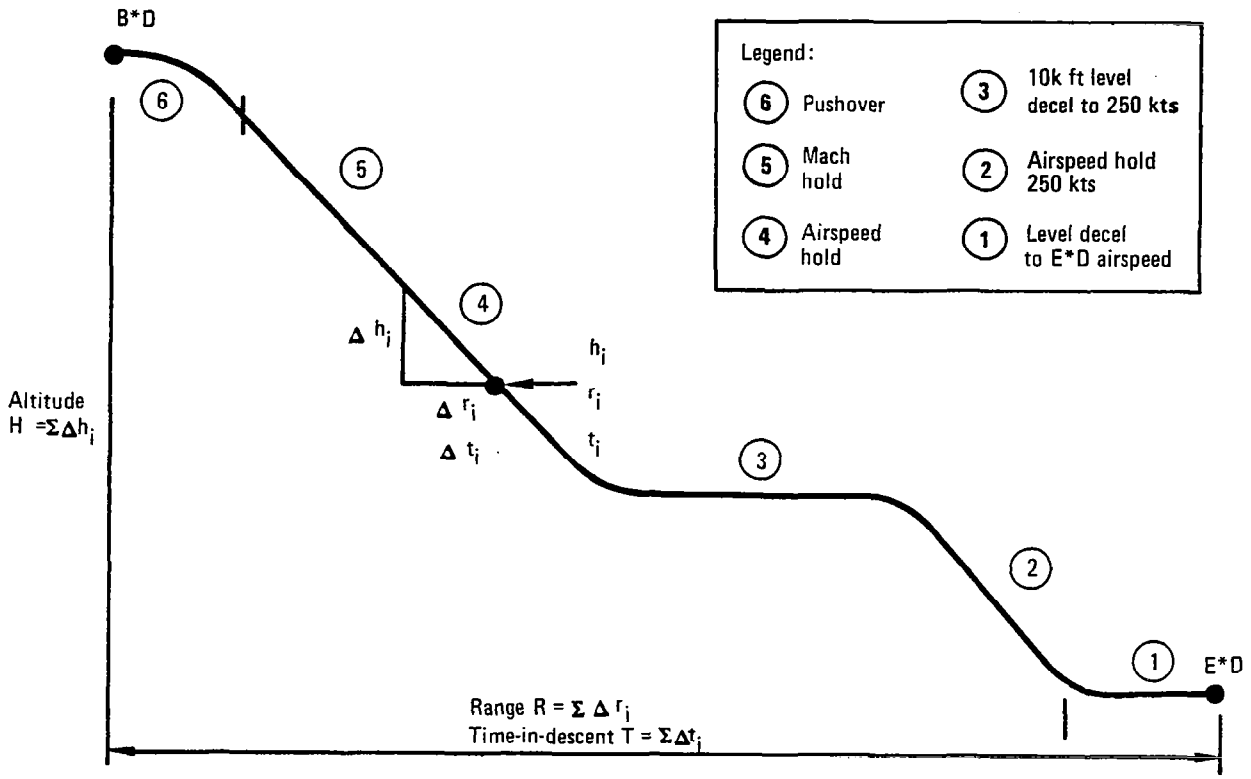

Figure 4. - Computation of 4-D descent profile.

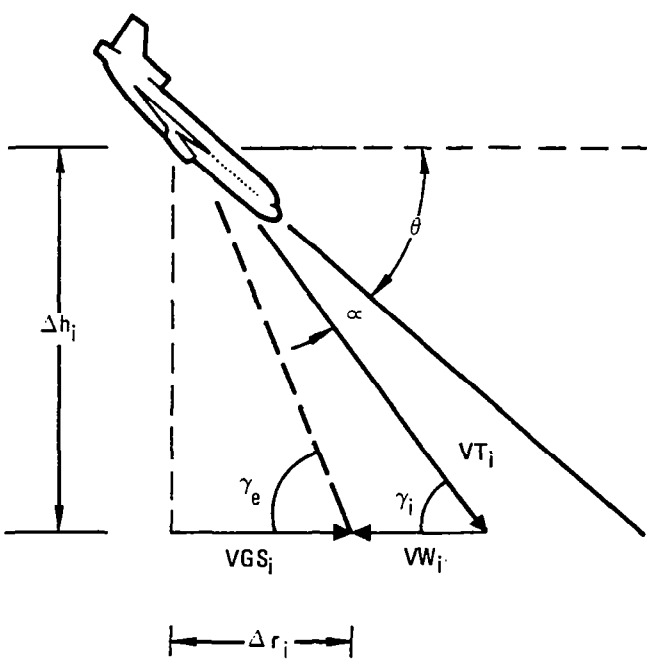

Figure 5. - Incremental segment relationships.

$$VGS_i = VT_i \cos \gamma_i + VW_i$$

$$\Delta t_i = \frac{\Delta r_i}{1/2\ (VGS_i + VGS_{i+1})}$$

$$= \frac{2\,\Delta r_i}{(VT_i + VT_{i+1})\cos \gamma_i + VW_i + VW_{i+1}}$$

where $\cos\gamma_i$ is approximated by the earth referenced path angle γ_e:

$$\cos \gamma_i \approx \cos \gamma_e = \frac{\Delta r_i}{\sqrt{\Delta h_i^2 + \Delta r_i^2}}$$

This approximation, used because the wind-referenced path angle γ_i was not calculated by the existing FMS software, results in an open loop error of 2 seconds or less, and therefore had negligible effect on the closed-loop performance of the prototype system.

The time-in-descent algorithms developed for all six segments of the descent profile are included in Appendix A.

1.2.4 Descent profile sensitivities and error sources. - The effects of speed schedule, aircraft weight, temperature and E*D altitude on descent trajectory range and time-in-descent were analyzed. The results of this analysis are summarized in figures 6 and 7 and presented in more detail in Appendix B.

Error sources which can significantly affect the quality of the descent trajectory and time-in-descent models were determined to be:

- aircraft performance modeling
- engine modeling
- navigation sensors
- modeling of winds aloft and along the descent

The aerodynamic performance model used for this program was the latest available for production aircraft. Figure 8 illustrates the operational quality of the 3-D profile using this model. No attempt was made to tailor the trajectory computations specifically for the flight test aircraft, S/N 1001, because it is continually being used for a wide variety of flight test activities involving engine testing and the development of other advanced systems (e.g.,

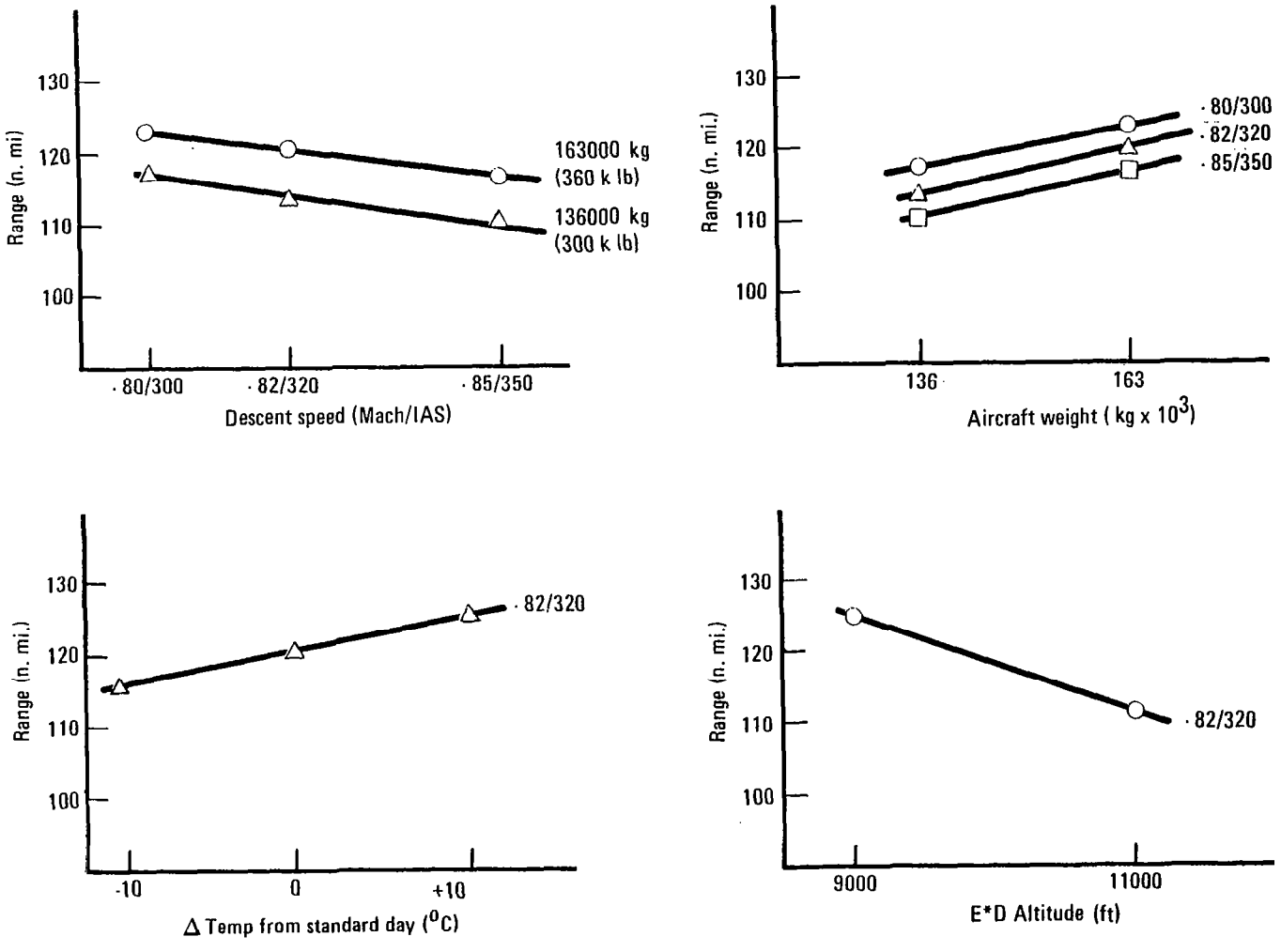

Figure 6. - The effects of speed, weight, temperature and E*D altitude on descent trajectory range (42000 to 9000 ft descent)

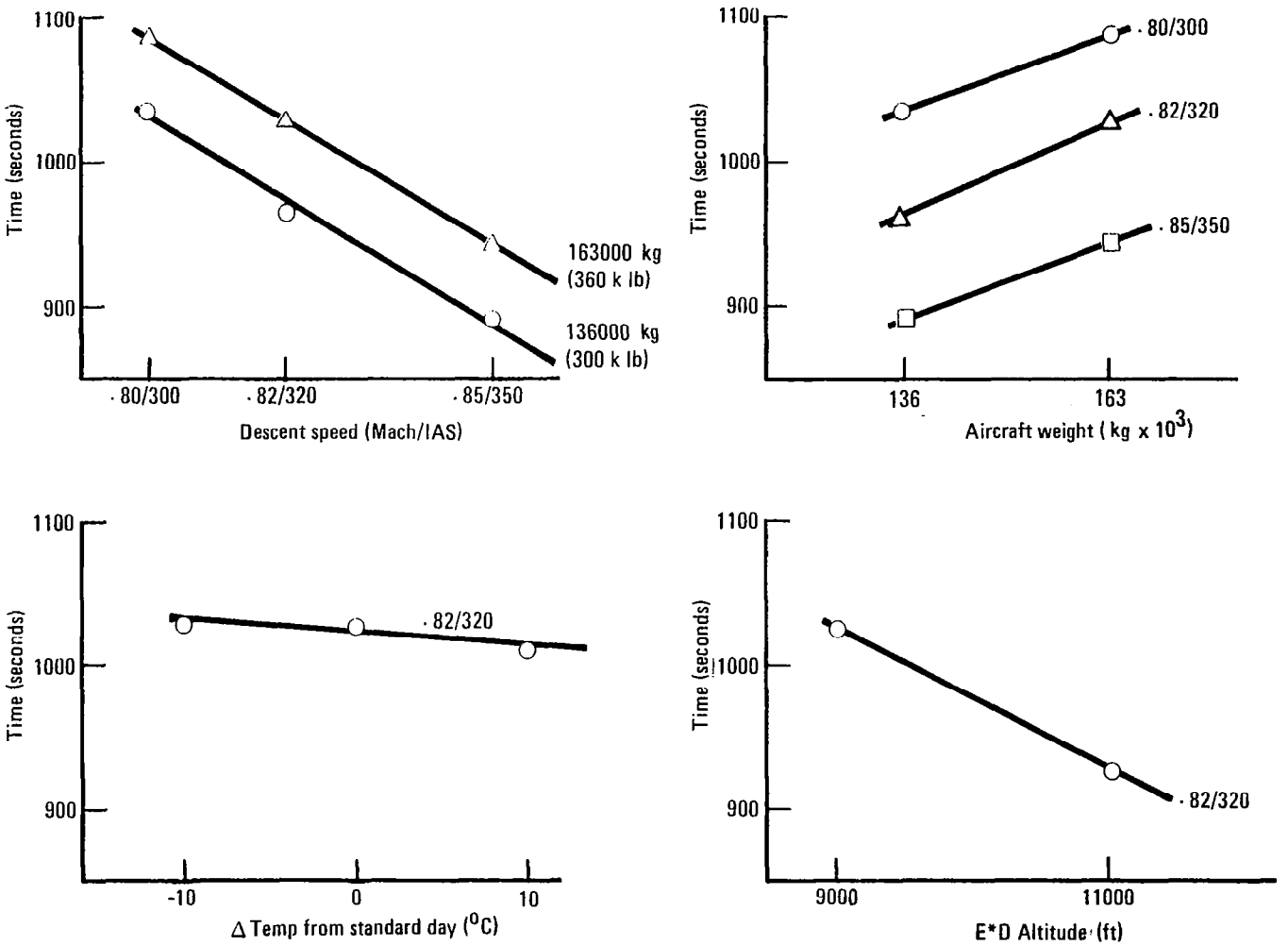

Figure 7. - The effects of speed, weight, temperature and E*D altitude on time-in-descent (42000 to 9000 ft descent)

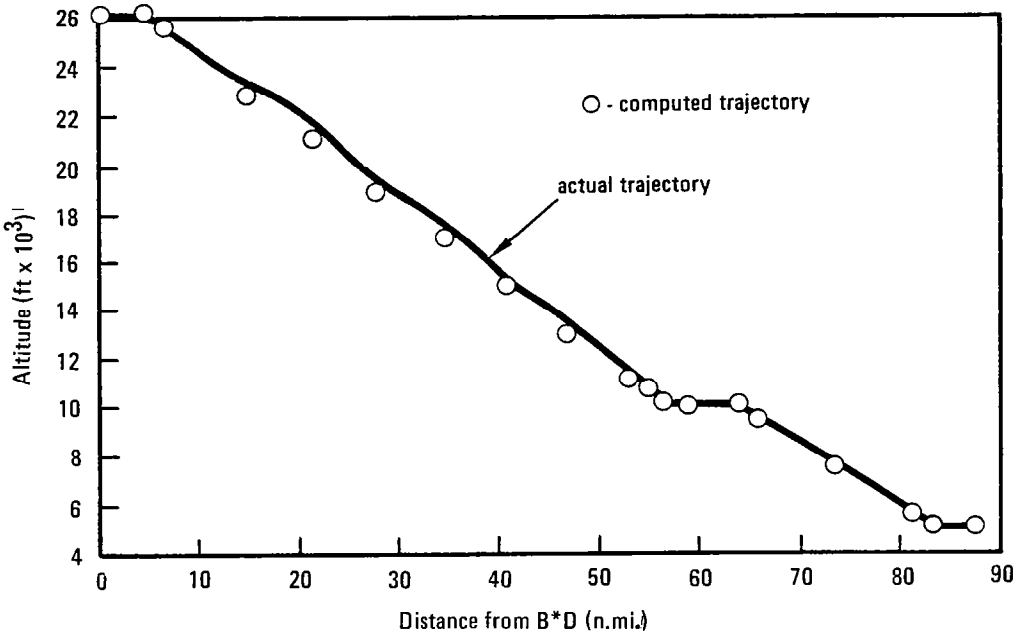

Figure 8. - Descent profile, Test No. 216, 8/6/79.

active controls). It is not uncommon to fly with a "mix" of various engine types and various control surface configurations, which are subject to change on short notice. Producing a more flexible model, that could be modified as the aircraft configuration was changed, was not possible in the short span of the study. It was noted that the engine mixes, of which there were several during the program, and the presence of wing tip extensions, that were not represented in the production modeling, made appreciable differences in actual descent trajectories. The closed loop nature of the 4-D control system suppressed errors from these sources. For future flight testing it is, however, recommended that more exact modeling be used.

The FMS inertial/radio navigation solution with DME/DME updating which offers position accuracies of 0.5 n.mi. or better was considered to be more than adequate for this application. However, as discussed in a later section of this report, further consideration concerning the logic utilized in blending the navigation sensor "mixes" appears necessary to preclude the position updating processes from introducing apparent time errors during 4-D flight.

Wind has the potential of causing the largest 4-D descent performance errors. Therefore it is necessary to accurately measure the wind existing in cruise just prior to descent, and to construct a realistic model for the winds existing at lower altitudes, so that the descent trajectory can be accurately computed. The measurement of winds in cruise presented no problem; true airspeed, ground speed, ground track and heading were used for this calculation. The descent wind model used in the FMS during flight testing was a linear decay of the wind velocity at cruise to zero at sea level.

1.3 Wind Study

The accurate modeling of winds along the descent trajectory is a critical factor in the computation of the descent profile and in the calculation of the time-in-descent. The following paragraphs describe a study of existing wind data and the basis for selecting the linear wind model that was used in the flight test experiments.

1.3.1 Statistical wind data. - In earlier NASA studies wind data (see references 2 and 3) were compiled for seven geographical locations of the world. The data, collected over a period of several years at each location, were presented as monthly tabulations of the zonal (east-west) and meridional (north-south) mean wind components at integral kilometers of altitude. Standard deviations from the mean were also presented for each altitude, along with the correlation coefficients relating the winds at one level upon another. Table 2 is an example of this data for Tripoli, Libya, during the month of February.

In the present study the monthly data from each location, up to the certified operational ceiling altitude of the L-1011 (42000 ft), were entered into an IBM 370 computer at Burbank for additional analysis. This effort is described in paragraphs 1.3.2 through 1.3.4.

1.3.2 Linear wind model development. - Reference 4, reporting the results of a study concerning the correlation of interlevel wind velocities, states that a linear relationship exists between winds at cruise and the winds along the lower altitudes. This relationship is illustrated by the scatter diagrams presented in figure 9 where linear regression techniques were used to provide a best fit to the observed interlevel wind velocity data. The slopes and intercepts of these regression lines can be determined using conditional probability density functions; the resulting linear equations can then be used to compute the expected values of wind velocities of all lower altitudes when the winds at cruise are known.

$$V_i = \overline{V}_i + \beta_{ij} \, (V_j - \overline{V}_j)$$

where

$$\beta_{ij} = \rho_{ij} \, \sigma_i / \sigma_j$$

TABLE 2. - NASA WIND DATA

INTERLEVEL AND INTRALEVEL CORRELATIONS BETWEEN WIND SPEED COMPONENTS WITH MEANS AND STANDARD DEVIATIONS OF WIND SPEED COMPONENTS BY ALTITUDE LEVELS

ZONAL AND MERIDIONAL WIND COMPONENT CORRELATIONS

TRIPOLI, LIBYA

FEBRUARY

STATION
Tripoli, Libya

REFERENCE PERIOD
February

STATION ELEVATION
12 meters MSL

STATION COORDINATES
32 deg 54 min N, 13 deg 17 min E

PERIOD OF OBSERVATION
January 1951 - December 1957

DATA SOURCE
National Weather Records Center
U. S. Weather Bureau
Asheville, North Carolina

PREPARED BY
Army Ballistic Missile Agency
Aeroballistics Laboratory
Aerophysics and Geophysics Branch
Redstone Arsenal, Alabama
23 April 1960

No. of Obs.	Altitude (MSL) km	Zonal Mean m/s	SD m/s	sfc	1	2	3	4	5	6	7	8	9	10	11	12	13	14	15	16	17	18	19	20	21	22	23	24	25	26	27	28	29	30	31	32
		Meridional Mean m/s		-0.63	-0.22	-0.62	-0.63	-0.64	-0.17	0.16	0.06	0.53	0.52	-0.06	0.07	-0.14	-1.03	-1.31	-1.05	-1.02	-1.11	-1.50	-0.90	-1.45	-1.13	-0.75	-0.67	-0.36	-0.27	0.43	0.91	0.80	1.61	0.77		
		SD m/s		3.36	5.65	6.31	7.47	8.43	9.98	11.49	13.40	15.71	16.79	15.51	15.11	13.50	12.43	10.26	8.82	7.70	7.66	6.42	6.67	4.52	4.77	5.00	3.93	4.33	4.74	5.58	6.79	7.32	6.90	4.36		
389	sfc	1.94	4.08	-.083	.479	.380	.279	.221	.227	.198	.190	.178	.167	.183	.157	.136	.170	.236	.204	.187	.264	.216	.142	.089	.072	-.034	-.045	.097	.058	.035	-.026	-.049	-.036	-.115		
386	1	6.63	6.98	.700	-.018	.770	.610	.570	.538	.469	.445	.429	.392	.459	.497	.422	.360	.439	.404	.399	.388	.232	.177	.141	.132	.126	.021	-.038	.004	.013	-.004	-.062	-.156	-.370		
385	2	9.60	7.03	.498	.790	.094	.805	.773	.738	.681	.637	.607	.563	.591	.584	.574	.491	.530	.495	.455	.500	.323	.313	.216	.250	.147	.084	-.013	-.002	.056	.032	-.054	-.107	-.207		
381	3	12.01	7.79	.376	.627	.822	.226	.893	.834	.773	.712	.673	.675	.670	.642	.618	.494	.562	.523	.490	.470	.361	.297	.245	.275	.232	.114	.046	.080	.137	.083	.039	-.091	-.083		
376	4	14.68	9.83	.273	.490	.691	.873	.268	.904	.841	.784	.728	.702	.691	.669	.640	.522	.573	.534	.478	.490	.401	.343	.295	.268	.219	.166	.013	.078	.137	.137	.056	.018	-.043		
372	5	17.75	12.02	.253	.457	.655	.809	.933	.274	.911	.844	.784	.750	.732	.693	.671	.583	.598	.572	.502	.491	.395	.380	.298	.266	.235	.100	-.047	-.005	.062	.087	.029	.050	-.008		
363	6	21.04	13.59	.197	.418	.617	.766	.873	.927	.310	.921	.859	.814	.779	.743	.709	.621	.611	.569	.496	.519	.414	.373	.268	.228	.175	.055	-.029	.005	.092	.087	.022	.047	.055		
351	7	24.69	16.13	.171	.386	.587	.705	.805	.873	.936	.341	.933	.887	.823	.772	.742	.660	.642	.605	.541	.582	.497	.441	.316	.319	.168	.038	-.090	-.017	.059	.048	.007	-.016	.051		
335	8	27.95	18.42	.134	.337	.547	.655	.747	.806	.865	.932	.353	.947	.856	.774	.756	.683	.638	.595	.520	.537	.454	.417	.320	.297	.185	.057	-.052	-.031	.064	.083	-.015	-.047	.086		
315	9	31.63	19.78	.115	.314	.498	.606	.699	.746	.795	.862	.935	.332	.919	.824	.780	.714	.671	.611	.526	.532	.457	.452	.336	.322	.243	.089	.008	.016	.106	.069	-.014	-.043	.200		
290	10	34.89	21.29	.078	.280	.470	.563	.639	.674	.745	.789	.859	.924	.331	.894	.826	.758	.705	.647	.564	.542	.475	.473	.316	.294	.252	.074	.039	.060	.161	.115	.029	-.009	.226		
266	11	38.38	21.75	.116	.248	.426	.521	.620	.665	.677	.727	.803	.863	.925	.392	.920	.842	.798	.713	.643	.528	.431	.427	.261	.228	.184	.019	.034	-.032	.036	-.097	-.205	-.244	.126		
249	12	39.77	19.67	.086	.201	.389	.504	.617	.648	.655	.695	.754	.810	.857	.914	.396	.908	.833	.744	.693	.545	.449	.426	.284	.245	.136	.000	.069	-.057	.060	-.047	-.130	-.148	.194		
225	13	37.45	16.93	-.012	.134	.366	.463	.56.	.649	.639	.660	.678	.686	.721	.771	.851	.252	.808	.768	.694	.556	.426	.389	.242	.214	.128	.017	-.088	-.083	.064	.004	-.070	-.004	.213		
214	14	34.96	15.81	-.028	.170	.315	.396	.507	.587	.592	.599	.599	.605	.625	.716	.773	.849	.281	.850	.828	.730	.602	.580	.302	.300	.169	.010	-.014	.043	.085	.043	-.106	-.050	.195		
194	15	30.38	14.06	-.080	.145	.298	.393	.507	.568	.581	.562	.553	.550	.586	.649	.677	.763	.829	.287	.811	.733	.645	.644	.338	.305	.243	.078	.031	.110	.145	.163	.008	.004	.178		
171	16	26.10	11.84	-.113	.074	.239	.329	.429	.471	.502	.456	.420	.396	.437	.514	.584	.662	.685	.791	.192	.772	.681	.620	.313	.283	.142	.016	.110	-.066	-.083	.041	-.054	-.119	-.136		
154	17	21.27	9.76	-.134	.009	.218	.294	.312	.336	.359	.289	.206	.207	.227	.331	.422	.498	.555	.593	.750	.166	.786	.732	.478	.467	.182	.010	.033	.014	-.012	.125	-.057	-.086	-.130		
148	18	18.09	9.53	.010	.222	.188	.410	.376	.401	.447	.391	.358	.348	.369	.442	.497	.573	.604	.581	.682	.706	.319	.822	.560	.496	.185	.085	.107	.042	-.021	.061	.130	-.058	-.005		
144	19	15.22	10.31	-.015	.162	.321	.358	.392	.419	.445	.397	.375	.359	.374	.417	.445	.527	.550	.591	.664	.616	.783	.484	.636	.634	.356	.218	.241	.149	.121	.141	.091	-.178	.288		
142	20	11.29	10.33	.029	.225	.332	.376	.380	.356	.348	.306	.310	.314	.322	.336	.366	.395	.365	.453	.470	.457	.593	.794	.152	.698	.497	.361	.273	.174	.013	.158	.136	-.255	-.079		
136	21	9.04	11.54	.072	.124	.197	.217	.239	.190	.197	.213	.243	.224	.249	.208	.279	.280	.201	.209	.391	.407	.523	.701	.775	.268	.630	.443	.439	.355	.251	.325	.307	-.104	.172		
135	22	8.97	11.66	.036	.157	.238	.317	.303	.257	.255	.279	.282	.217	.254	.213	.231	.247	.205	.169	.184	.407	.551	.691	.686	.862	.273	.639	.572	.519	.398	.505	.560	.260	.096		
132	23	8.35	11.82	.040	.107	.183	.323	.313	.240	.241	.284	.296	.261	.269	.254	.371	.385	.534	.297	.460	.442	.586	.606	.634	.698	.843	.196	.705	.627	.607	.677	.645	.544	.265		
124	24	8.33	12.28	.076	.099	.164	.305	.271	.178	.189	.258	.289	.266	.294	.248	.345	.334	.298	.248	.395	.433	.559	.597	.631	.687	.792	.907	.263	.798	.751	.779	.785	.589	.333		
111	25	8.83	12.94	-.108	.075	.119	.309	.257	.182	.241	.314	.361	.336	.355	.309	.390	.387	.349	.306	.438	.456	.594	.567	.559	.675	.759	.852	.909	.326	.853	.786	.813	.678	.559		
94	26	9.92	13.37	-.151	.016	.005	.256	.226	.164	.207	.251	.349	.340	.350	.295	.416	.429	.413	.350	.358	.301	.470	.482	.395	.509	.553	.729	.794	.924	.414	.911	.849	.684	.487		
77	27	10.40	13.56	-.195	.040	.067	.158	.159	.087	.136	.141	.247	.220	.221	.163	.350	.357	.313	.240	.246	.277	.374	.371	.311	.434	.520	.756	.772	.874	.950	.510	.876	.782	.267		
67	28	11.92	15.18	.197	.034	.014	.221	.192	.116	.208	.255	.333	.296	.298	.235	.380	.374	.338	.268	.333	.354	.445	.428	.333	.425	.480	.648	.763	.859	.909	.930	.567	.852	.823		
51	29	11.17	15.44	.227	.200	.333	.002	.028	.021	.024	.041	.077	.049	.029	.054	.216	.306	.284	.274	.328	.367	.425	.415	.316	.328	.404	.715	.714	.778	.877	.908	.963	.437	.656		
31	30	15.56	13.50	.301	.281	.287	.216	.103	.195	.108	.083	.002	.090	.227	.242	.088	.163	.184	.224	.326	.351	.443	.455	.324	.188	.261	.581	.516	.498	.682	.752	.881	.911	.004		
10	31			Correlations were not determined for the last 11 altitude levels when less than twenty observations were available																																	
5	32																																			

NOTE: Zonal Mean, Positive for Wind Component from West. Meridional Mean, Positive for Wind Component from South.

Underlined Values Indicate Intralevel Correlations

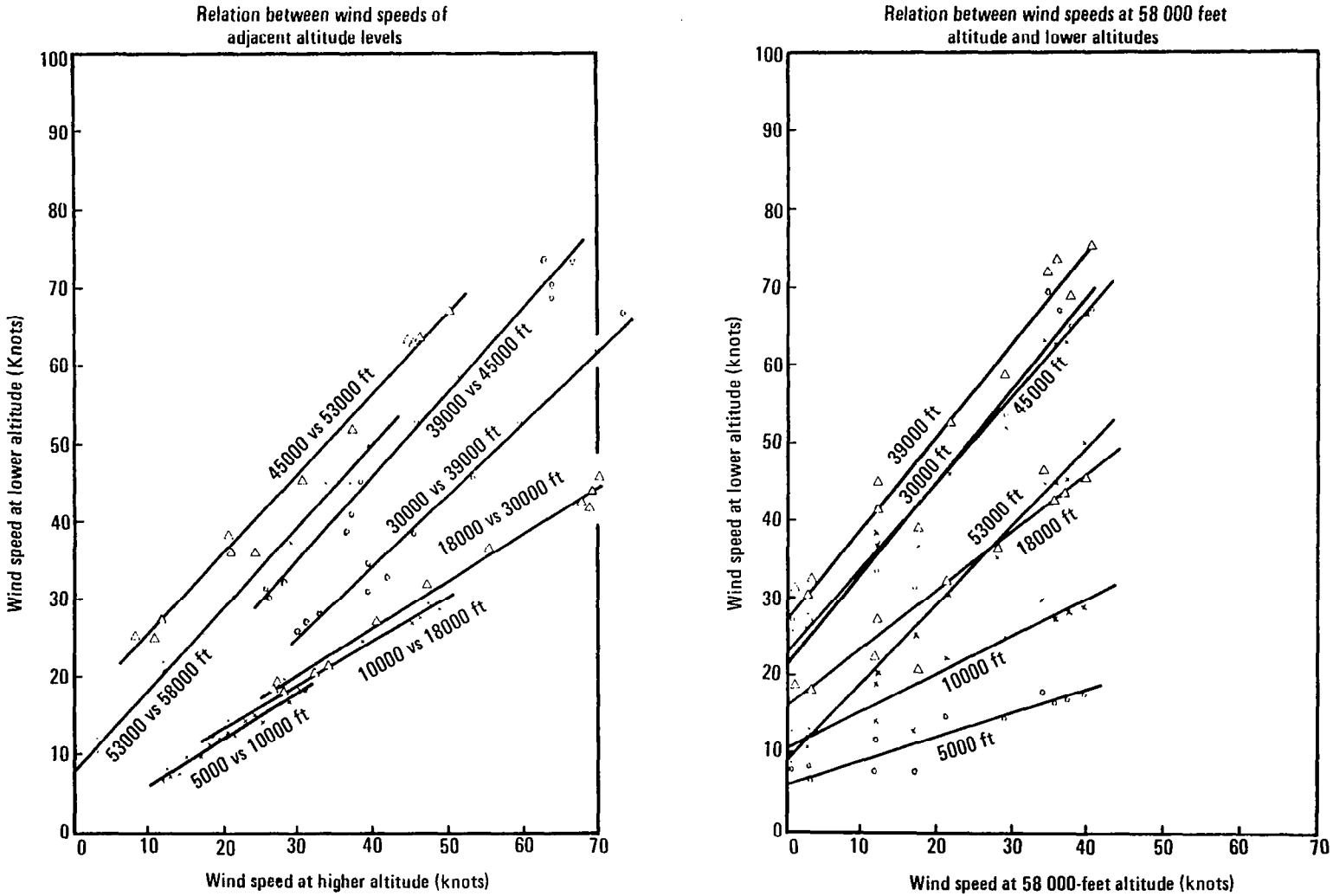

Figure 9. - Interlevel wind velocities.

is the regression coefficient; i = 0,1,2 - - - (j-1) are the lower altitude levels at which the expected values of wind velocities are to be computed; j is the altitude level at which the known wind velocity is given; V_i is the computed wind velocity at level i; V_j is the known wind velocity measured at level j; $\overline{V}_i$ and $\overline{V}_j$ are the mean wind velocities; ρ_{ij} is the interlevel correlation coefficient for level j on level i; σ_i and σ_j are the standard deviations. The 95-percentile confidence envelope for the conditional wind profile is given by:

$$V_i' = V_i \pm 2\sigma_i \left[1 - \rho_{ij}^2\right]^{1/2}$$

A computer program was written for the IBM 370 to investigate the possible application of these techniques in developing a suitable wind model for the descent trajectory computation. Wind profiles based on the linear regression techniques were computed and plotted for each of these locations.

Figure 10 shows the February zonal mean wind profile together with the $\pm 2\sigma$ raw data envelope and the $\pm 2\sigma$ conditional profile envelope. Figure 11 shows the February zonal mean profile and the conditional profiles resulting from $\pm 1\sigma$ and $\pm 2\sigma$ winds existing at a descent entry altitude of 42000 feet.

A review of the graphic results concluded that, for the flight regime of the L-1011 aircraft, wind velocities at cruise altitudes decay in a fairly linear fashion to zero knots at zero feet altitude.

1.3.3 Simulation wind model development. - For the seven geographical locations studied, winds were observed to be predominantly east-west; the worst case wind (i.e. the monthly wind velocity with the highest standard deviation) was seen to occur at Tripoli, Libya in the month of February. For this reason, the February zonal Tripoli wind profiles were chosen for use as a worst case statistical representation for simulation studies in the course of development of the 4-D descent control algorithm. To add realism to the descent simulations using the Tripoli model, a random component, taken from Palmdale flight test data, was added. The Palmdale wind, with a standard deviation of 7.6 kts, was added to the Tripoli wind as shown in figure 12. The resulting wind was then applied as a headwind or a tailwind during the analyses.

1.3.4 The effect of wind estimation error on open loop performance. - The following descent performance criteria were established at the beginning of the program: the E*D position error goal was ±1 n.mi. and E*D time-of-arrival error was to be kept within ±30 seconds (2σ). The Tripoli 2σ raw wind profile and the mean wind profile, shown in figure 10, were applied as headwinds to the descent profile algorithm described in section 1.2. The

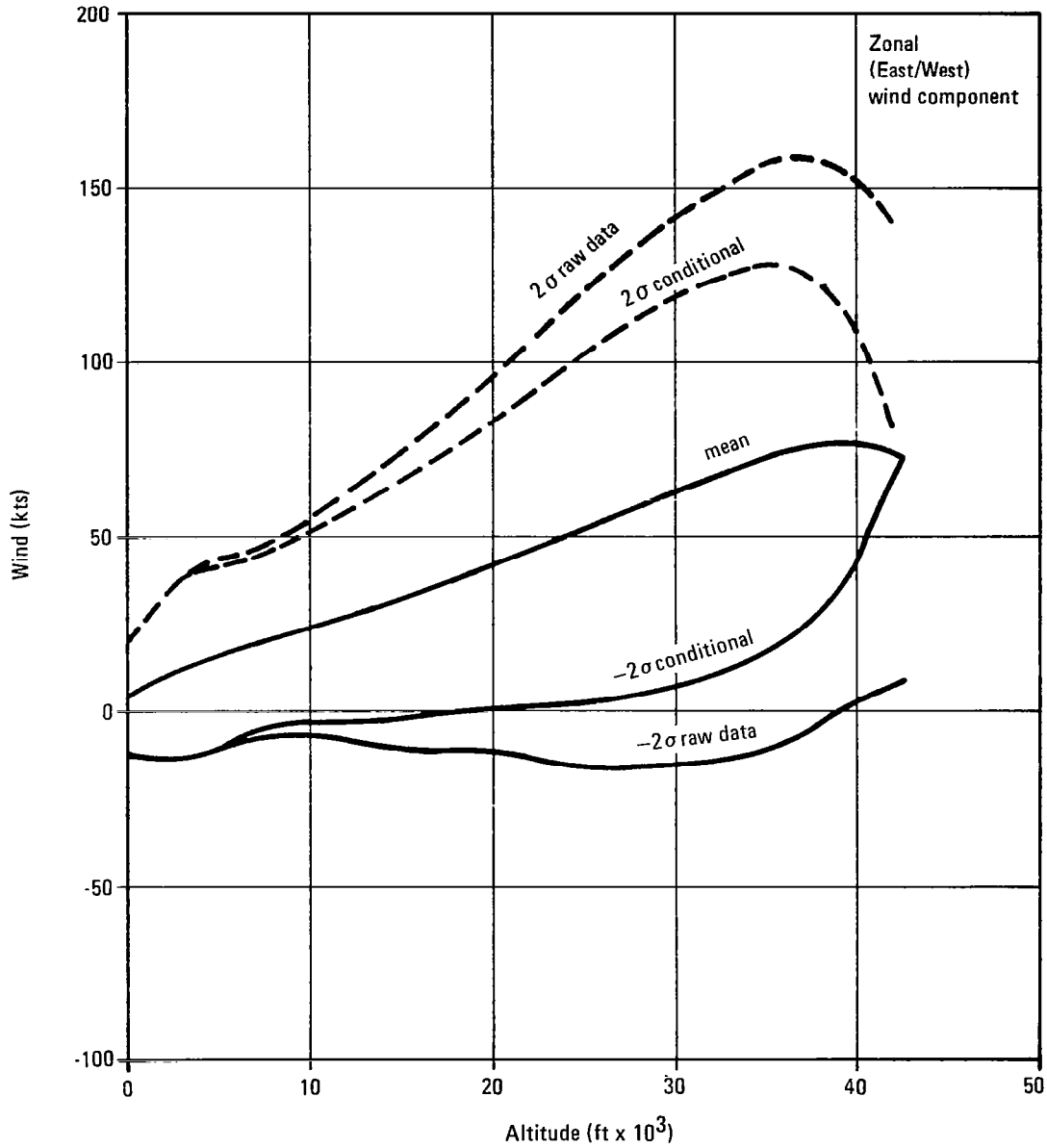

Figure 10. - Wind statistics, Tripoli, Libya, February.

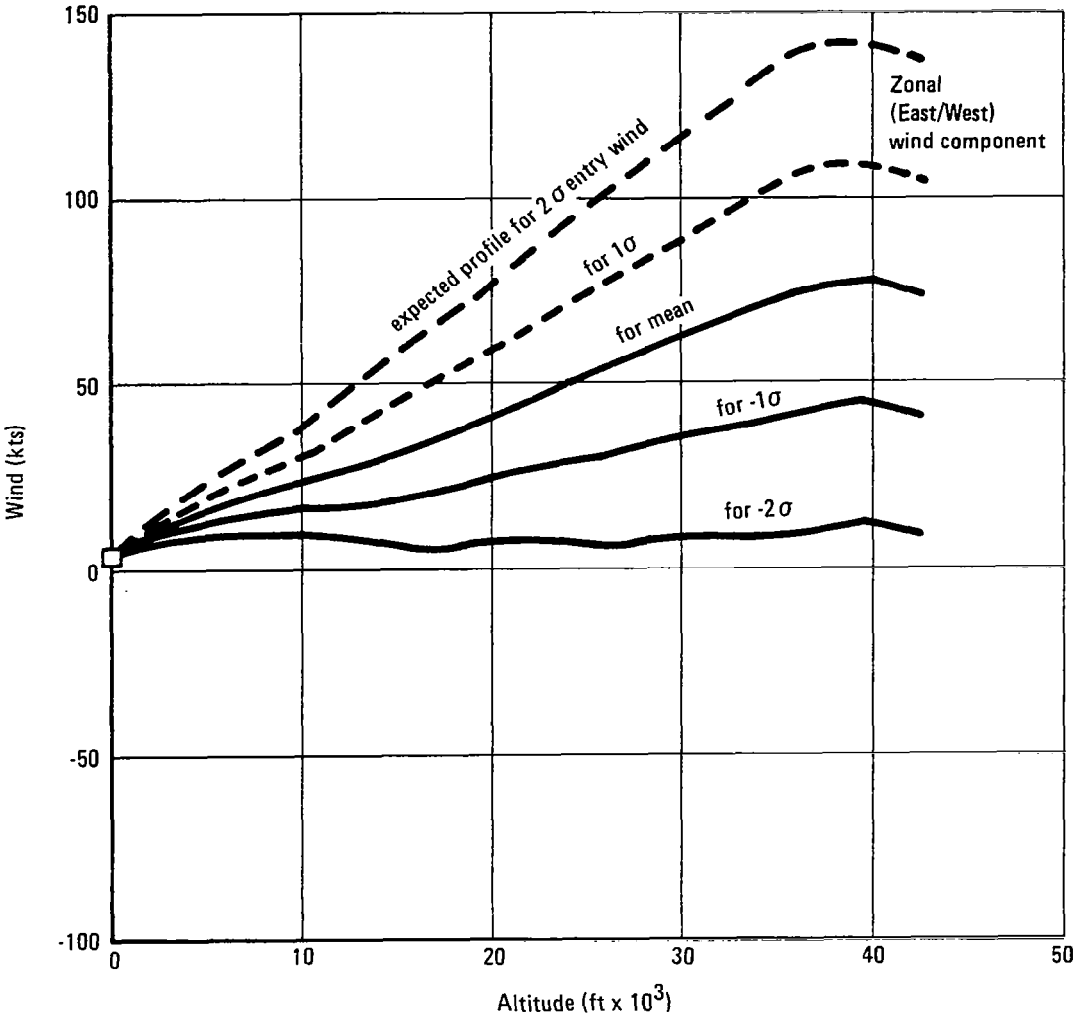

Figure 11. - Derived wind profiles, Tripoli, Libya, February.

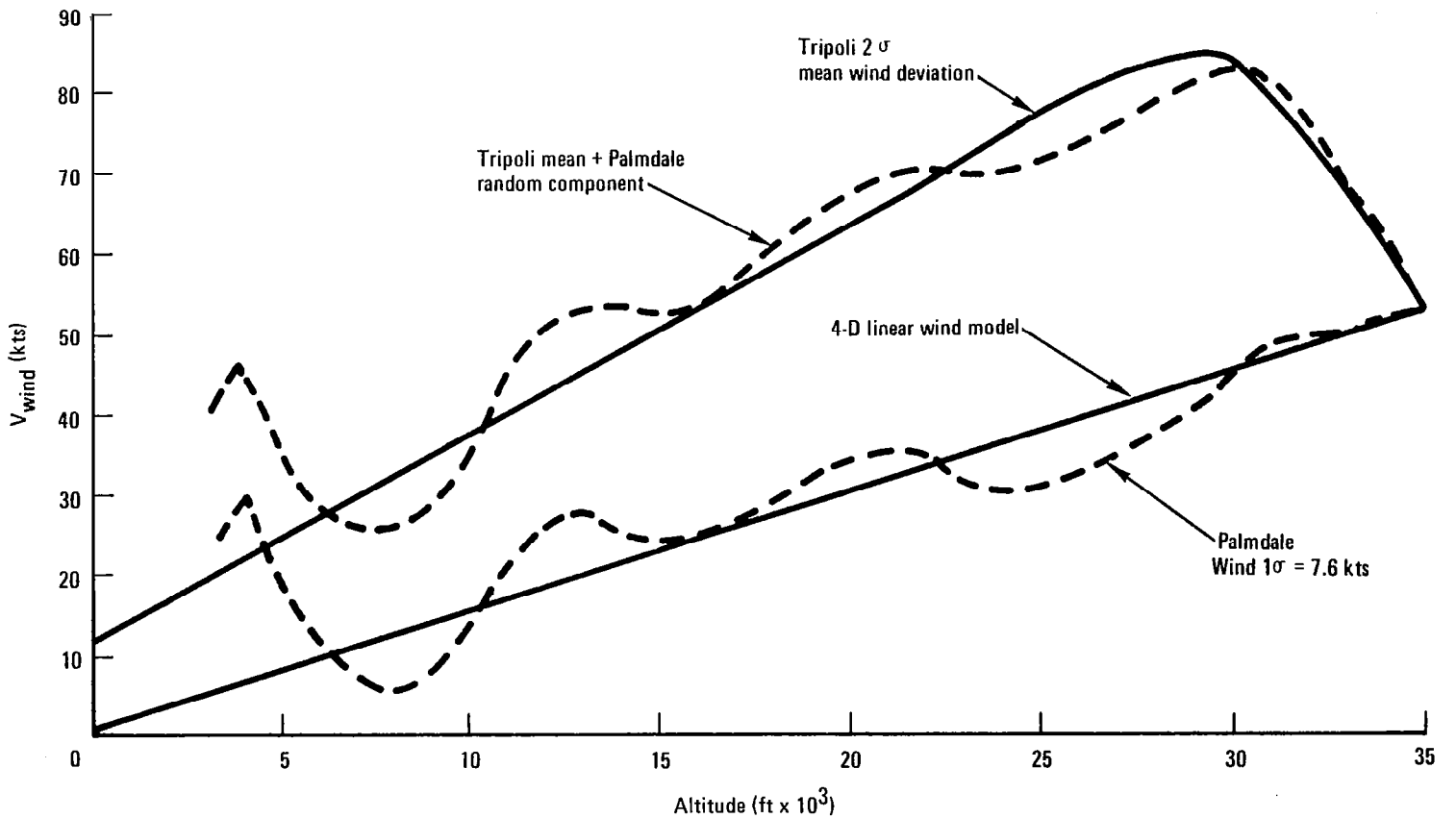

Figure 12. - Simulation wind models.

differences in the descent time and descent range values resulting from the application of these two wind profiles represent the open-loop 3-D descent errors that can result from a worst-case unmodeled wind. The results of this study showed that E*D could be overflown within about ±40 seconds of the required time, however, E*D altitude would be captured with range errors of approximately ±20 n.mi. This is presented by figure 13 which illustrates the inadequacy of an open loop solution for achieving the desired results.

1.4 4-D Control Law Development

1.4.1 Altitude and range errors as feedback variables. - With the need for improved 4-D control clearly justified by simulation results, several candidate schemes were identified and traded-off. The technique eventually chosen was to:

- Precompute a fixed 3-D trajectory prior to descent
- Feedback trajectory altitude errors to the spoilers or throttle
- Feedback trajectory range errors through the aircraft pitch autopilot

Figure 14 depicts the feedback variables of altitude error and range error that are used for control.

Control of altitude errors was not automated because of the extensive hardware modifications that would be required for the aircraft's flight control systems. Instead, advisories of altitude deviations from the 3-D profile were displayed to the flight crew for manual deployment of spoilers (to increase the rate of descent for the "too high" case) or manual application of thrust (to slow the descent rate for the "too low" case). The range error feedback was completely automatic through the pitch autopilot.

It was decided to apply control only during the airspeed hold portion of the descent (below 29,000 ft altitude) for two reasons: simulation studies showed that altitude and range (time) errors that might accumulate early in the Mach-hold portion of descent were not significant and could be compensated for by applying control in the airspeed region; the Mach-hold control laws and logic in the existing FMS are fairly complex and not easily modified by additional software.

One descent speed schedule was mechanized for the prototype system. This schedule consisted of a 0.82 Mach-hold descent until indicated airspeed (IAS) increases in value to 320 kts (which occurs at approximately 29000 ft); after this, the system holds 320 kts IAS until level-off at 10000 ft or at E*D altitude, whichever comes first. A 0.82 mach/320 kts descent was selected primarily because a ±40 kts airspeed variation would be available for closed loop control of range errors. It also represented fairly closely a minimum cost speed schedule.

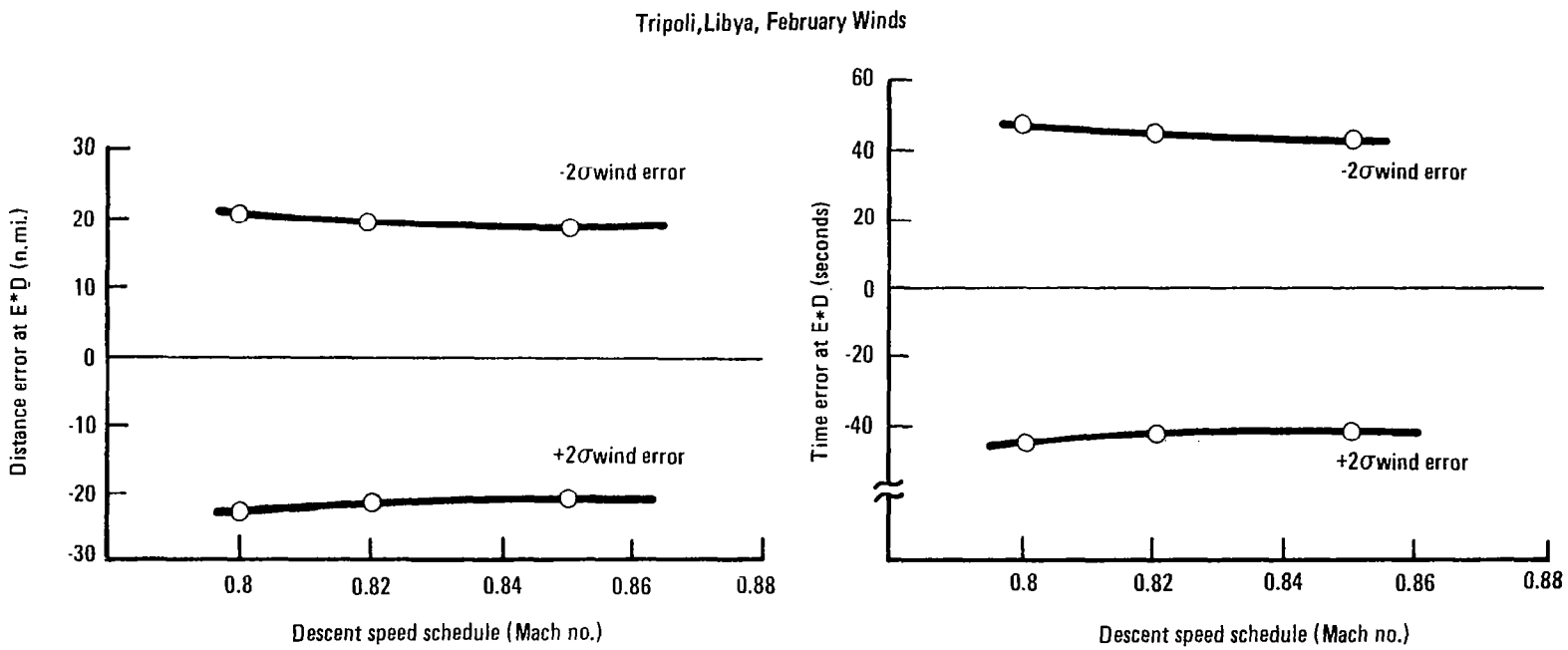

Figure 13. - Effect of wind estimation error.

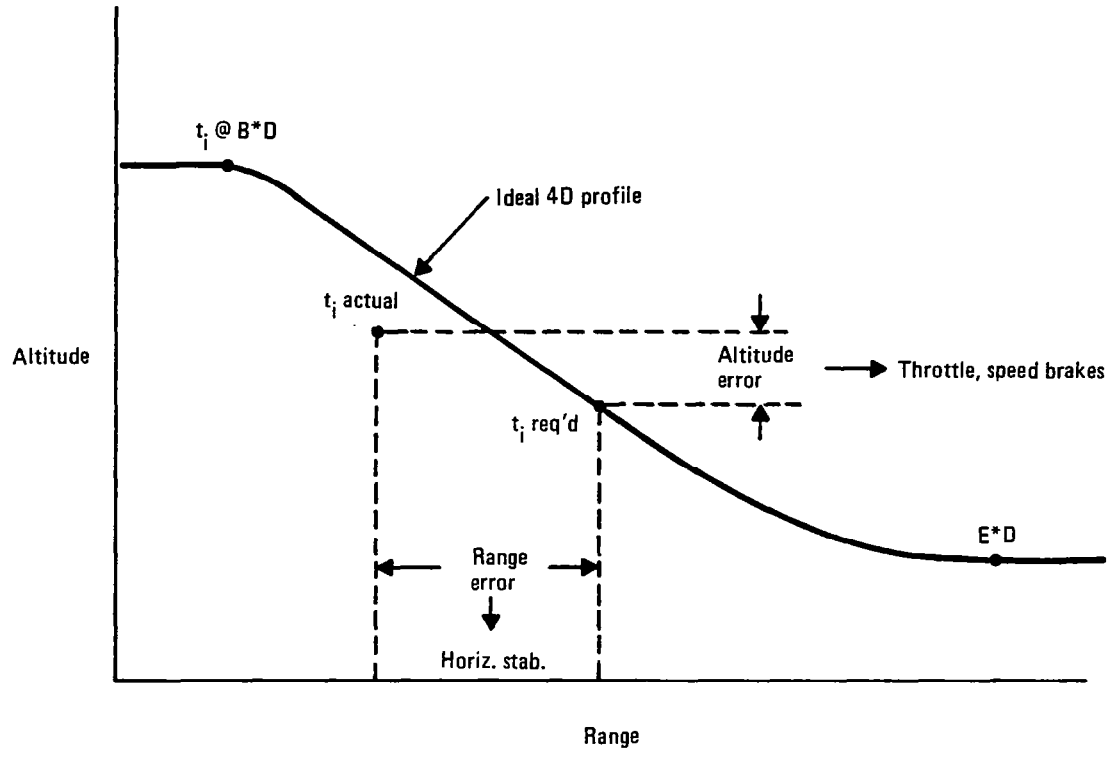

Figure 14. - Feedback variables.

1.4.1.1 Altitude error feedback. - Figure 15 shows the manual control scheme utilized for making good the 3-D or spatial profile. The aircraft's actual altitude is compared to the altitude required by the descent profile to derive altitude error. For positive errors, i.e., when the aircraft is above the desired spatial profile, spoilers are deployed to increase the aircraft's descent rate; conversely, thrust is applied to slow the aircraft's descent when the aircraft is below the profile. A "bang-bang" control strategy was adopted, wherein errors were allowed to build up to ±300 ft and specified spoiler/EPR schedules were followed to reduce the error to ±150 ft. This was done because a proportional control strategy:

- would have been subject to interpretation by the crew and resulting performance would have been more difficult to evaluate by simulation analysis
- would have caused more throttle cycling than the bang-bang approach

The EPR schedule shown in figure 15 was calculated for an L-1011 with a full complement of RB 211-524B engines.

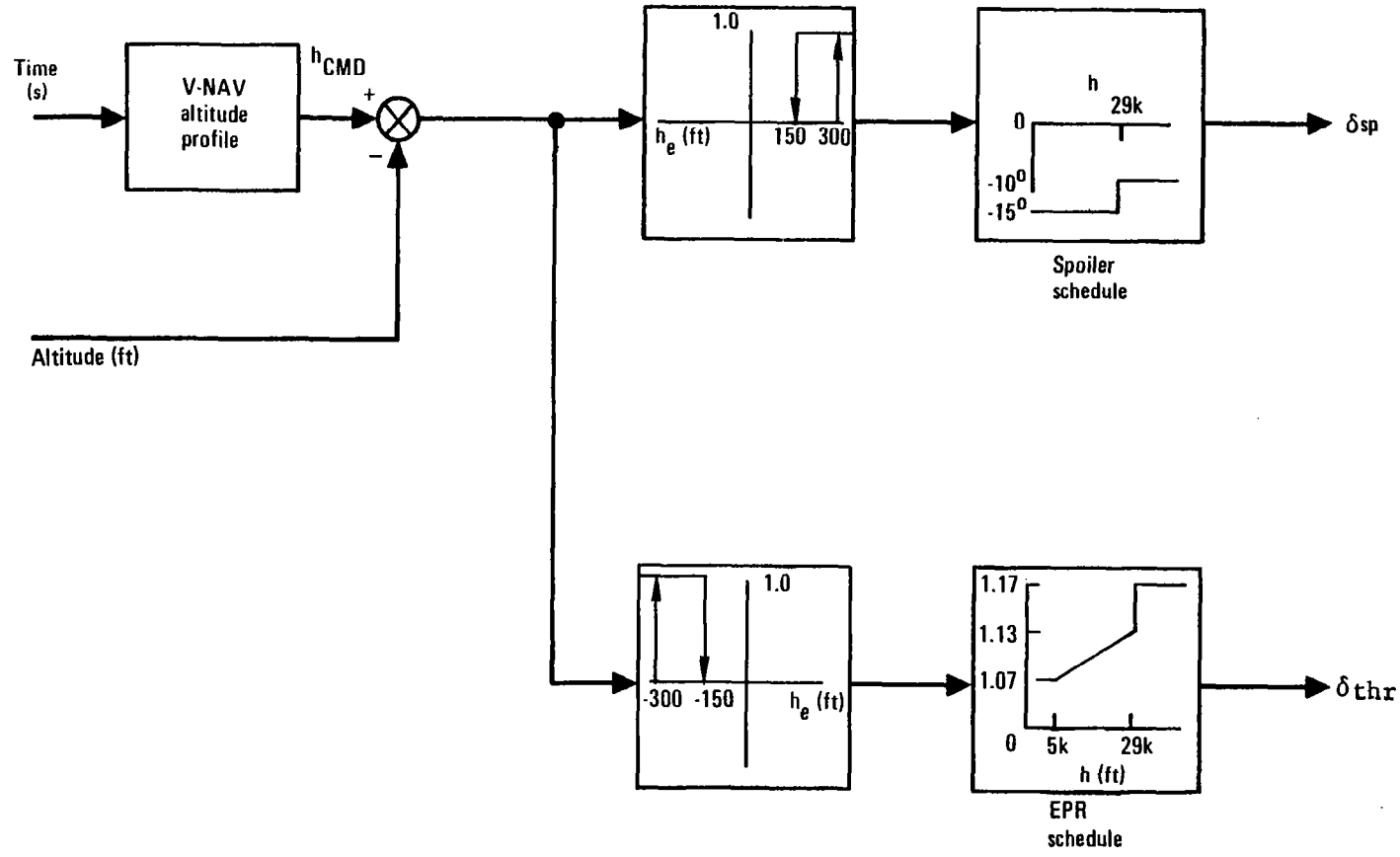

Figure 15. - Altitude error feedback.

1.4.1.2 Range error feedback. - The time control loop shown in figure 16 is switched in as the aircraft transitions from mach hold to airspeed hold in the descent, for a speed schedule of 0.82 mach/320 kts, this occurs nominally at 29000 ft. Control remains active to 10000 ft or until the aircraft captures E*D altitude, whichever comes first. Gains were chosen to allow the airspeed to vary slowly (0.2 kts/sec) between 280 and 360 kts (320 ±40 kts) during airspeed "hold" to make good the E*D arrival time requirement.

1.4.2 Descent simulation errors. - Several simulation runs were made to examine the performance of the altitude and range control strategies discussed above. The wind profiles shown in figure 12 were used to introduce unmodeled wind errors during descent; a three degree-of-freedom dynamic aircraft model was used to evaluate the effectiveness of the 4-D control laws. Table 3 tabulates the errors in time, range, and E*D altitude/speed resulting from these simulations. Time response plots are presented in Appendix C.

TABLE 3. - DESCENT SIMULATION ERRORS

Errors at End of Descent	4-D Control Off				4-D Control On			
	Time (s)	Altitude (ft)	IAS (kts)	Range (n.mi.)	Time (s)	Altitude (ft)	IAS (kts)	Range (n.mi.)
Palmdale Wind	–4.3	97.6	3.4	0.33	3.5	16.7	3.3	–0.36
Palmdale Wind + Head Wind	59.1	0	2.2	–4.2	22.0	11.9	3.4	–1.6
Palmdale Wind + Tail Wind	–64.3	1000	11.3	5.4	–15.7	141	5.2	1.3

Note: Time, altitude, and IAS errors were measured when the aircraft position was at the metering fix.
Range error was measured at the required-time-of-arrival at the metering fix.

1.5 FMS Software Development

The actual preparation of software incorporating the 4-D descent capability into the L-1011 Flight Management System was funded internally by Lockheed because of the proprietary nature of the existing FMS algorithms and control laws. This report therefore contains no detailed software coding or other related information in order to protect the rights of Lockheed and ARMA, Division of AMBAC, the system's manufacturer. The software developmental approach is discussed, however.

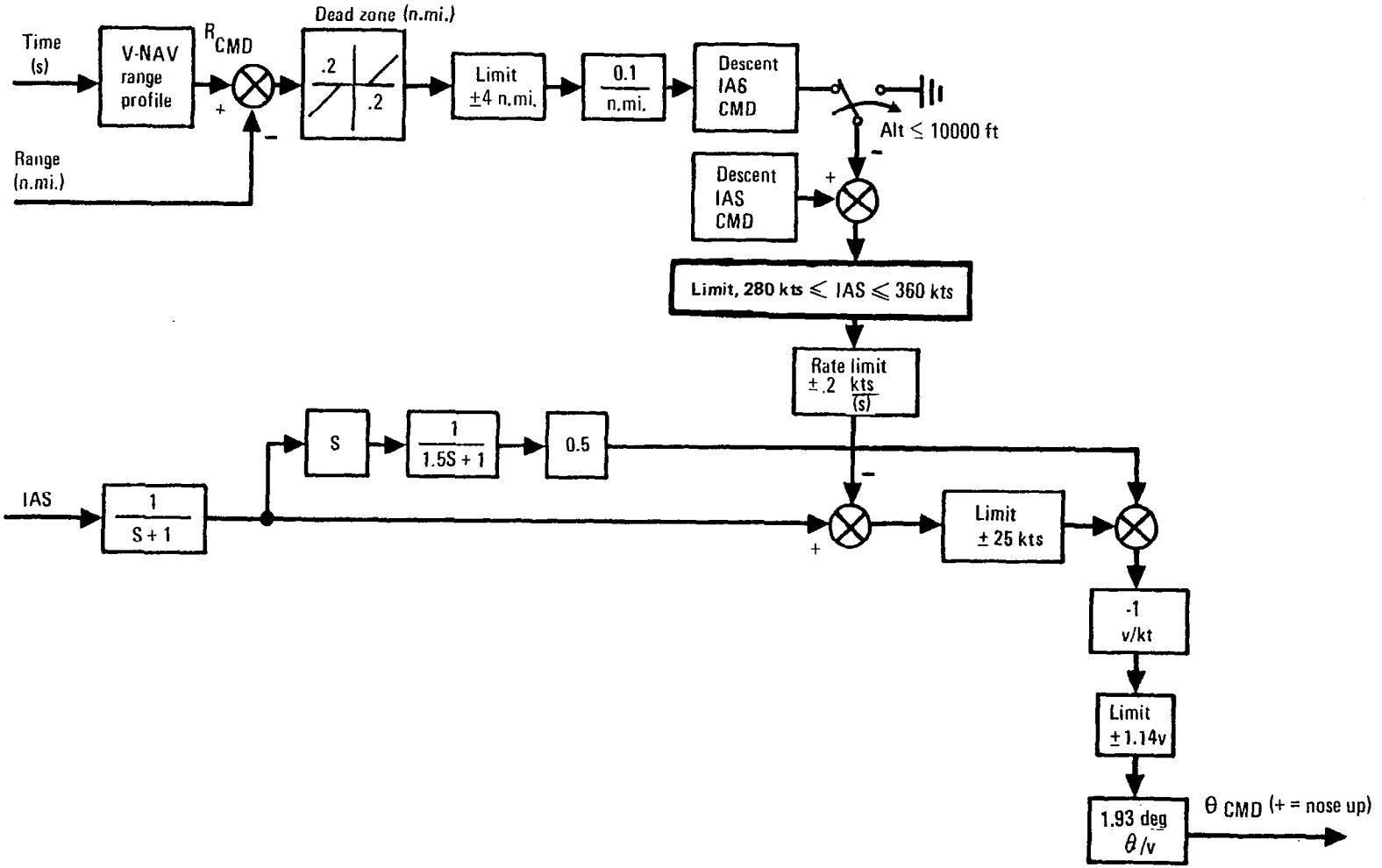

Figure 16. - Range error feedback.

1.5.1 Computer organization. - The L-1011 Flight Management System computer used for this work was an ARMA model 1808 with 32K words (18 bit/word) of core memory; the CPU has 56 different instructions. The functional characteristics of the ARMA 1808 are:

- .909 MHz clock rate
- 700 μsec memory access time
- fixed point 2's complement arithmetic
- execution time: 6.6 μsec add/subtract
  26.4 μsec multiply/divide
- programming registers: 1 upper accumulator (A)
  1 lower accumulator (B)
  3 index (X1, X2, X3)
  1 program counter
- address modes: direct
  indirect
  indexed
- A/D and D/A conversion
- Synchro I/O
- A/C DC I/O
- VOR/DME auto tune
- Discrete I/O
- CDU keyboard interface
- Serial digital I/O channels
- Direct memory access (up to 151,000 words/sec)
- Priority interrupt
- 4.5 msec real time counter

1.5.2 Emulator development. - The 4-D descent software was written as machine language patch code to the basic Saudia Airlines FMS operational program assembly. Coding relating to the FMS engine-out mode was removed and the 4-D patch code was developed in this section of core, thereby preserving the rest of the FMS functional capability.

A FORTRAN IV emulation, reproducing the instruction set of the ARMA 1808 on a bit-by-bit basis, was prepared and used for the initial development of the 4-D software code. In this way, code could be written in the same format required by the airborne computer and tested statically in an interactive environment. The code could be stepped through, one instruction at a time, or the program executed with various check points in the flow; the results of any operation could be displayed in engineering units rather than fixed-point binary, and logic and branching processes easily reviewed.

1.5.3 Data bank preparation. - The Flight Management System data bank is a section of memory in the computer which is reserved for storing necessary information primarily related to the navigation function of the system. Examples of information stored in the data bank include:

- waypoint names and locations
- VORTAC data
- route structures

Data for the Dallas/Ft. Worth area were collected, and a punched computer tape made in preparation for the demonstration flights that were performed on 01 August, 1979. Appendix D presents this information in detail.

1.5.4 Hot mock-up checkout. - After the software changes to the operational program had been checked out on the emulator and the data bank information prepared, the machine code patches were transferred to the airborne computer and system level testing conducted on the Palmdale Hot Mock-up facility; this facility allows the airborne system and its interface to be exercised in a dynamic simulation of the aircraft. In this way, the total FMS software package and its interaction with the 4-D patch code was evaluated prior to installation and flight testing in the Lockheed L-1011 test aircraft.

The overall process of software development is illustrated in figure 17.

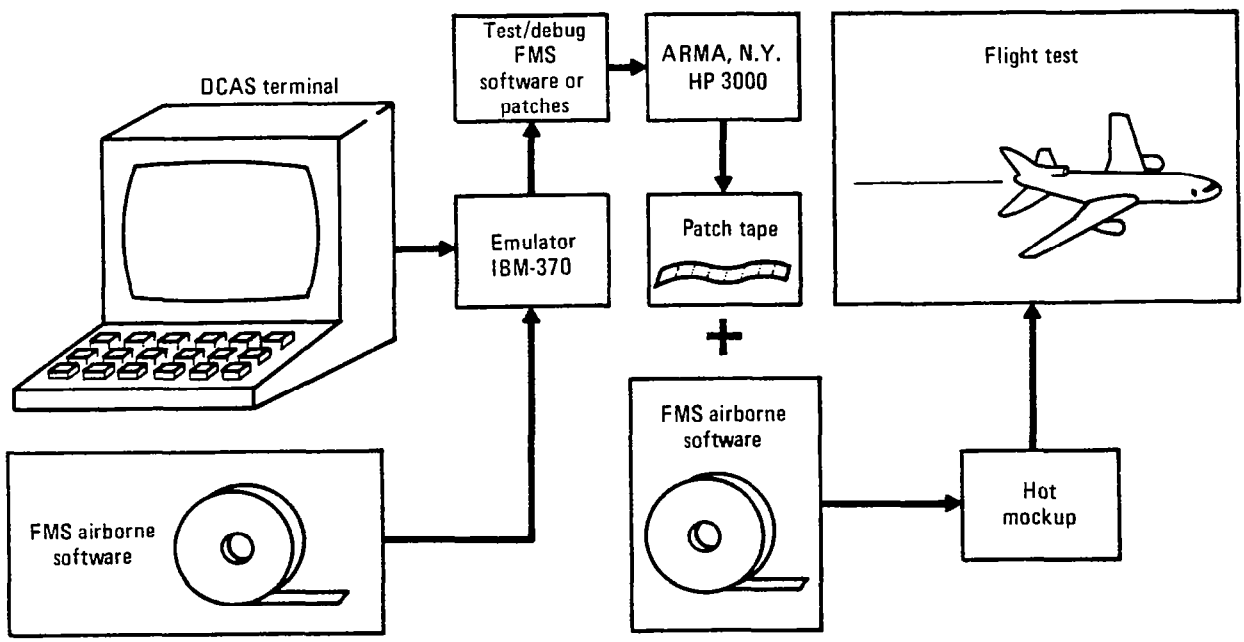

Figure 17. - Software development.

2.0 FLIGHT TESTING

Flight testing of the new 4-D descent capability was conducted on L-1011 S/N 1001, shown in figure 18. A total of eleven descents were performed - eight in the local area around the Flight Test Center at Palmdale, California and off the Pacific coast, and three in the arrival air space of the Dallas/ Ft. Worth Regional Airport (DFW). Approximately sixteen flight hours were used in the flight test evaluation of the 4-D descent.

2.1 Local Area Flight Testing

The flight test effort began on June 25, 1979, with two straight-in descents performed between 31000 and 11000 ft to minimize any possible errors that might be introduced by turns in the descent and by extended operation in the mach-hold region.

Two more straight-in descents were performed on the 26th and the 29th - the first between 37000 and 11000 ft to test the exposure to uncontrolled flight in the mach region, the second between 31000 and 9000 ft to test the exposure to uncontrolled flight at altitudes below to 10000 ft.

Four descents took place on July 30 in final preparation for the Dallas demonstration flights. The descents were conducted off the Pacific coast over an altitude range and a course which simulated the approach geometry of the Acton Standard Terminal Arrival Route (STAR) at DFW.

2.2 Dallas/Ft Worth Demonstration Flights

The last three descents in the flight test program were performed as part of a demonstration flight into DFW on August 1, 1979. Figure 19 shows the flow of air traffic to DFW for final approach and landing to the south. Four "corner post" VORTACS are used as the metering fix gateways defining the approximate boundaries between the Ft. Worth Center and Dallas approach control. All three descents were performed from the southwest, via the Acton Six STAR. The waypoint Flato was chosen as E*D with an altitude and speed requirement of 11000 ft and 250 kts.

Figure 20 illustrates the westerly approach (Wink transition) to the Acton STAR that was flown for the first demonstration. For this first descent, B*D was calculated to lie between Tuscola and Gramy at a point along the flight plan 92.4 n.mi. before Flato. Although not a primary objective of the demonstration, Wink, Texas, was overflown within 30 seconds of the time requested by Ft. Worth Center prior to the aircraft's departure from Palmdale, California.

The L-1011 FMS had no capability for performing controlled (closed loop) 4-D cruise flight, however, full use was made of the system's preflight planning capability to achieve a very credible approximation to 4-D flight

Figure 18. - Lockheed Advanced TriStar, L-1011 S/N 1001

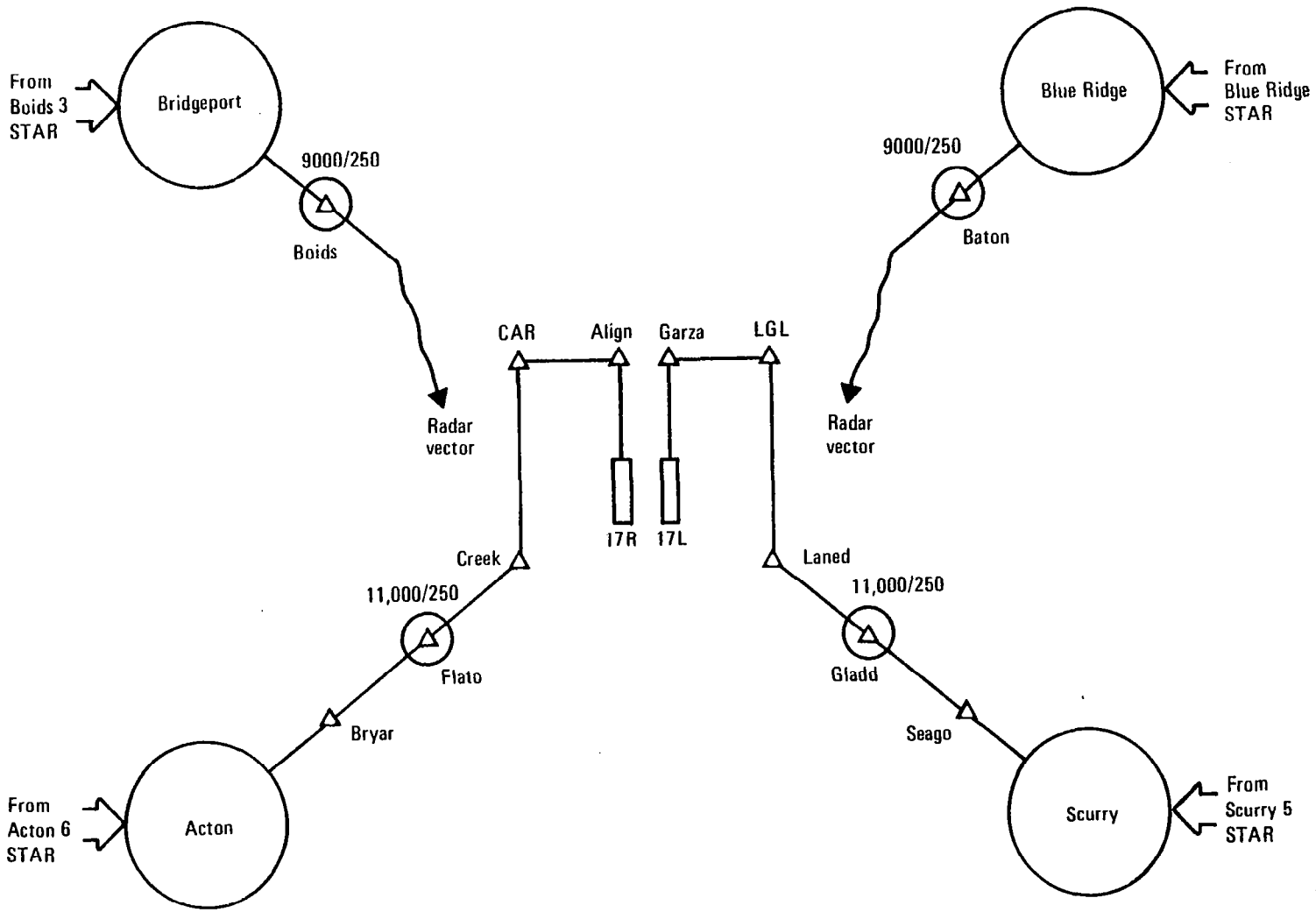

Figure 19. - Dallas/Ft. Worth south flow.

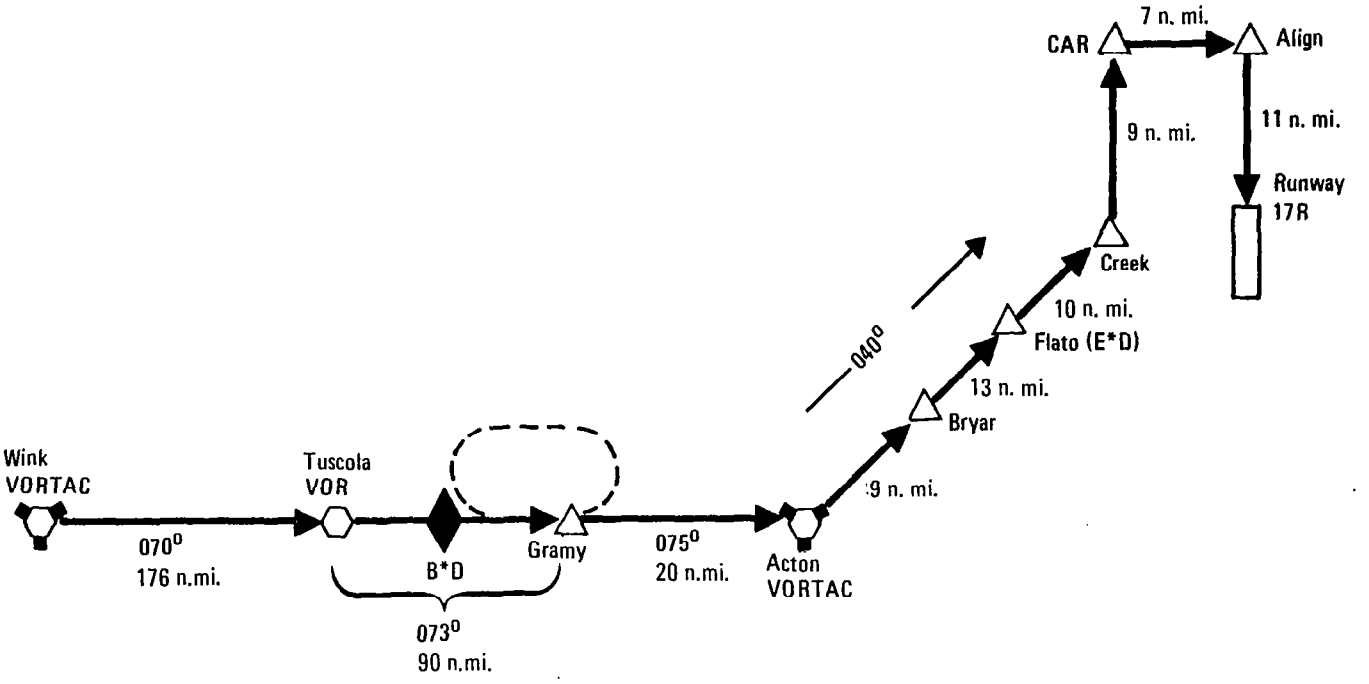

Figure 20. - Acton arrival Wink transition.

management. Prior to takeoff at Palmdale, Lockheed Jet Plan wind and temperature data were entered into the FMS for the cruise portion of flight to obtain an accurate projection of time enroute to Wink. The take-off time was then backcomputed to meet the 13:00 Wink arrival time requirement. The L-1011 took off at this time, 09:17 local, and flew to Wink under automatic FMS control.

Figure 21 is a schematic representation of the demonstration flight scenario. The first high profile descent, using the inertial navigation system as a reference, was performed at the end of the flight which originated in Palmdale, California. The aircraft, still under automatic control, coupled to the ILS for final approach and landing. After landing, observers from NASA, FAA, and the airlines were boarded for two more descent demonstrations. An inertial/radio mix was used for these descents for improved accuracy. After the third descent, the aircraft again made a fully automatic approach and landing. The day after the flight, a debriefing workshop was held in which representatives from NASA, the FAA, Delta Airlines, and Lockheed discussed the results of the demonstrations.

Table 4 lists in detail the initial conditions for each of the eleven descents, performed in the course of the flight test effort.

TABLE 4. - FLIGHT TEST INITIAL CONDITIONS

Descent	Date	Altitude B*D/E*D (kft)	Wind at B*D (kts)	Gross Weight (kg)	SAT (°C)	Descent range (n.mi.)	Descent Time (s)	Nav mode	NCU S/N
1	6/25/79	31/11	46 HW	138 300	-37	68.7	568	INERTIAL/ RADIO	251
2	6/25/79	31/11	38 TW	126 300	-39	74.6	571		
3	6/26/79	37/11	56 TW	136 000	-54	98.1	761		
4	6/29/79	31/9	33 TW	143 800	-38	85.7	731	INERTIAL	
5	7/30/79	31/11	19 HW	173 275	-32	81.5	633		2103
6	7/30/79	31/11	26 HW	160 800	-32	76.5	604		
7	7/30/79	31/11	31 HW	150 595	-32	73.4	581		
8	7/30/79	31/11	24 HW	133 980	-32	71.5	554		
9	8/1/79	33/11	27 TW	171 000	-36	92.4	693	INERTIAL/ RADIO	
10	8/1/79	33/11	28 TW	161 000	-36	88.1	686		
11	8/1/79	33/11	29 TW	150 000	-36	87.0	658		

Note: Speed schedule for all descents – 0.820/320/250

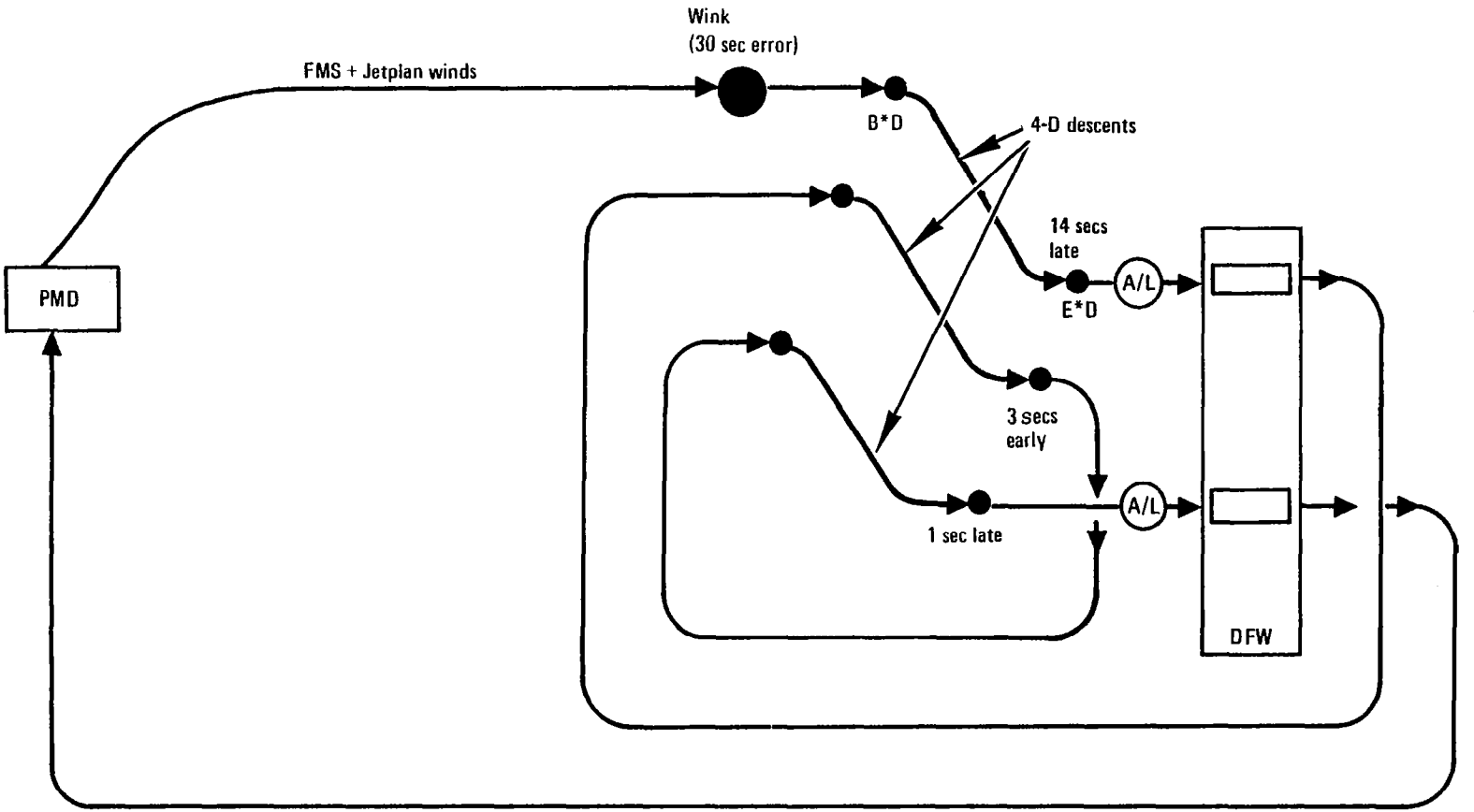

Figure 21. - Dallas/Ft. Worth scenario.

2.3 Flight Test Results

As shown in Table 5 the most important flight test goals, arrival time, airspeed, position, and altitude accuracies, were mainly achieved; arrival time accuracy is of greatest interest in a 4-D experiment. It was an objective to arrive at the end-of-descent point within ±30 seconds of the predicted time; this goal was achieved with a 2σ error of 19 seconds about a mean of -2 seconds. Figure 22 is a histogram of all eleven descents reflecting the even distribution of E*D errors based on the last estimate made by the FMS computer before descent. The values in Table 5 were obtained from nine of the eleven descents; two were eliminated because of test procedure problems. The position and altitude errors of Table 5 are also within the pre-established test goals. Airspeed error was high, i.e., within ±15 kts instead of ±5. This amount of error is not substantial and will be reduced with system improvements discussed in paragraph 2.5.

The terminal errors observed at E*D for each of the eleven descents are presented in table 6. Time errors presented under the column heading "Initial Estimate" were computed by the FMS in cruise, prior to B*D, as described in paragraph 1.2.3. The arrival time estimate for E*D given in this column would vary with changing winds. There was concern therefore that the predicted time of arrival given to ATC by the crew about 5 minutes before descent might not be accurate, however, this concern was unfounded. Mean and 2σ values in table 7 for the initial and final estimates agree within one second.

The method used to measure terminal errors at the end-of-descent was to analyze recorded time, altitude, and airspeed for the interval when E*D was overflown. System position error was not measured against a ground-based reference for the first four descents. DME range was used as a position reference for descents five through eight; approach control radar data provided the position reference for the last three descents, which were performed at Dallas.

The pre-selected E*D altitude is captured by the autopilot prior to E*D as the aircraft begins to decelerate to the required final speed; altitude errors at E*D are therefore determined by the accuracy of the autopilot's altitude hold mode and are typically less than ±50 feet. E*D speed is controlled by the autothrottle system using commands from the FMS. Unfortunately, a wiring problem which caused the autothrottle to disconnect at E*D altitude capture, existed on the aircraft during the period the first eight descents were performed; as a result, the autothrottle could not automatically capture and hold the required speed of 250 kts at E*D. The problem was corrected, however, in time for the last three descents performed at Dallas.

Two descents were degraded by procedural problems. The third descent, performed on June 26, 1979, was initiated over the Pacific Ocean at a large distance from the VORTAC station being used as a navigation reference. As the descent progressed toward the mainland, radio position updating caused the position of the descending aircraft to change and the spatial path of the

TABLE 5. - FLIGHT TEST RESULTS

Error		4-D Test Goals	Summary (9 Descents)
End of Descent Arrival Time	Mean	Not specified	2s Early
	2 σ	<30 s	19s
Airspeed		±5 kts	±15 kts
Position		±1 n.mi.	±0.2 n.mi.
Altitude		±150 ft	±50 ft

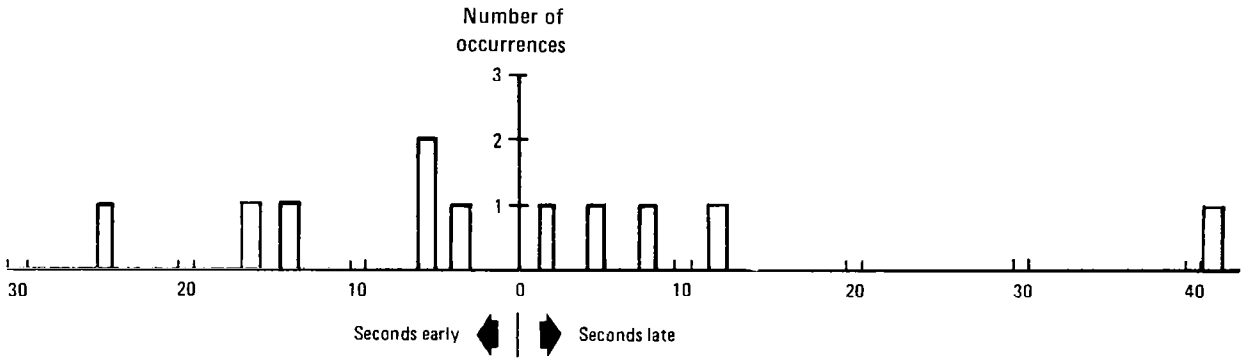

Figure 22. - E*D time error histogram (final estimate).

descent to move towards the updated E*D position. It is estimated that 20 of the 25 seconds of time error observed could be attributed to this cause. The largest time error recorded during the flight test program occurred on July 30,1979, during the eighth descent. Data analysis indicates that incorrect data were entered into the system prior to descent. Aircraft weight was manually input to the computer as an expedient during this test program; it is planned to use an automatic weight computation for future 4-D testing as is the practice on production FMS systems.

Figure 23 depicts the aircraft ground track for the first two descents into the Dallas terminal area on August 1,1979, as recorded by approach control radar. The first descent was performed using an inertial system as

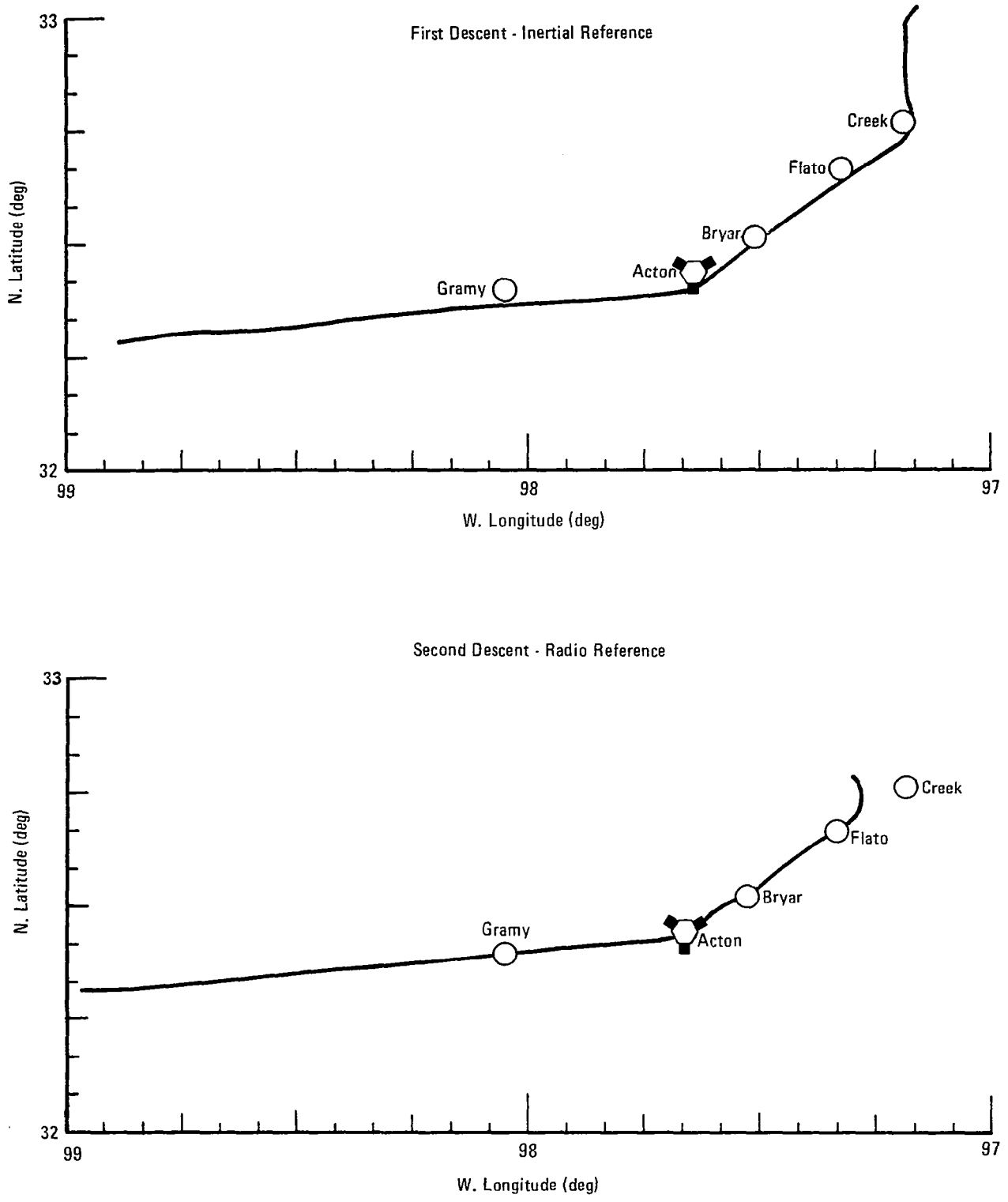

Figure 23. - Comparison of navigation with inertial and radio references.

TABLE 6. - FLIGHT TEST TERMINAL ERRORS AT E*D

Descent	Time (Initial Estimate) (s)	Time (Final estimate) (s)	Altitude (ft)	Speed (kts)	Position	
					Ref	Error (n.mi.)
1	No estimate made	4 Early	±50	60 Fast (A)	RNAV	Not measured
2	↓	8 Late	↓	0	↓	↓
3		25 Early (B)		0		
4		14 Early		0		
5	3 Early	2 Late		45 Fast	DME	<2
6	13 Early	16 Early		50 Fast	↓	↓
7	3 Early	6 Early		20 Fast		
8	66 Late (C)	41 Late (C)		0		
9	14 Late	12 Late		10 Fast	RADAR	2.5
10	3 Early	6 Early		15 Fast	↓	<0.2
11	1 Late	5 Late	↓	8 Fast	↓	<0.2

Notes:

(A) Autothrottle did not automatically capture and hold 250 kts at E * D for descents 1 through 8

(B) Most of this error caused byradio position updating during descent

(C) Caused by incorrect input data to the system.

TABLE 7. - ARRIVAL TIME ERROR COMPARISON

	Initial Estimate Error (6 Descents)	Final Estimate Error (9 Descents)
Mean	1s Early	2s Early
2σ	18s	19s

the navigation reference; radar data shows the aircraft's position to have a southerly error of 2.5 n.mi. The inertial system had not been updated since its preflight check nearly three hours before the end of descent. The second and third descents of the day were performed using radio reference navigation for improved accuracy; radar data shows the errors observed during these descents to be less than 0.2 n.mi.

2.3.1 Wind modeling. - On two sets of flights, wind profile data were collected for several descents performed over the same course. Figure 24 shows wind profile data for the 7/30/79 tests in which four descents were made off the California coast starting at Saint Nicholas Island and ending over the Catalina Channel. The aircraft encountered descent headwinds which varied little in the 5 hours 29 minutes between the first and last descents. Figure 25 illustrates data from the three descents performed 8/1/79 on the Acton STAR to DFW. These winds were predominately tailwinds and are seen to be less correlated than those of figure 24; the diminished correlation was caused by frontal activity and weather cells in the vicinity of the approach path. These two sets of data afforded an opportunity to compare the system linear wind model with a segmented model. (the linear model was the one used for the flight test experiments as described in paragraph 1.3.2). The segmented model is one in which actual wind measurements made at three thousand foot altitude increments are connected by straight line segments which could then be used as a model for subsequent descents. These measurements could be collected at an airport from meterological instruments or from descending aircraft and radio-linked up as segments to other approaching aircraft.

Figure 26 shows a segment fit to the winds encountered during the first descent on 7/30/79, similarly, figure 27 shows the segment fit to the first descent of 8/1/79. These segments were then plotted against the actual winds encountered during the last descent of each day.

These plots were reconstructed with wind velocity on the ordinate and time on the abscissa as the right hand graphs of figures 28 and 29, also shown on figures 28 and 29, in the left hand graphs, are the linear models programmed for the last descent of each day superimposed on the actual wind profiles. (Note that the linear models have breaks to accommodate the course change made during the descents.) The areas between the curves on each graph were integrated to obtain a measure of the trajectory error, expressed in nautical miles, that would accrue during these descents for the respective models; these errors are summarized in table 8.

As expected for the well-correlated 7/30/79 data, the segmented model has less absolute error than the linear model (0.16 n.mi. and 1.13 n.mi. respectively). For the descents performed on 8/1/79, the segmented model did not improve matters, in fact its error was worse (-1.9 n.mi. compared to -0.13 n.mi.). These two data sets are not meant to provide quantitative guidelines for a phenomena that is best described by statistical means; they do, however, suggest some possibilities for future research. The persistence of wind velocity profiles in unstable weather conditions is such an area.

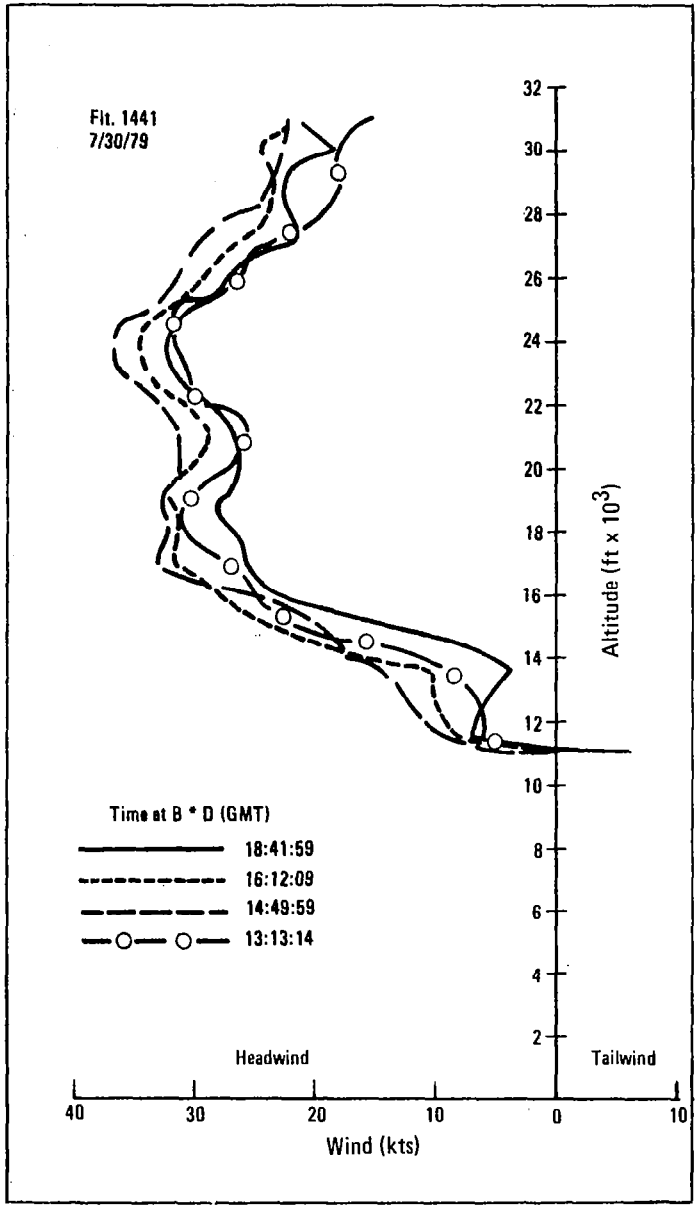

Figure 24. - Wind persistence, 7/30/79.

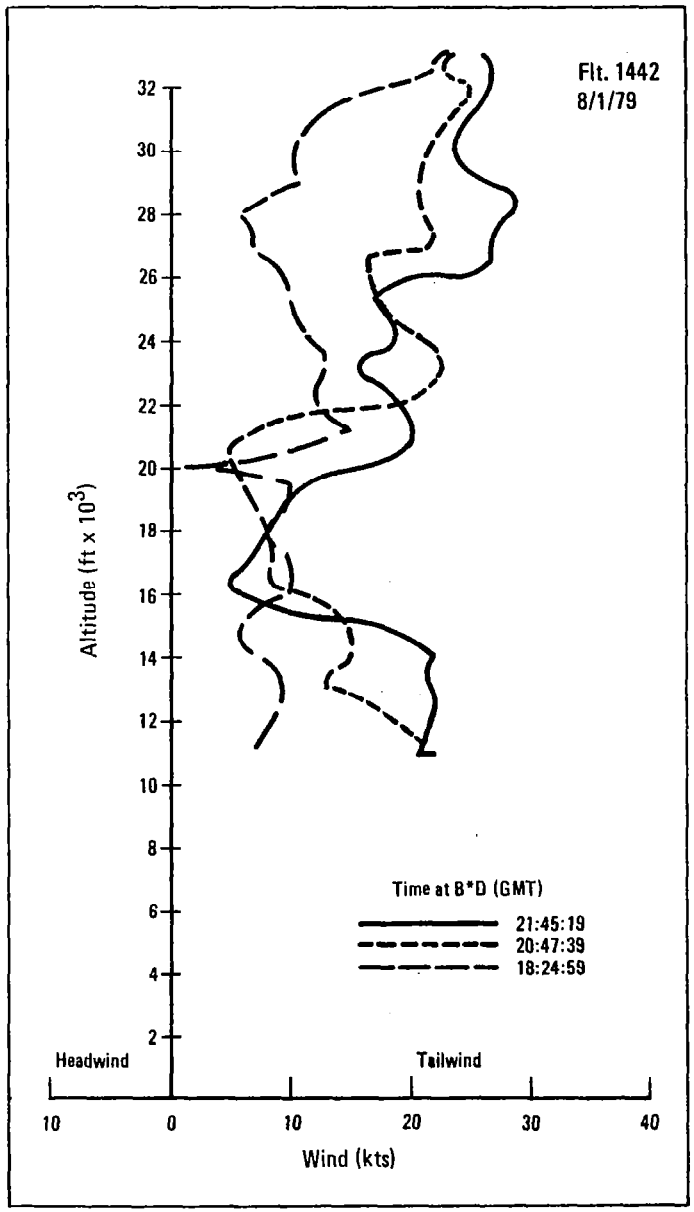

Figure 25. - Wind persistence, 8/1/79.

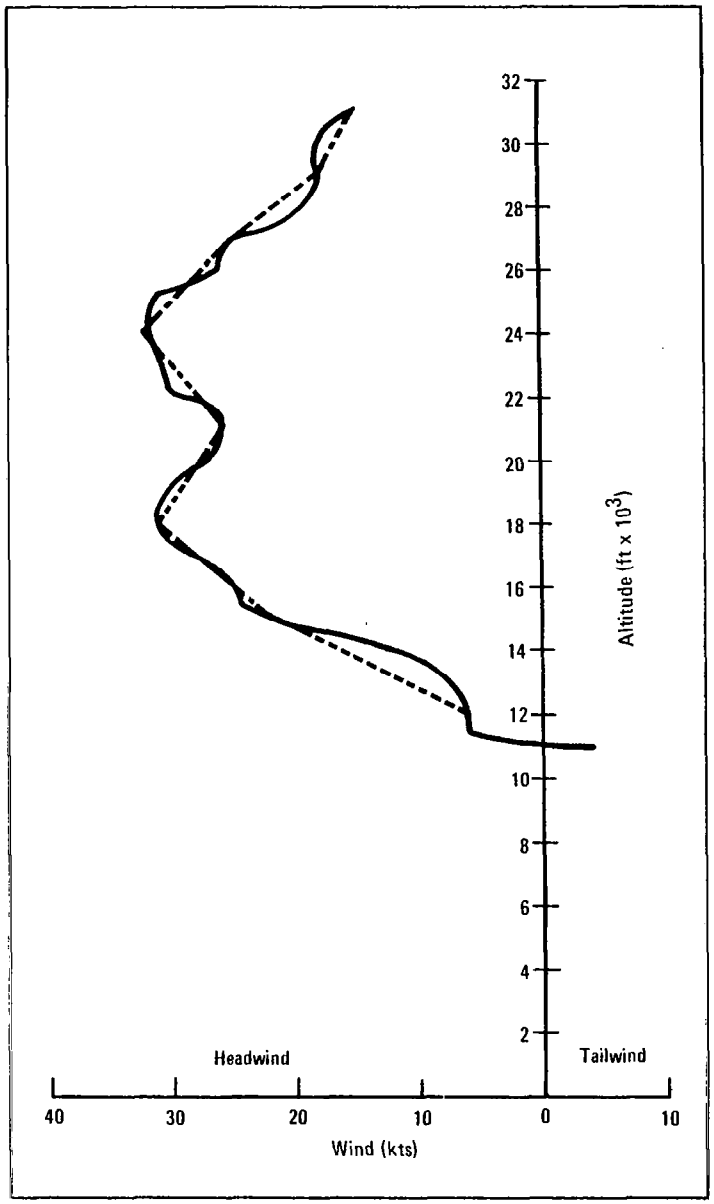

Figure 26. - Segment fit to 7/30/79 wind profile, first descent.

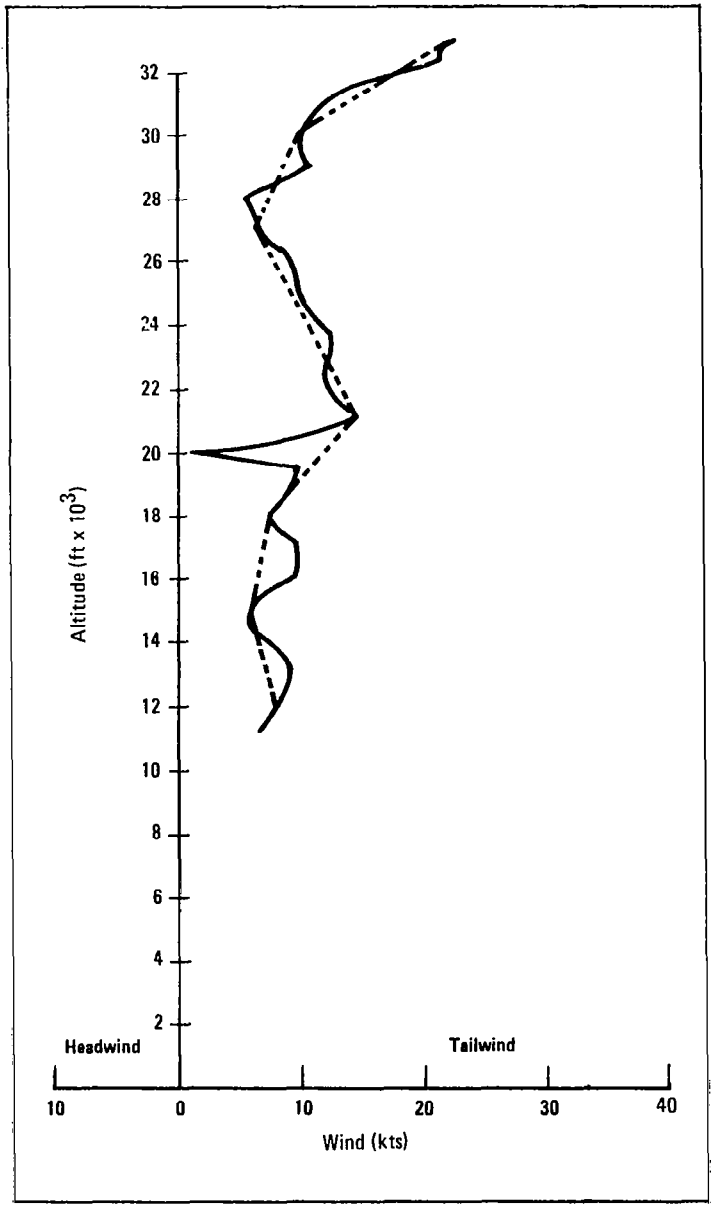

Figure 27. - Segment fit to 8/1/79 wind profile, first descent.

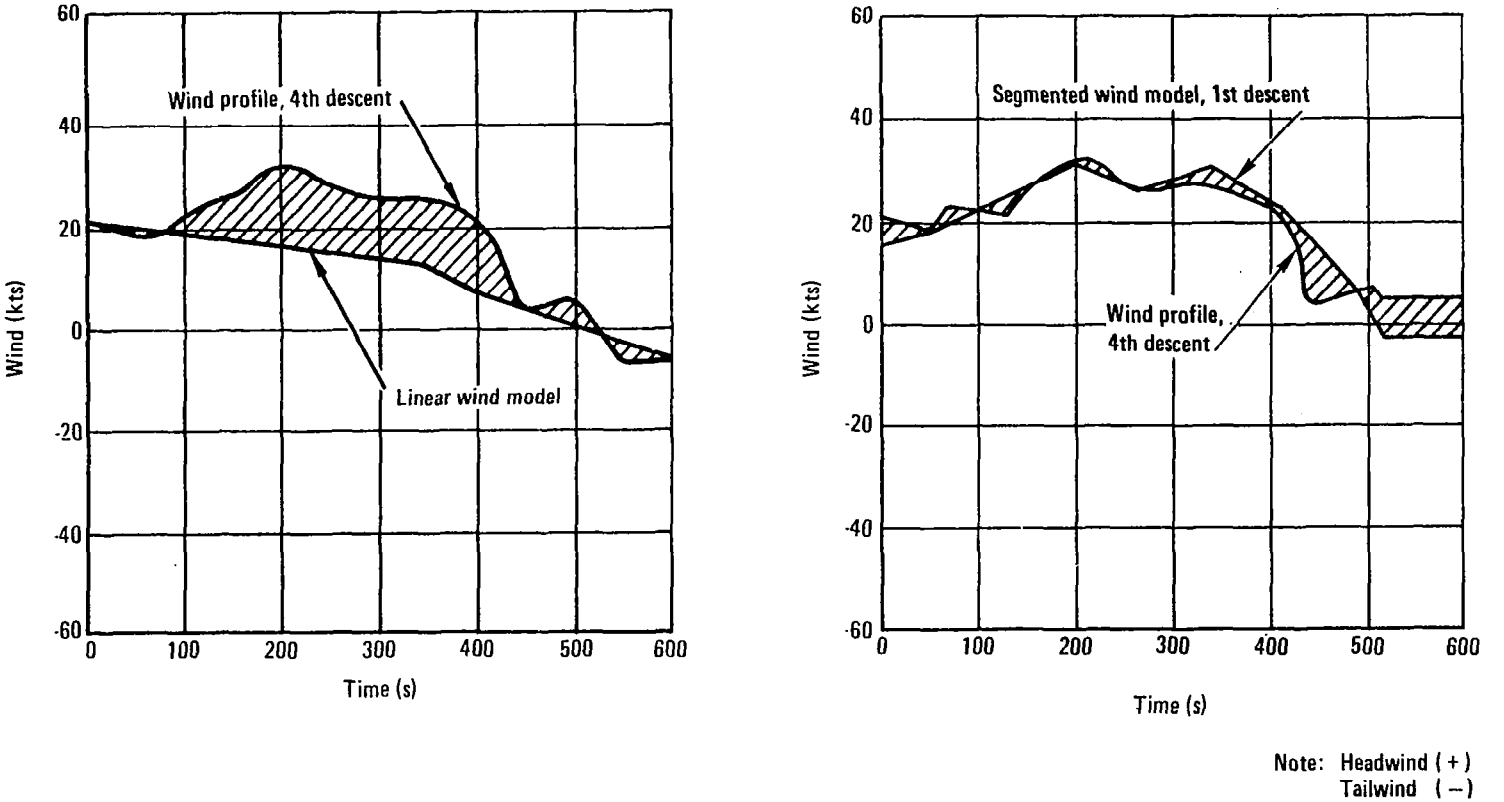

Figure 28. - Comparison of linear and segmented wind models, 7/30/79 flight tests, L-1011, S/N1001.

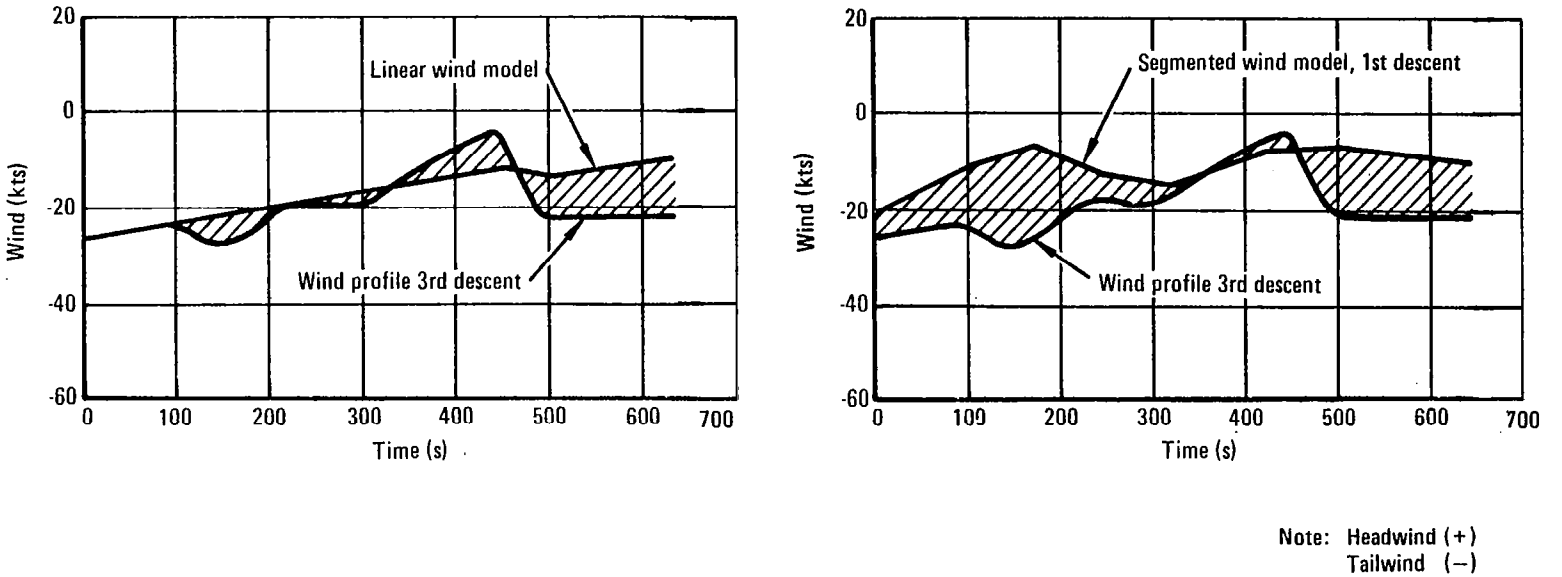

Figure 29. - Comparison of linear and segmented wind models, 8/1/79 flight tests, L-1011 S/N1001.

TABLE 8. - WIND MODEL ERROR

Flight test date	7/30/79	8/1/79
Linear model	1.13 n.mi.	−.13 n.mi.
Segmented model	.16 n.mi.	−1.9 n.mi.
Age of segmented model	5 hrs, 29 min	3 hrs, 20 min
−Denotes tail wind error + Denotes head wind error		

Wind persistence in stable conditions has been researched and it has been shown to be quite good for periods up to six hours. (See reference 5.) The 7/30/79 data in figure 24 are consistent with this finding.

2.3.2 Effects of wind modeling errors on 4-D descent. - Unmodeled wind errors are corrected by aircraft speed changes. The amount of speed change possible varies widely as a function of the descent speed schedule flown. Changes in E*D arrival time are also effected by varying the descent speed. A practical 4-D descent system must have the flexibility to vary its E*D arrival time somewhat to properly interface with the ground controller. This flexibility to vary arrival time without a change in flight path is eroded by unmodeled wind errors. The 4-D systems of the future therefore will require accurate wind models that will not cause a serious degradation of arrival time flexibility.

2.4 Air Traffic Control Integration

The development of 4-D techniques must be pursued with the goal of eventually integrating them into the national air traffic control system. Based on the results of this study and the NASA TCV flight tests at Denver, it appears as if that goal is possible without major changes in ATC methods. (See references 6, 7, and 8.) DFW and Denver both make use of automated time-based metering, a method of local flow control that will be extended to other busy airports in the next few years. The integration of 4-D will be discussed from the standpoint of interfacing with such an automated metering system.

2.4.1 Metering and spacing. - Time-based metering uses computer-aided techniques to control the flow of aircraft into the terminal area at a rate that does not exceed the acceptance rate of the airport. Metering is the responsibility of the Air Route Traffic Control Center (ARTCC). As shown in figure 30, spacing of aircraft in the vicinity of the airport is the responsibility of Terminal Radar Approach Control (or TRACON). The metering program computes the arrival time of all aircraft approach the airport when they are about 25 minutes away. Arriving aircraft and their associated arrival times are then displayed on a CRT scope in their order of arrival for the ATC flow controller to determine if the rate of arrival will exceed the acceptance rate of the airport, if so, the arrival times are then delayed to match the current rate of acceptance. The various sector controllers are each given the metering fix arrival times assigned by the flow controller; they then radio speed or path changes to incoming aircraft to meet the assigned times for the aircrafts in their respective sectors.

An aircraft with 4-D flight management capability can fit neatly into this system. To do so it is necessary for the ground controller to radio the assigned metering fix time to the aircraft so that the 4-D descent can be programmed to cross the metering fix at exactly that time. This can be done now without any change in the metering program. The FMS computation would have to have sufficient flexibility to handle an assigned time that may not correspond exactly with the aircraft's ETA at the metering fix. At least thirty seconds of flexibility would be required to accommodate the fact that the metering fix times are given in integral minutes. Additional flexibility will be necessary to accommodate delays caused by weather or traffic peaks.

Substantial reductions in ground controller workload are possible with 4-D techniques; additionally, 4-D can do the job better. A controller can bring aircraft to the metering fix within one to two minutes of the assigned time whereas the 4-D equipped aircraft can get there within seconds of the assigned metering fix time.

Extending 4-D back to takeoff has the potential of greatly reducing congestion. As was demonstrated in the DFW flight test, the L-1011 flew over Wink, Texas, within 30 seconds of the time assigned by ATC before takeoff. Often the same scheduled flights are delayed at the same time every day when approaching busy hub airports. If all scheduled aircraft were assigned arrival times and used 4-D now, it is apparent that the delays which occur at peak periods could be reduced or eliminated because there wouldn't be bunching up at the metering fixes.

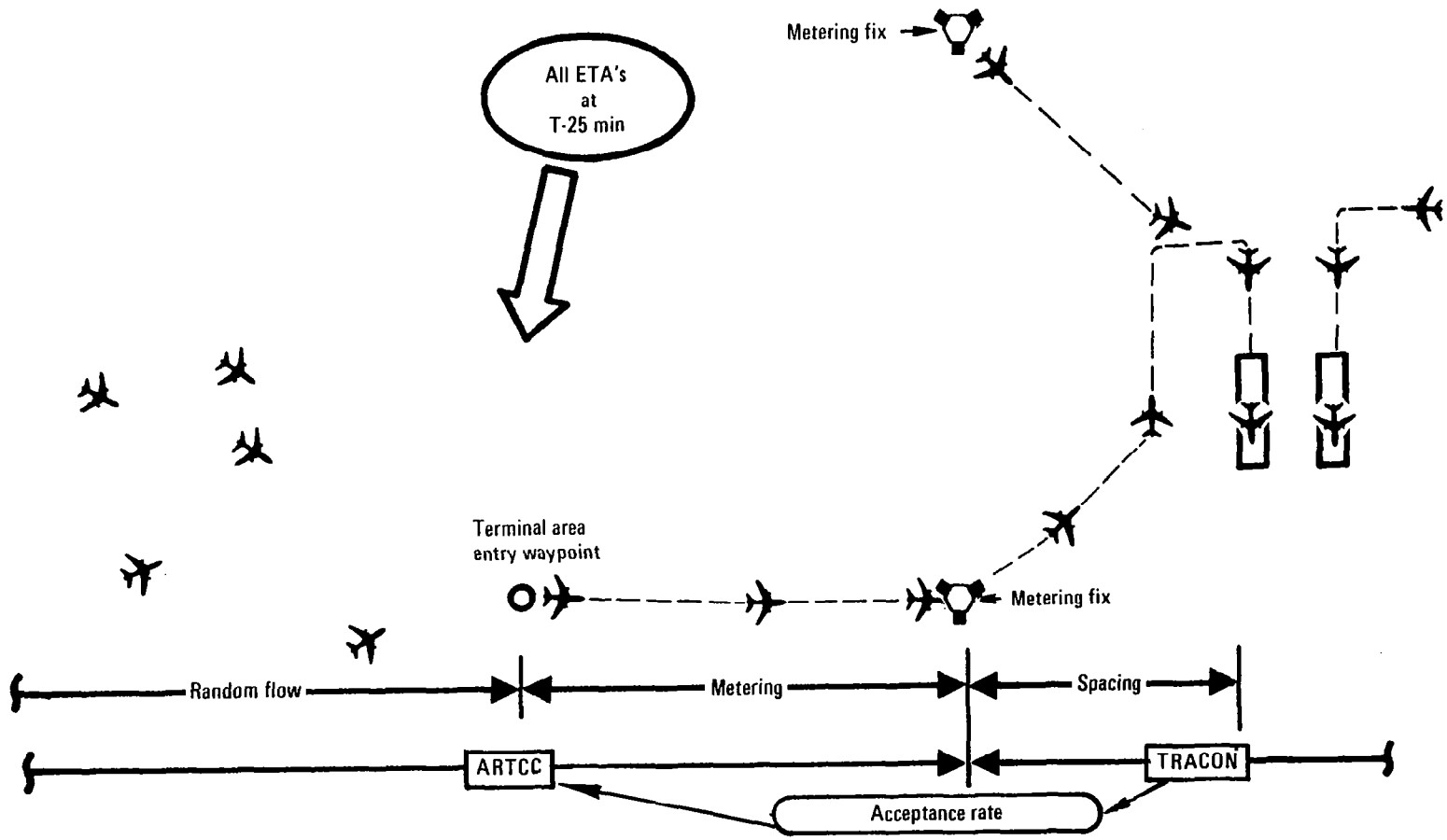

Figure 30. - Metering and spacing.

The FAA is already using the Fuel Advisory Delay System wherein aircraft scheduled into a busy airport, such as O'Hare Airport in Chicago are advised to delay takeoff if their normal arrival occurs at a time when the airport acceptance rate is projected to be exceeded. Total 4-D flight planning would integrate well with this system also.

Four-D nav must be flexible with regard to arrival time. It is envisioned, that during a flight the crew would receive periodic updates of the assigned metering fix time. When updated, the aircraft computer would determine the best speed and altitude for the remainder of the flight to achieve the assigned time in a reasonably fuel efficient fashion. It is recommended that subsequent R&D develop total 4-D flight, with arrival time flexibility.

The experience of this test program also highlighted the need for a very close collaborative effort with ATC personnel to plan and conduct meaningful flight test programs and to develop 4-D techniques that integrate well with the ground control function.

2.5 Future 4-D Flight Management

The results of the current study can be improved upon with relatively simple system improvements. These would include:

1) Exact aerodynamic/propulsion modeling
2) Use of RNAV with either radio or radio-inertial position reference
3) Completely automatic altitude control
4) Improved vertical damping

These features will reduce the 2σ arrival error dispersion from 19 seconds to an estimated 8 seconds. Research by Menga and Erzberger (reference 9) has shown that arrival errors of this order are possible.

The use of direct lift control is another way of maintaining altitude control without unduly cycling the engines. It is recommended that subsequent research include these fixes in a fuel efficient, flexible 4-D flight management approach that combines climb, cruise, and descent from altitude to the runway threshold.

3.0 CONCLUSIONS AND RECOMMENDATIONS

3.1 Conclusions

The following are conclusions reached as a result of the activities performed during this program:

- The L-1011 demonstrated the capability of executing a 4-D descent and achieving 2σ end-of-descent accuracies of 19 seconds with a 2 second early mean.

- It is estimated that the dispersion can be reduced to 8 seconds with a mean of zero seconds utilizing improvements in wind modeling, aero-engine modeling, automation of the altitude feedback loop, and improved procedures.

- It is also estimated that altitude error at the end of a 4-D descent could be less than 50 feet, airspeed error less than 5 kts, and position error less than 0.5 n.mi.

- The 4-D system arrival times should be made flexible so that the end-of-descent arrival time can be made to match the ATC assigned metering fix time.

- The 4-D descent appears to decrease air traffic controller workload.

- Wind modeling should be improved so that arrival time flexibility is not severely restricted.

- A segmented wind model based on actual wind measurements appears to offer an improvement over the linear model for stable weather conditions.

- Unstable weather conditions sharply decrease the persistence of wind velocity profiles.

3.2 Recommendations

The following items are recommended for additional research and development to further the state-of-the-art of 4-D descents:

- A flexible 4-D descent control law should be designed and flight tested to improve ATC integration.

- The 4-D capability should be extended back through departure, and arrival time flexibility worked back as early in the flight as possible.

- Future L-1011 testing should include fully automatic altitude control that makes use of both altitude error and vertical velocity feedback.

- Wind modeling research should be directed toward providing improved segmented models.

- Further analysis should be performed on wind persistence data relating to unstable weather conditions.

- An ongoing dialogue should be maintained with ATC, the airlines, and the system developers such as Lockheed and NASA, in order to ensure that the progress made satisfies real needs and fits into the ATC system.

APPENDIX A

TIME-IN-DESCENT ALGORITHMS

This appendix presents the derivation of algorithms describing the computation of incremental times required for each of the six segments of the L-1011 Flight Management System's 3-D descent profile. Total time-in-descent is then simply the sum of each of the six segments.

SYMBOL DEFINITIONS

H	Aircraft altitude	(ft)
H_c	Cruise altitude	(ft)
H_{E*D}	E*D altitude	(ft)
IAS	Indicated-Air-Speed	(kts)
K	3600	(sec/n.mi./kt)
K_c	Independent Time-Profile "Bending" factor (Set equal to 1.0)	
K_T	Temperature Correction Factor = (1 + .0043Δ Temp)	
R	Range	(n.mi.)
T	Time	(s)
V_T	True-Air-Speed	(kts)
V_W	Wind Velocity	(kts)
V_{W_C}	Wind Velocity at Cruise Altitude	(kts)
γ	Flight path angle	(deg)
θ	Desired track	(deg)
α	Wind bearing	(deg)

① E*D SEGMENT

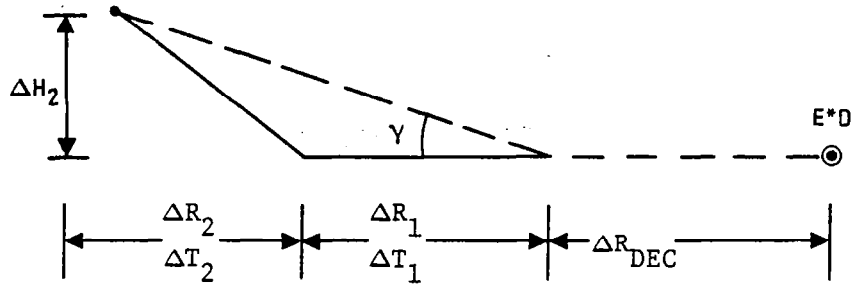

R_3	R_2	$R_1 = \Delta R_{DEC}$	$V_{T_{E*D}}$
H_3	H_2	$H_1 = H_{E*D}$	IAS_{E*D}
T_3	T_2	T_1	
IAS_3	IAS_2	IAS_1	
V_{T_3}	V_{T_2}	V_{T_1}	
V_{W_3}	V_{W_2}	V_{W_1}	

Level Decel to E*D IAS

If E*D IAS is equal to descent IAS, set $T_1 = 0$ and omit this step; otherwise, compute T_1 as follows:

$$T_1 = \left\{ \frac{K(R_1)}{1/2\left(V_{T_{E*D}} + V_{T_1} + 2\,V_{W_1}\right)} \right\} K_c$$

where:

$$V_{T_{E*D}} = K_T \left\{ \left(K_0 + K_1 H_1 + K_2 H_1^2\right) + \left(K_3 + K_4 H_1 + K_5 H_1^2\right) IAS_{E*D} \right\}$$

$$V_{T_1} = K_T \left\{ \left(K_0 + K_1 H_1 + K_2 H_1^2\right) + \left(K_3 + K_4 H_1 + K_5 H_1^2\right) IAS_1 \right\}$$

} See Table A-1 for value of constants

$K = 3600$ sec/n.mi./kt

$K_T = 1 + .0043 \ \Delta \text{ TEMP}$

$K_c = 1.0$

$$IAS_1 = IAS_3 - \frac{(R_3 - R_1)}{R_3} \left(IAS_3 - IAS_{E*D}\right)$$

IAS_3 = Descent IAS

$$= \begin{cases} 285, 300, 320, 350 \text{ or } 365, & H_{E*D} \geq 10000 \text{ FT} \\ 250, & H_{E*D} < 10000 \text{ FT} \end{cases}$$

$$V_{W_1} = \frac{V_{W_c}}{H_c} H_1 \cos(\theta - \alpha)$$

Autopilot Capture

$$\Delta T_1 = \left\{ \frac{K(R_2 - R_1)}{1/2 \left[\left(V_{T_1} + V_{T_3}\right) \cos\gamma + V_{W_1} + V_{W_3} \right]} \right\} K_c$$

$$\Delta T_2 = \left\{ \frac{K(R_3 - R_2)}{1/2 \left[\left(V_{T_1} + V_{T_3}\right) \cos\gamma + V_{W_1} + V_{W_3} \right]} \right\} K_c$$

where:

$$V_{T_3} = K_T \left\{ \left(K_0 + K_1 H_3 + K_2 H_3^2\right) + \left(K_3 + K_4 H_3 + K_5 H_3^2\right) IAS_3 \right\}$$ See Table A-1

$K = 3600$ sec/n.mi./kt

$K_T = 1 + .0043 \ \Delta$ TEMP

$$K_c = 1.0$$

$$IAS_3 = \text{Descent IAS}$$

$$= \begin{cases} 285,\ 300,\ 320,\ 350 \text{ or } 365, & H_{E*D} \geq 10000 \text{ FT} \\ 250, & H_{E*D} < 10000 \text{ FT} \end{cases}$$

$$\text{Cos } \gamma = \frac{R_3 - R_1}{\sqrt{\left(\frac{\Delta H_3}{6076.103}\right)^2 + \left(R_3 - R_1\right)^2}}$$

$$V_{W_1} = \frac{V_{W_c}}{H_c} H_1 \text{ Cos } (\theta - \alpha)$$

$$V_{W_2} = \frac{V_{W_c}}{H_c} H_3 \text{ Cos } (\theta - \alpha)$$

(2) CONSTANT 250 KTS IAS SEGMENT

The equations derived in Segment 4 (Constant IAS) are also applicable to this segment with the exception that only the 250 kts IAS coefficients of Table A-2 are used.

③ 10,000 FT LEVEL DECEL TO 250 KTS SEGMENT

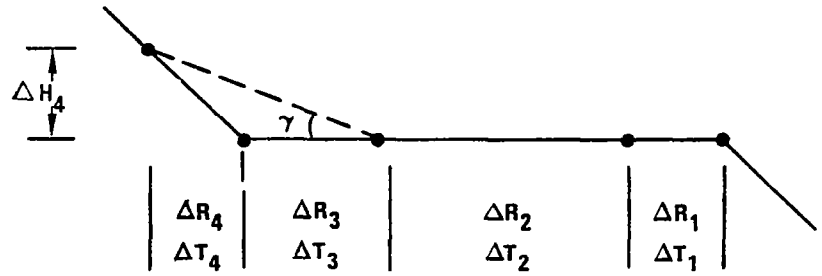

R_5	R_4	R_3	R_2	R_1
H_5	H_4	H_3	H_2	H_1
T_5	T_4	T_3	T_2	T_1
IAS_5	IAS_4	IAS_3	IAS_2	IAS_1
V_{T_5}	V_{T_4}	V_{T_3}	V_{T_2}	V_{T_1}
V_{W_5}	V_{W_4}	V_{W_3}	V_{W_2}	V_{W_1}

$$\Delta T_1 = \left\{ \frac{K \Delta R_1}{1/2\left(V_{T_1} + V_{T_2} + 2V_{W_1}\right)} \right\} K_c$$

$$\Delta T_2 = \left\{ \frac{K \Delta R_2}{1/2\left(V_{T_3} + V_{T_2} + 2V_{W_2}\right)} \right\} K_c$$

$$\Delta T_3 = \left\{ \frac{K \Delta R_3}{1/2\left[\left(V_{T_3} + V_{T_5}\right) \cos \gamma + V_{W_3} + V_{W_5}\right]} \right\} K_c$$

$$\Delta T_4 = \left\{ \frac{K \Delta R_4}{1/2 \left[\left(V_{T_3} + V_{T_5} \right) \cos \gamma + V_{W_3} + V_{W_5} \right]} \right\} K_c$$

where:

$$\left\{ \begin{array}{l} V_{T_1} = K_T \, (K_o + 250 \, K_1) \\ V_{T_2} = K_T \, (K_o + 270 \, K_1) \\ V_{T_3} = K_T \, (K_o + IAS_3 \, K_1) \end{array} \right\} \quad \text{See Table A-4}$$

$$V_{T_5} = K_T \left\{ (K_o + K_1 H_5 + K_2 H_5^2) + (K_3 + K_4 H_5 + K_5 H_5^2) IAS_5 \right\} \text{ (See Table A-1)}$$

$$IAS_3 = IAS_5 - \left(\frac{R_5 - R_3}{R_5 - R_2} \right) (IAS_5 - 270)$$

IAS_5 = Descent IAS

= 285, 300, 320, 350 or 365

$$V_{W_1} = V_{W_2} = V_{W_3} = V_{W_4}$$

$$= \frac{V_{W_c}}{H_c} \, (10{,}000) \, \text{Cos} \, (\theta - \alpha)$$

$$V_{W_5} = \frac{V_{W_c}}{H_c} \, H_5 \, \text{Cos} \, (\theta - \alpha)$$

K = 3600 sec/n.mi./kt

$K_T = 1 + .0043 \Delta \text{Temp}$

K_c = 1.0

$$\text{Cos}\,\gamma = \frac{R_5 - R_3}{\sqrt{\left(\Delta H_4 / 6076.103\right)^2 + (R_5 - R_3)^2}}$$

④ CONSTANT IAS SEGMENT

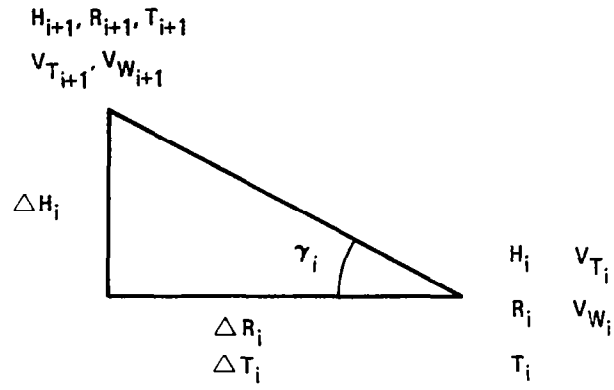

$$\Delta T_i = \left\{ \frac{K \Delta R_i}{1/2\left[\left(V_{T_i} + V_{T_{i+1}}\right) \text{Cos}\gamma_i + V_{W_i} + V_{W_{i+1}}\right]} \right\} K_c$$

where:

$$\left.\begin{aligned} V_{T_i} &= K_T \left(K_0 + K_1 H_i + K_2 H_i^2\right) \\ V_{T_{i+1}} &= K_T \left(K_0 + K_1 H_{i+1} + K_2 H_{i+1}^2\right) \end{aligned}\right\} \text{See Table A-2}$$

$K = 3600$ sec/n.mi./kt

$K_c = 1.0$

$K_T = 1 + .0043\ \Delta\ \text{TEMP}$

$$\text{Cos}\gamma_i = \frac{\Delta R_i}{\sqrt{\left(\frac{\Delta H_i}{6076.103}\right)^2 + \Delta R_i^2}}$$

$$V_{W_i} = \frac{V_{W_c}}{H_c} H_i \quad \text{Cos } (\theta - \alpha)$$

$$V_{W_{i+1}} = \frac{V_{W_c}}{H_c} H_{i+1} \quad \text{Cos } (\theta - \alpha)$$

⑤ CONSTANT MACH SEGMENT

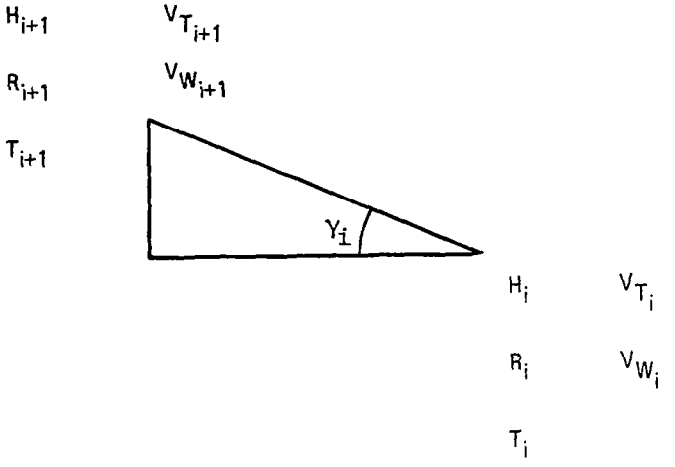

$$\Delta T_i = \left\{ \frac{K \Delta R_i}{1/2\left[\left(V_{T_i} + V_{T_{i+1}} \right) \text{Cos } \gamma_i + V_{W_i} + V_{W_{i+1}} \right]} \right\} K_c$$

$$\left.\begin{aligned} V_{T_i} &= K_T \left(K_0 + K_1 H_i + K_2 H_i^2 \right) \\ V_{T_{i+1}} &= K_T \left(K_0 + K_1 H_{i+1} + K_2 H_{i+1}^2 \right) \end{aligned}\right\} \text{See Table A-3}$$

$$V_{W_i} = \frac{V_{W_c}}{H_c} \; H_i \; \text{Cos} \; (\theta - \alpha)$$

$$V_{W_{i+1}} = \frac{V_{W_c}}{H_c} \; H_{i+1} \; \text{Cos} \; (\theta - \alpha)$$

$K = 3600$ sec/n.mi./kt

$K_T = 1 + .0043 \; \Delta\text{Temp}$

$K_c = 1.0$

$$\text{Cos} \; \gamma_i = \frac{\Delta R_i}{\sqrt{\left(\frac{\Delta H_i}{6076.103}\right)^2 + \Delta R_i^2}}$$

⑥ CRUISE PUSH-OVER SEGMENT

Above Mach-IAS Cross-Over Altitude

$\Delta T = K_c \; (K_o + K_1 \; \text{Mach}_{CRZ})$ } See Table A-5

Below Mach-IAS Cross-Over Altitude

$\Delta T = K_c \; (K_o + K_1 \; \text{IAS}_{CRZ})$ } See Table A-5

$K_c = 1.0$

TABLE A-1. V_{TAS} IN E*D ALTITUDE (kts)

K_0	K_1	K_2	K_3	K_4	K_5
3.12522	0.20176×10^{-3}	0.26710×10^{-7}	0.99230	0.12725×10^{-4}	0.7085×10^{-10}

TABLE A-2. V_{TAS} IN CONSTANT IAS SEGMENT (kts)

IAS	K_0	K_1	K_2
250	251.25	3.318×10^{-3}	4.525×10^{-8}
285	290.00	3.375×10^{-3}	6.045×10^{-8}
300	301.70	3.910×10^{-3}	5.300×10^{-8}
320	321.12	4.173×10^{-3}	5.238×10^{-8}
350	349.65	4.715×10^{-3}	4.815×10^{-8}
365	364.70	5.011×10^{-3}	4.710×10^{-8}

TABLE A-3. V_{TAS} IN CONSTANT MACH SEGMENT (kts)

Below 36,090 ft

Mach	K_0	K_1	K_2
0.800	525.5	-1.496×10^{-3}	-1.004×10^{-8}
0.820	542.4	-1.855×10^{-3}	-3.912×10^{-9}
0.850	562.5	-1.923×10^{-3}	-4.050×10^{-9}
0.865	577.2	-2.306×10^{-3}	1.908×10^{-9}

Above 36,090 ft

Mach	V_T (kts)
0.800	459.0
0.820	470.3
0.850	485.5
0.865	496.0

TABLE A-4. V_{TAS} IN 10 000 ft DECEL TO 250 kts SEGMENT (kts)

K_0	K_1
7.81382	1.12664

TABLE A-5. ΔT IN CRUISE PUSH-OVER SEGMENT (seconds)

Above Mach—IAS Cross-Over Altitude

Descent Mach	K_0	K_1
0.800	69.85	−55.17
0.820	127.20	−120.00
0.850	165.00	−164.90
0.865	165.00	−164.90

Below Mach—IAS Cross-Over Altitude

Descent IAS (kts)	K_0	K_1
285	156.70	−0.4292
300	156.70	−0.4292
320	130.90	−0.3258
350	114.00	−0.2400
365	95.54	−0.1559

APPENDIX B

OPEN LOOP DESCENT SIMULATIONS

This appendix contains computer-generated graphs illustrating the effects of descent speed schedule, aircraft weight, temperature and E*D altitude on time-in-descent and range for the L-1011. All simulations were performed under zero wind conditions.

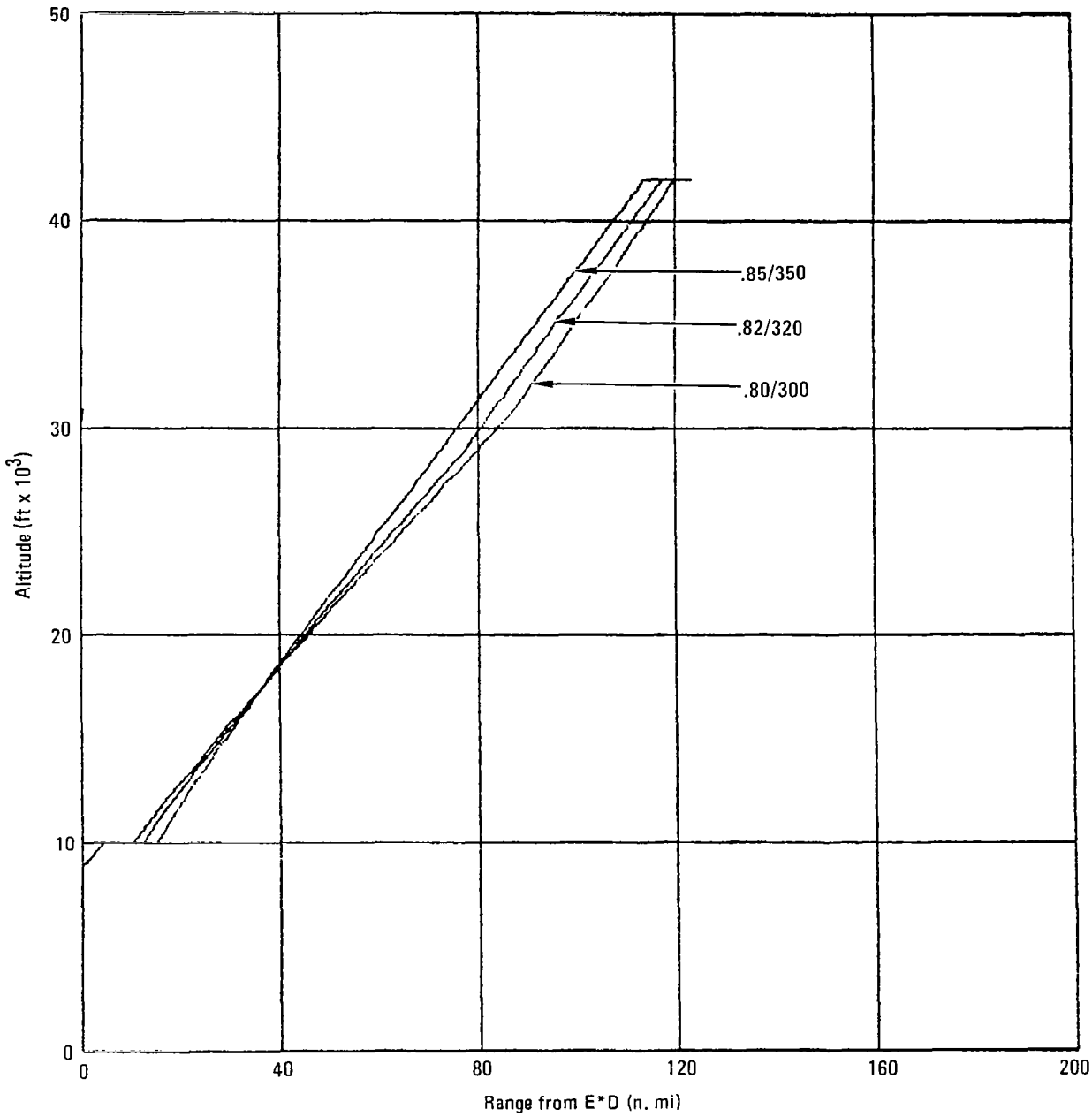

Figure B-1. - Altitude/range descent profiles, W = 163000 kg, E*D = 9000 ft/250 kts.

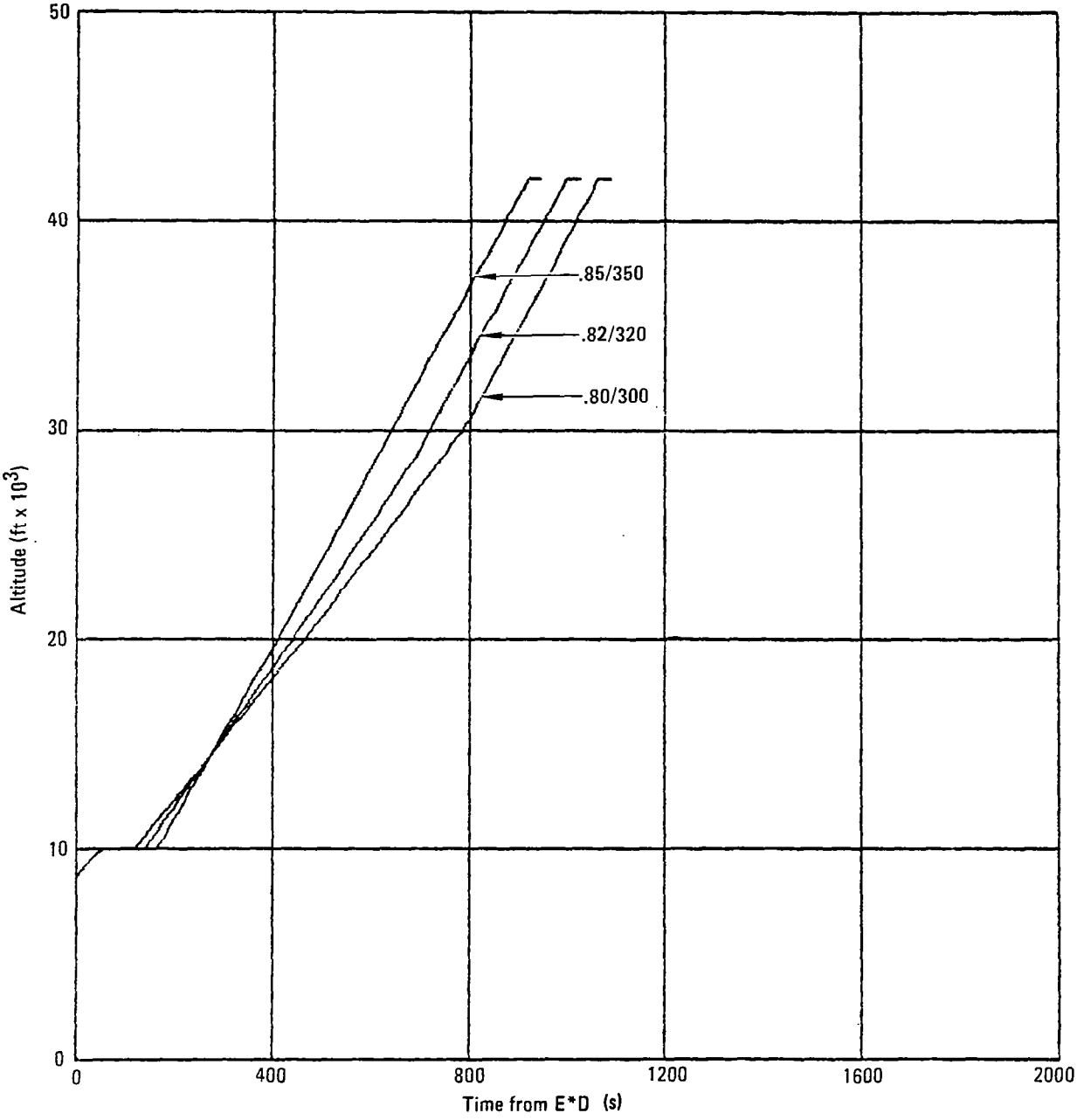

Figure B-2. - Altitude/time descent profiles, W = 163000 kg, E*D = 9000 ft/250 kts.

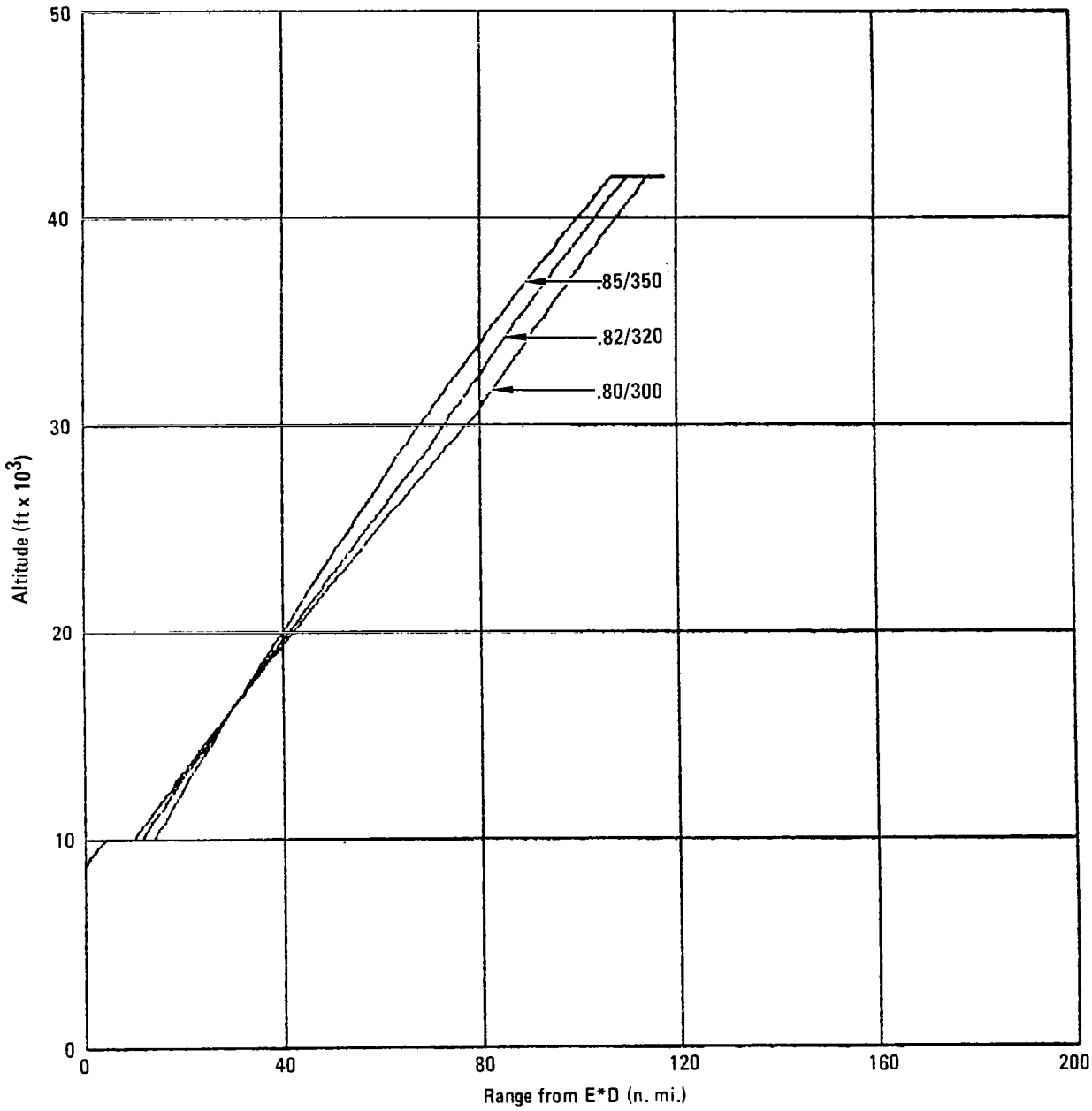

Figure B-3. - Altitude/range descent profiles, W = 136000 kg, E*D = 9000 ft/250 kts.

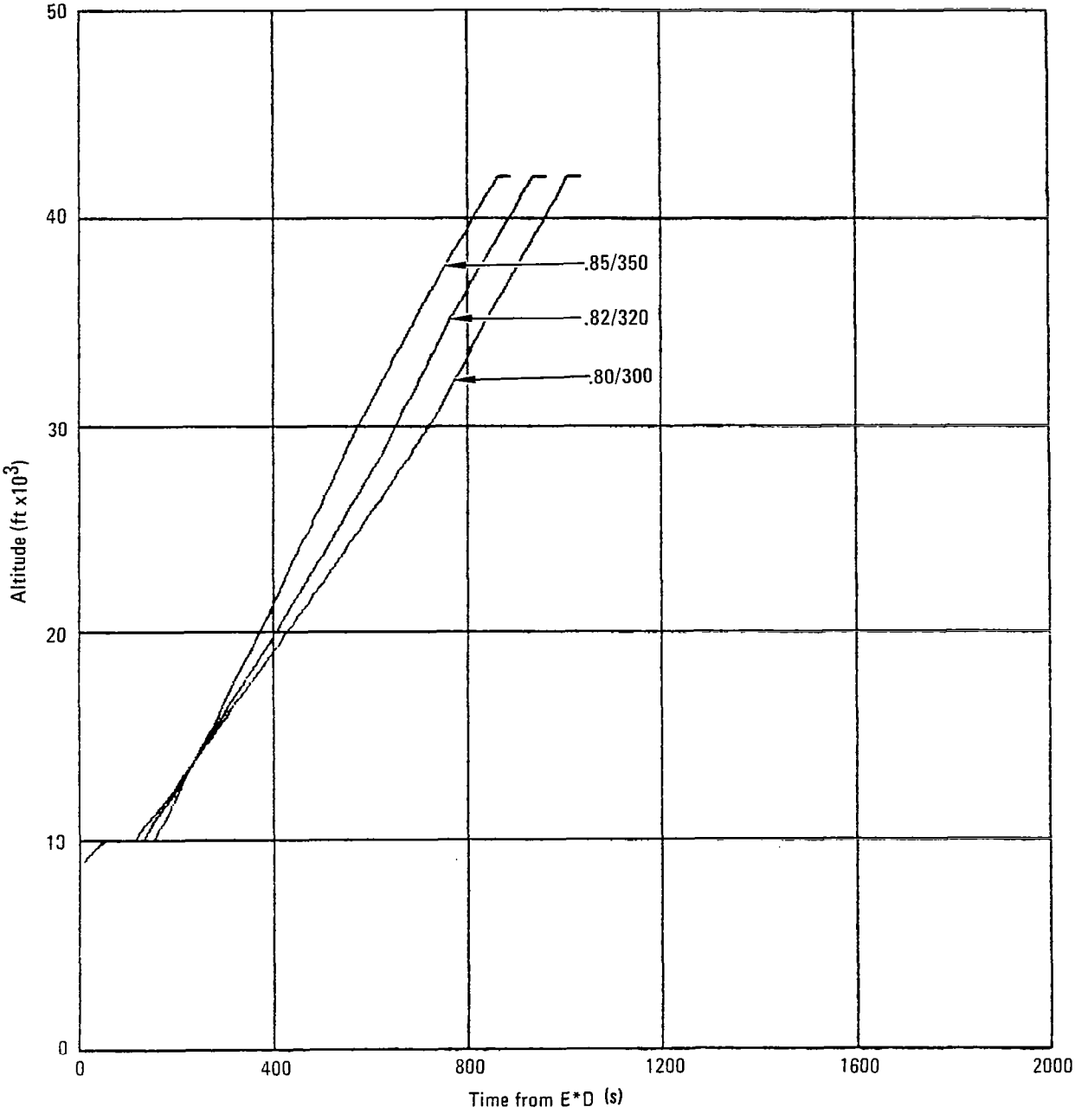

Figure B-4. - Altitude/time descent profiles, W = 136000 kg, E*D = 9000 ft/250 kts.

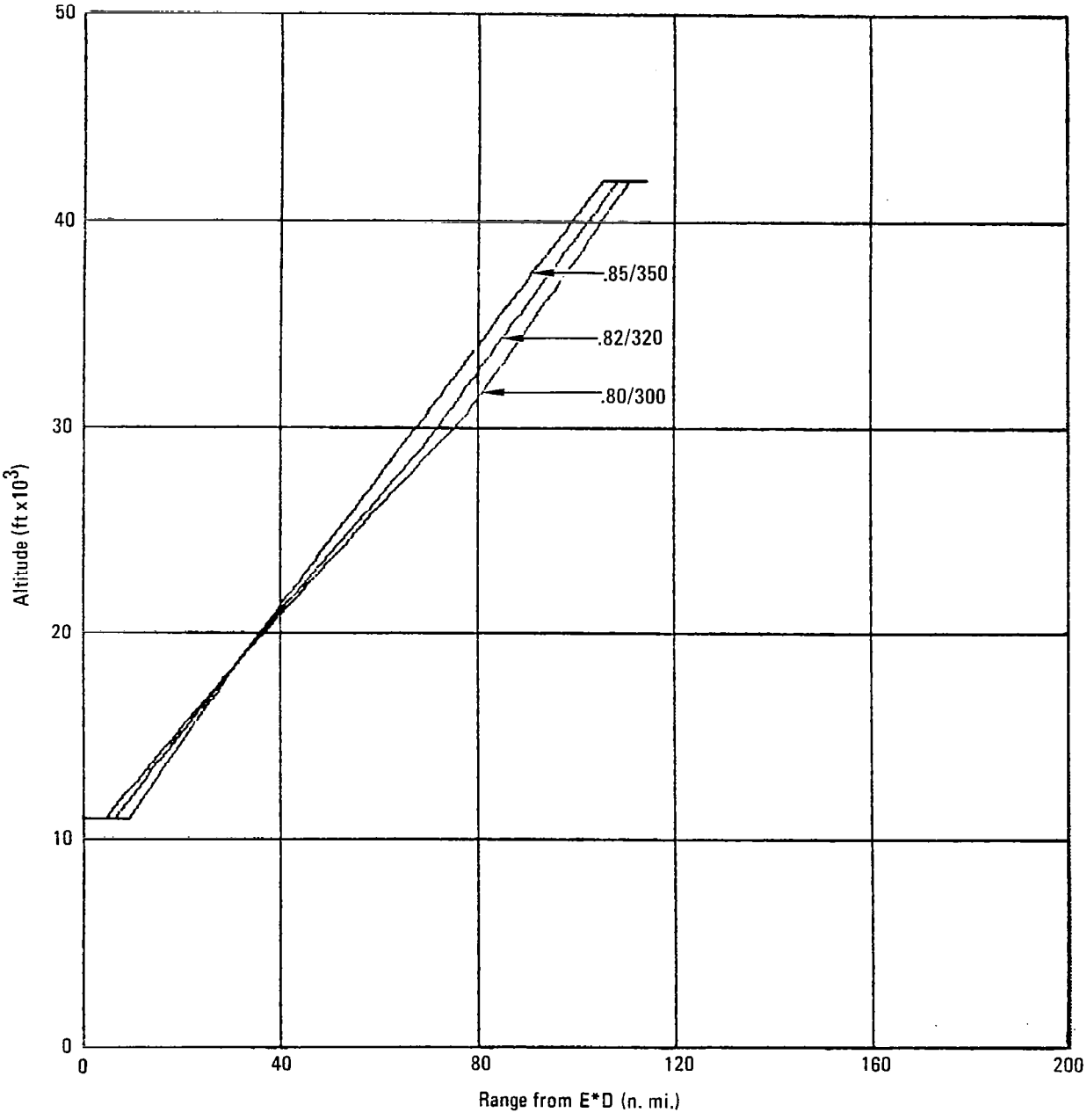

Figure B-5. - Altitude/range descent profiles, W = 163000 kg, E*D = 11000 ft/250 kts.

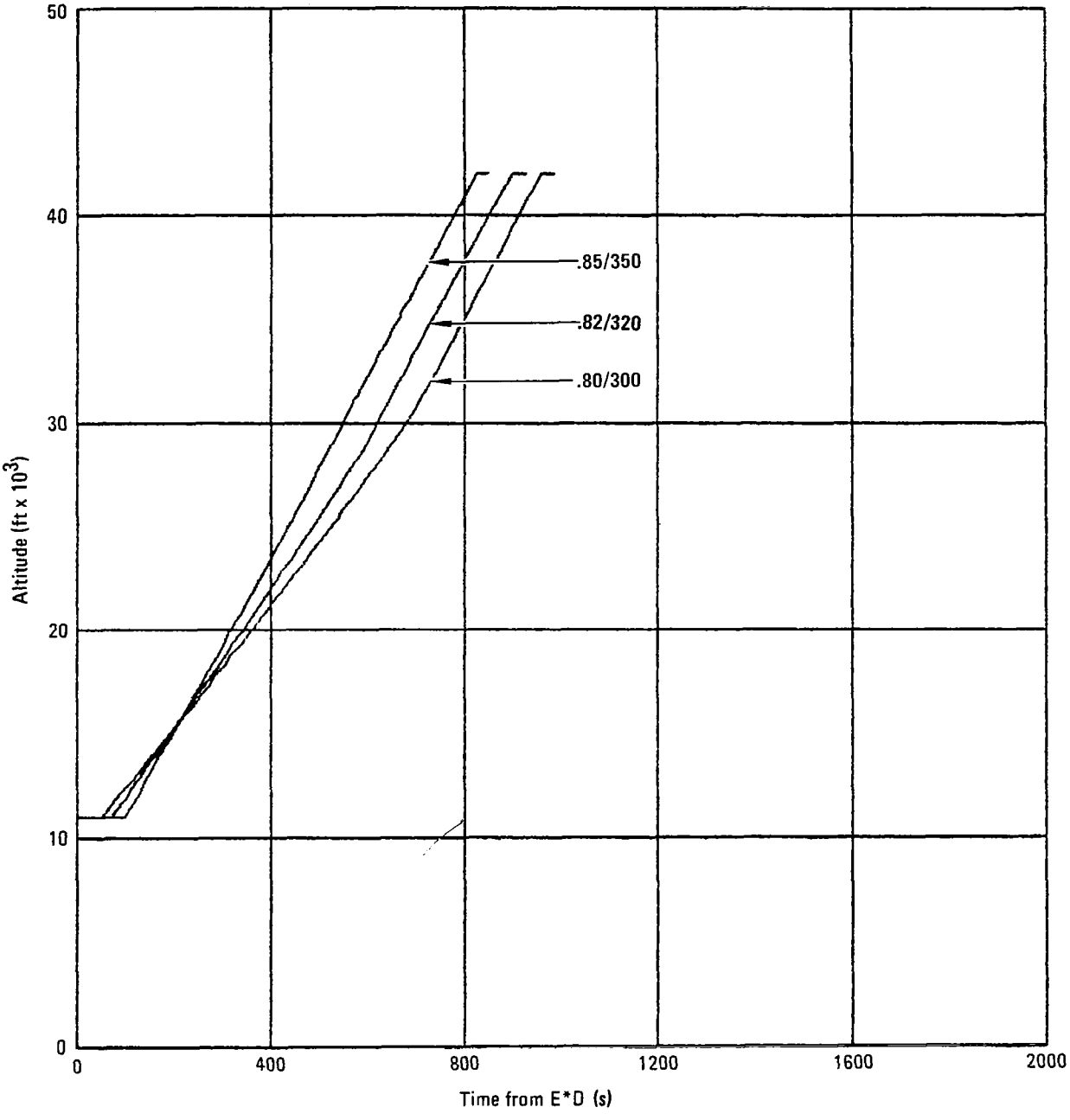

Figure B-6. - Altitude/time descent profiles, W = 163000 kg, E*D = 11000 ft/250 kts.

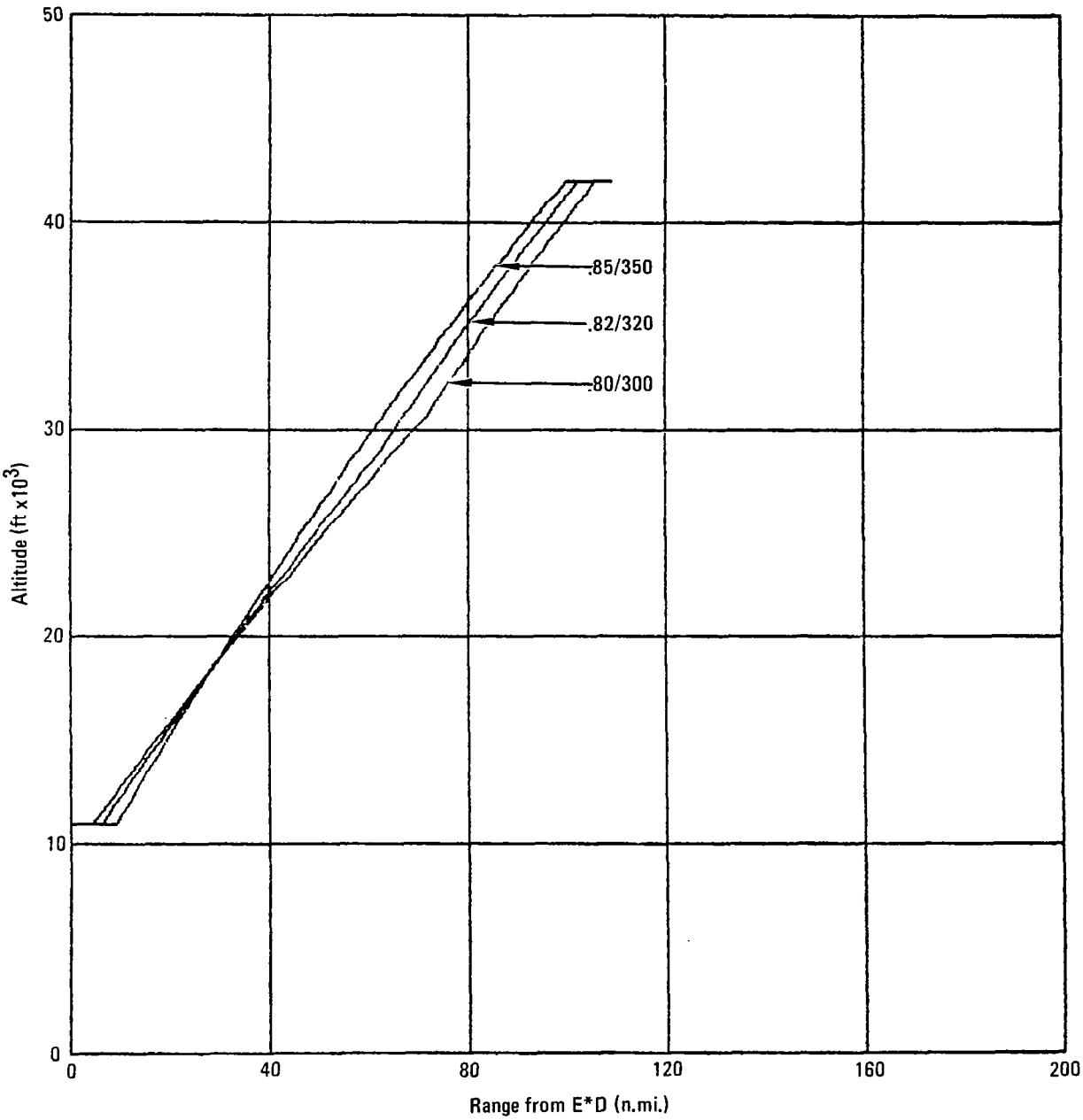

Figure B-7. - Altitude/range descent profiles, W = 136000 kg, E*D = 11000 ft/250 kts.

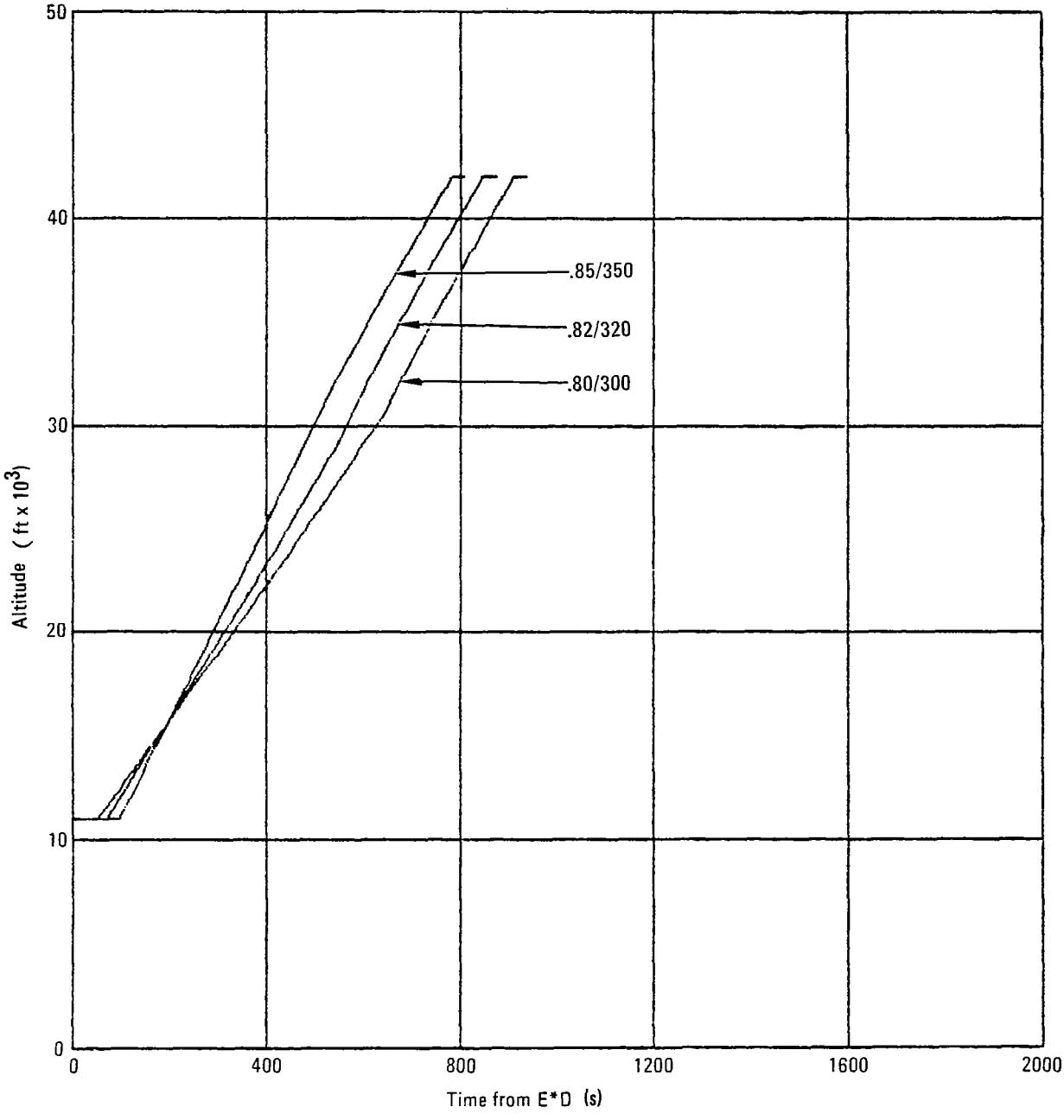

Figure B-8. - Altitude/time descent profiles, W = 136000 kg, E*D = 11000 ft/250 kts.

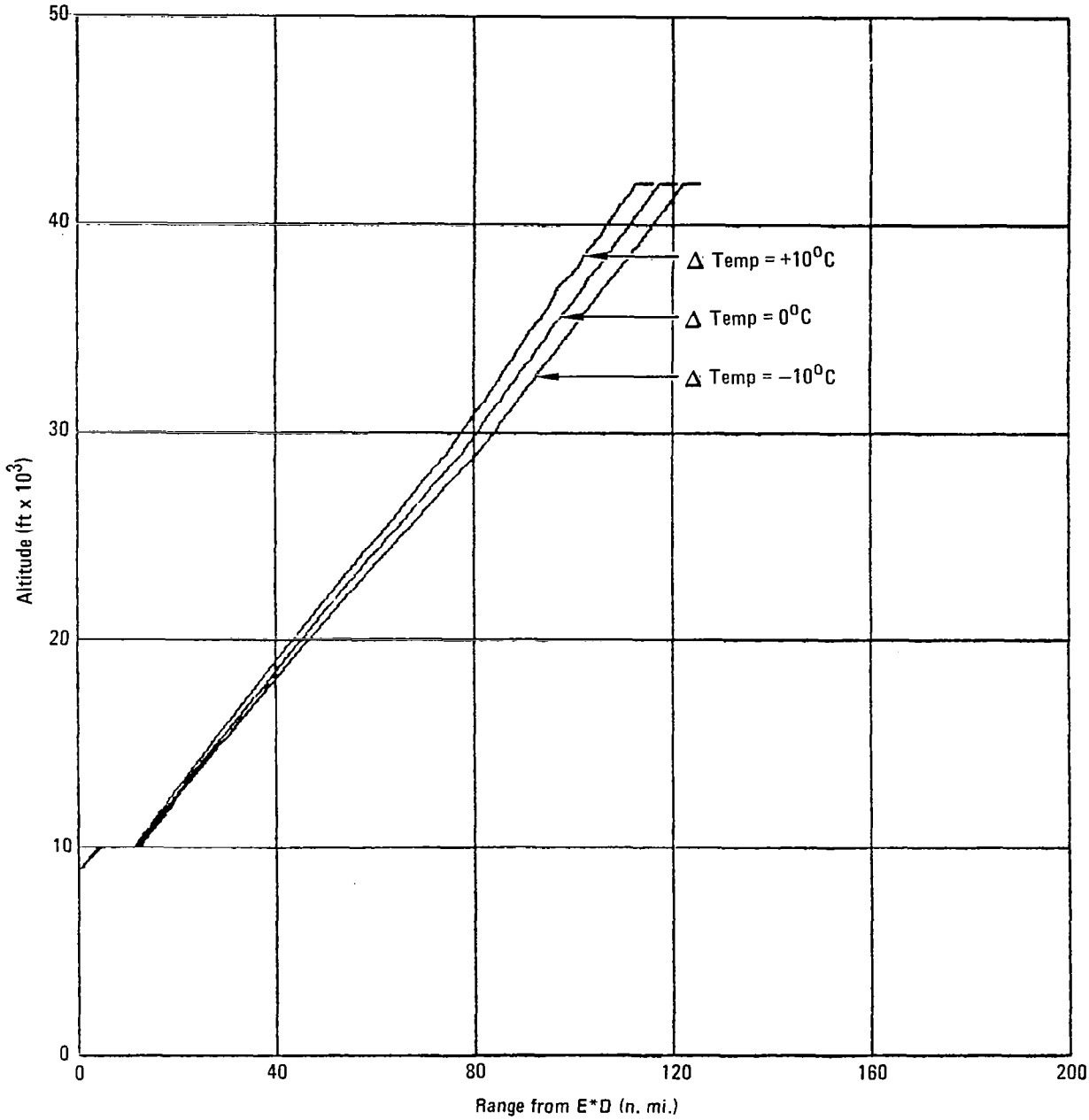

Figure B-9. - Altitude/range descent profiles, W = 163000 kg, E*D = 9000 ft/250 kts, M = .82/IAS = 320 kts.

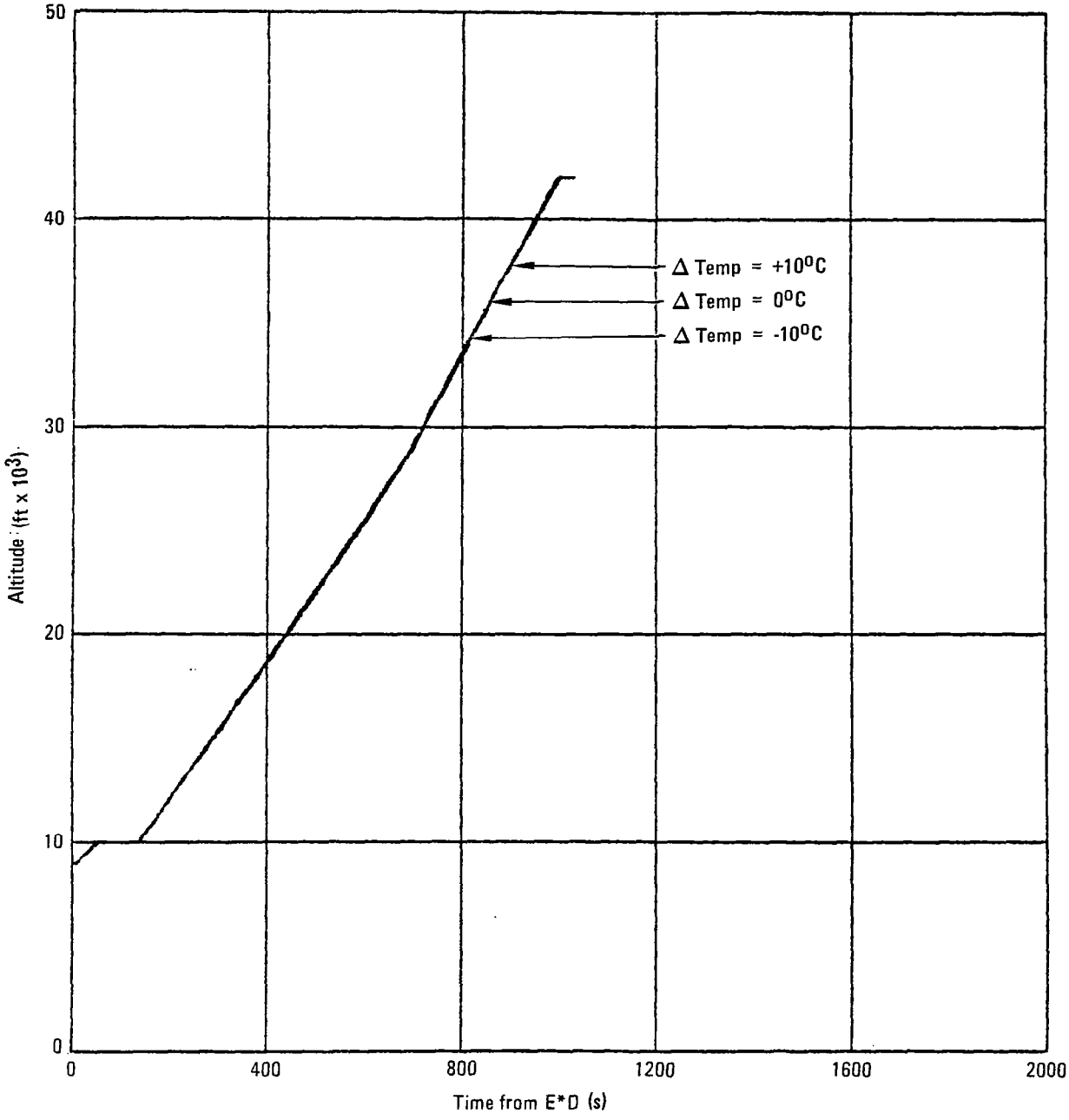

Figure B-10. - Altitude/time descent profiles, W = 163000 kg, E*D = 9000 ft/250 kts, M = .82/IAS = 320 kts.

APPENDIX C

CLOSED LOOP DESCENT SIMULATION PLOTS

This appendix contains computer-generated graphs illustrating the results of a closed-loop 4-D descent performed with the wind models of Figure 12. The effects upon altitude, descent range and speed are presented as well as control surface activity, attitude, and thrust and drag requirements. The descent speed schedule used to obtain this data was Mach = .82/IAS = 320 kts.

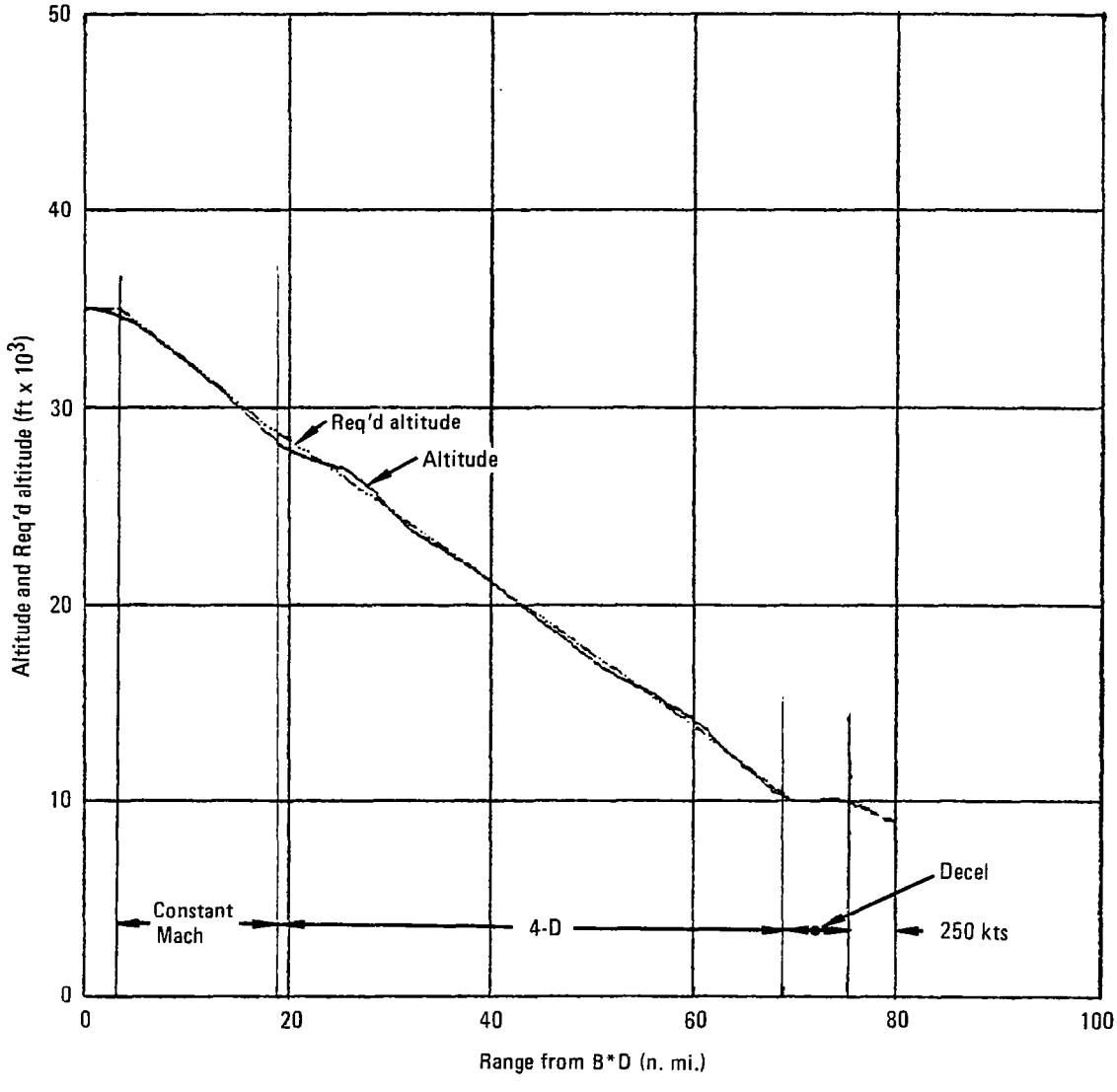

Figure C-1. - Descent profile, W = 136000 kg, E*D = 9000 ft/250 kts, Palmdale wind.

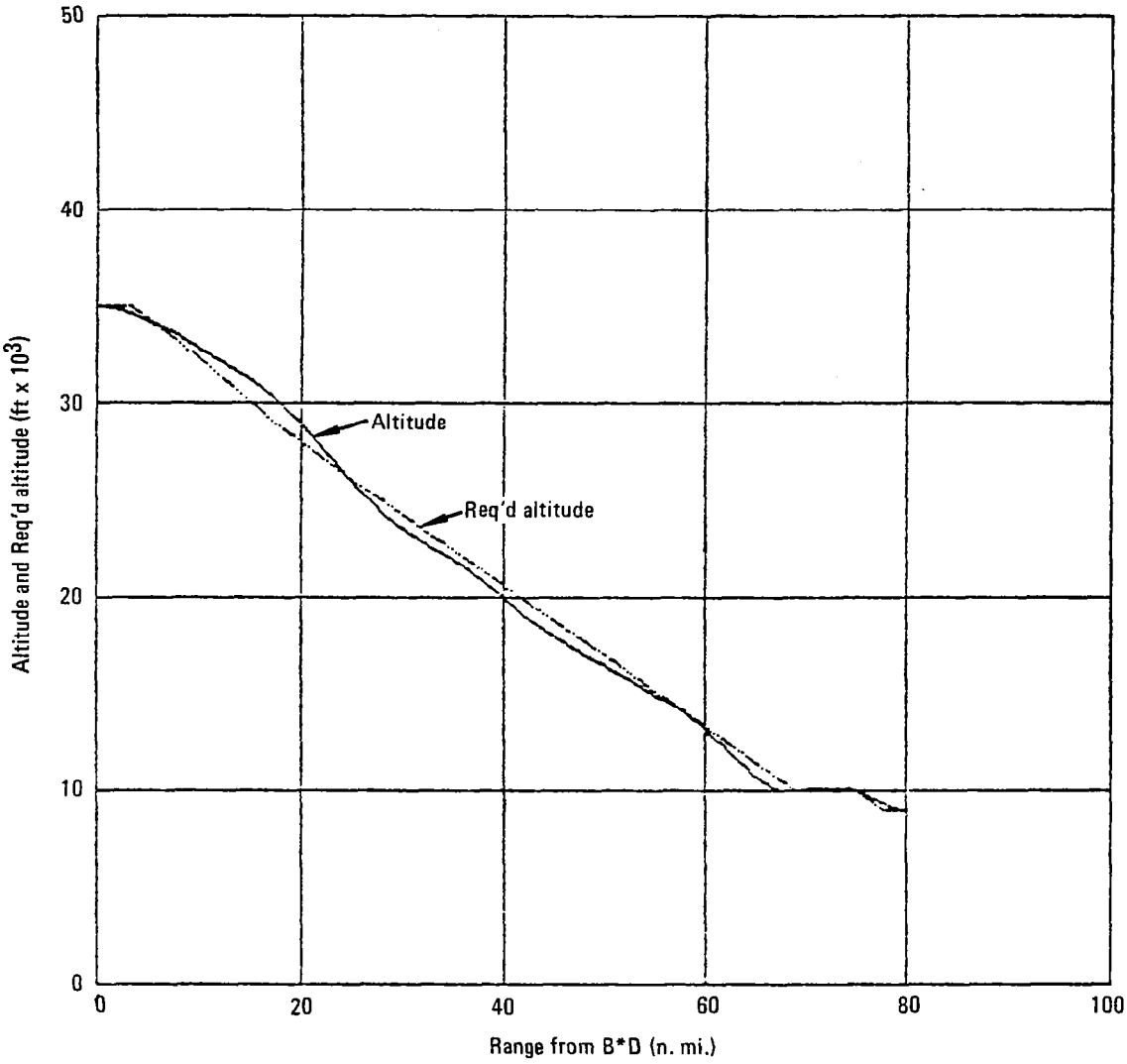

Figure C-2. - Descent profile, W = 136000 kg, E*D = 9000 ft/250 kts, Palmdale wind + Tripoli 2σ headwind.

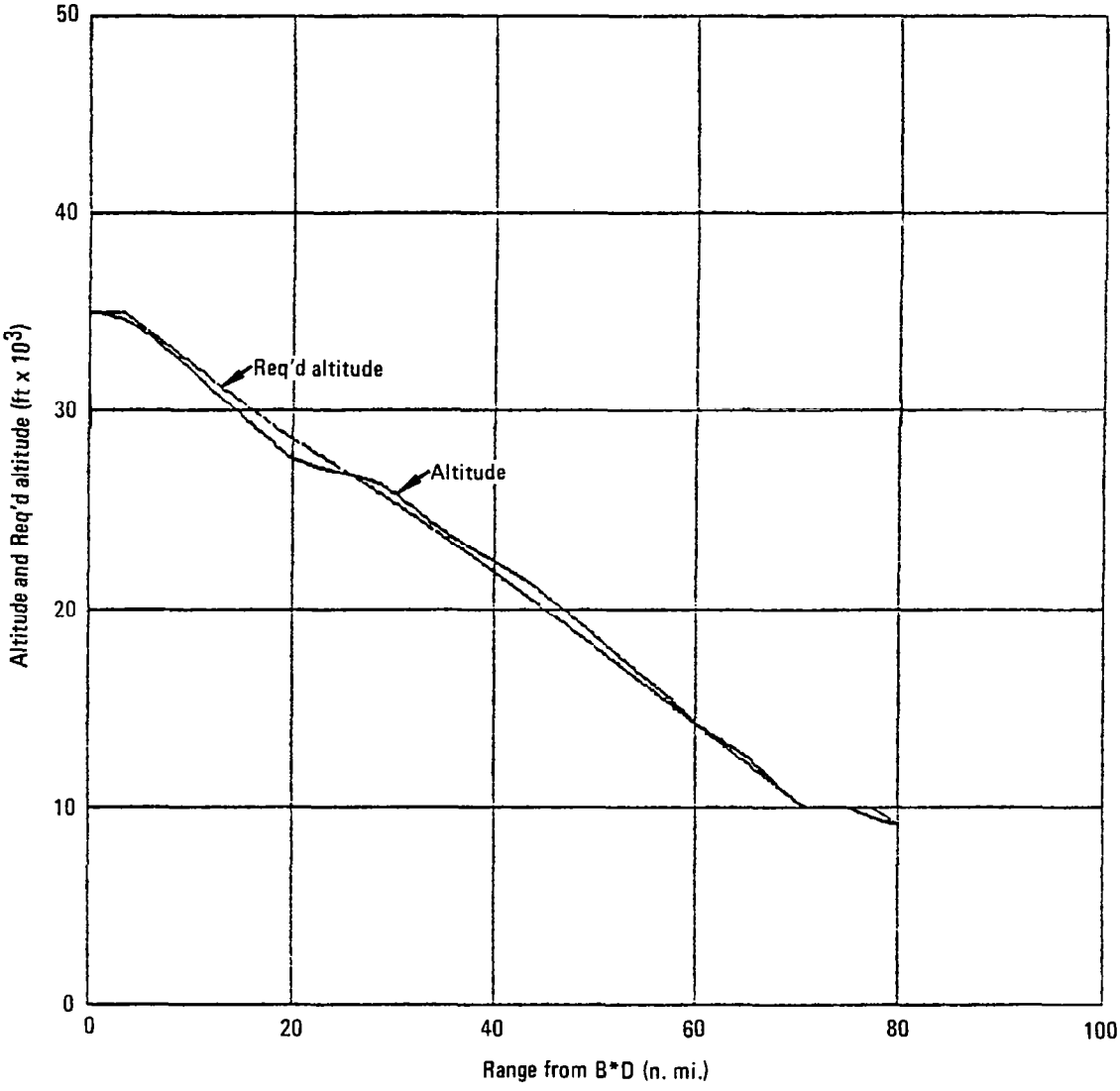

Figure C-3. - Profile descent, W = 136000 kg, E*D = 9000 ft/250 kts, Palmdale wind + Tripoli 2σ tailwind.

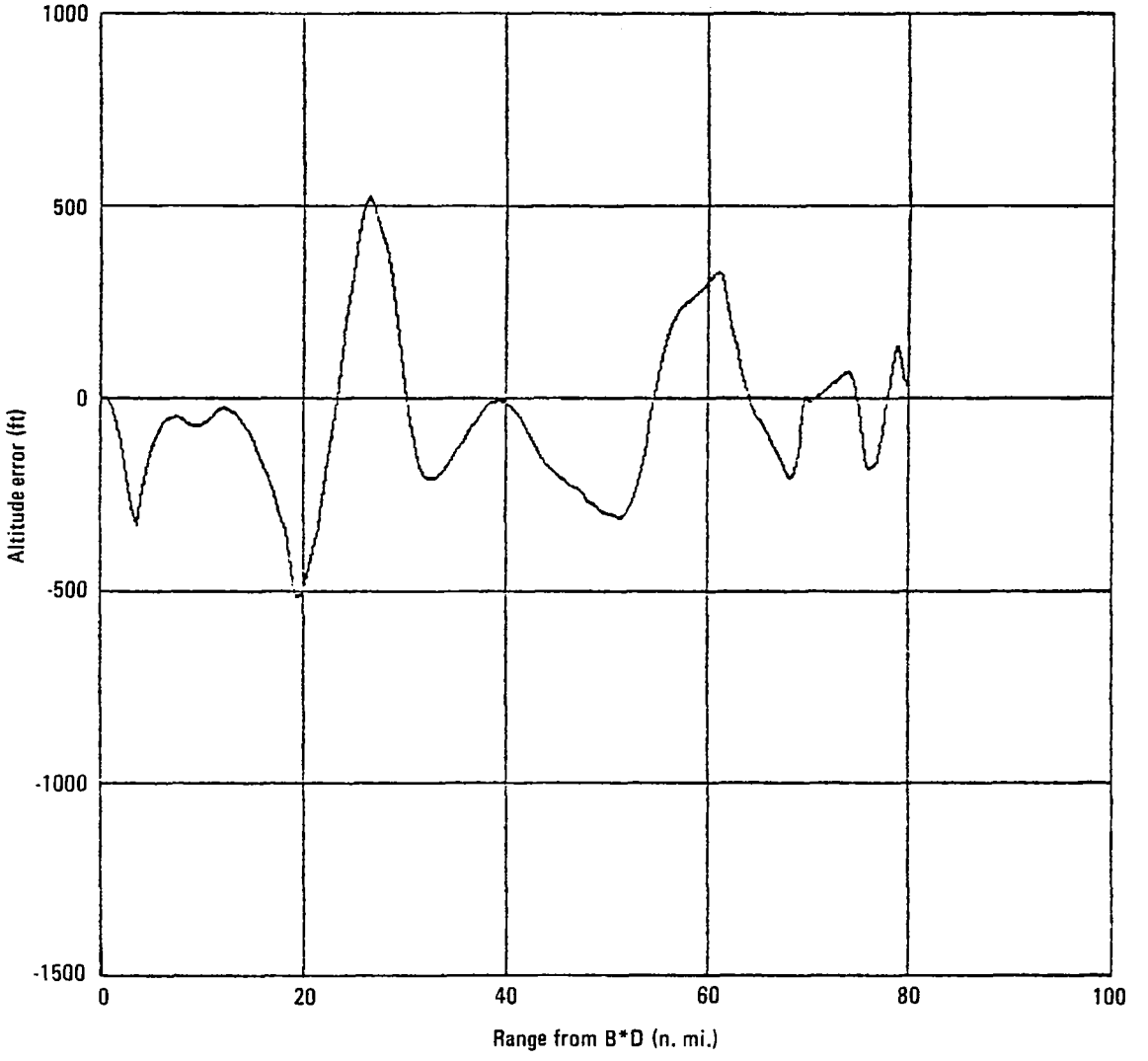

Figure C-4. - Altitude error for figure C-1 descent.

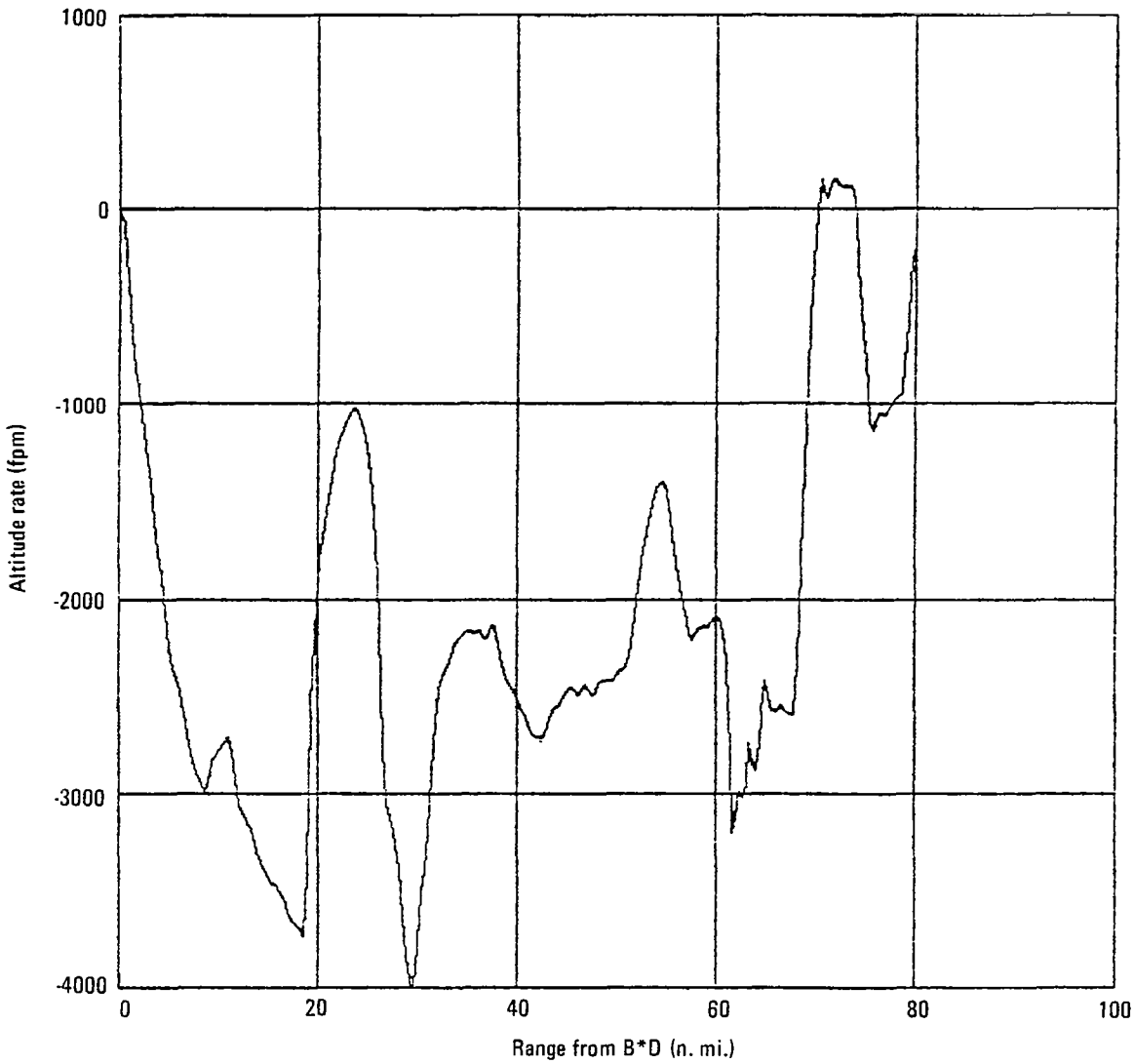

Figure C-5. - Altitude rate for figure C-1 descent.

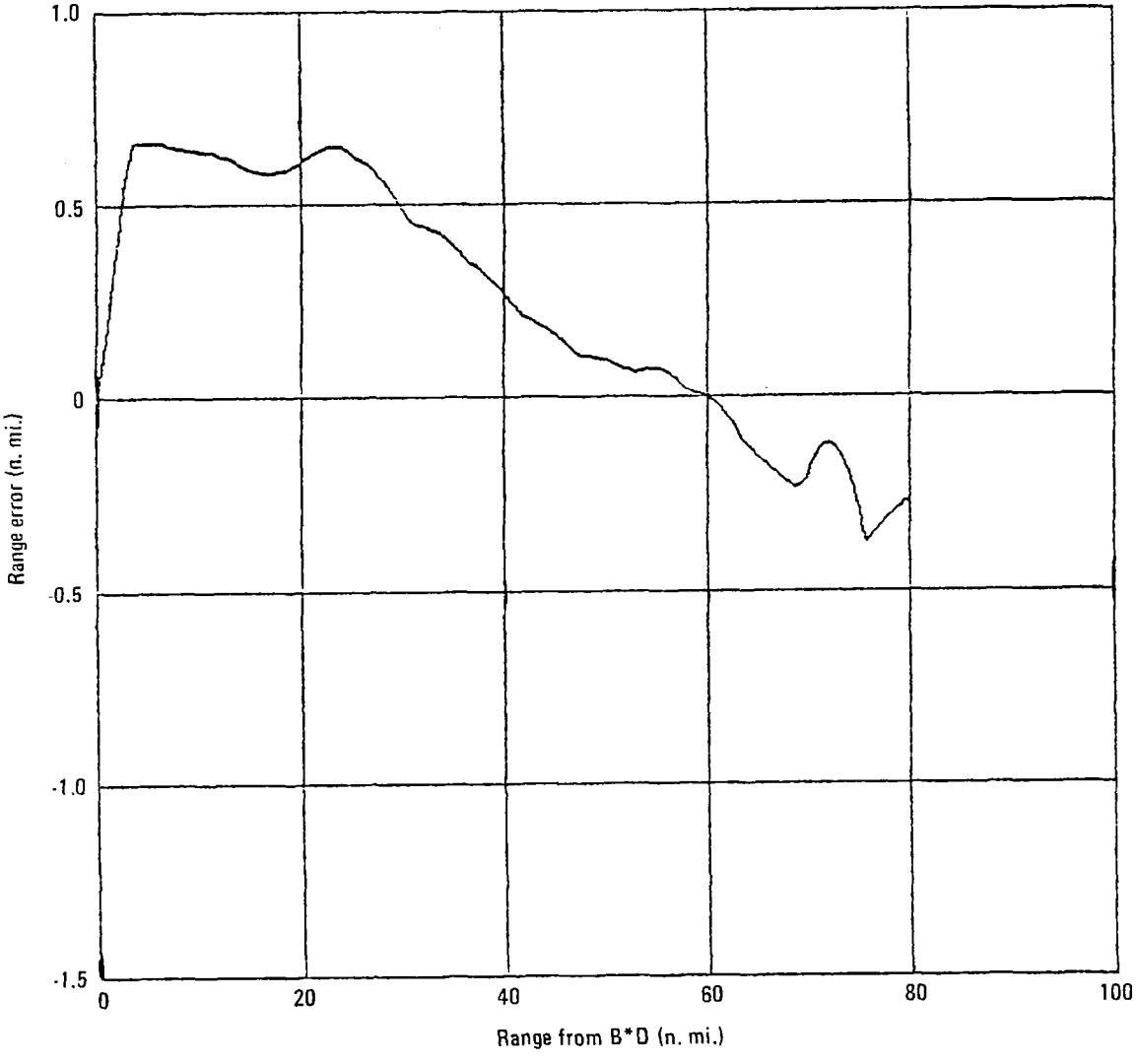

Figure C-6. - Range error for figure C-1 descent.

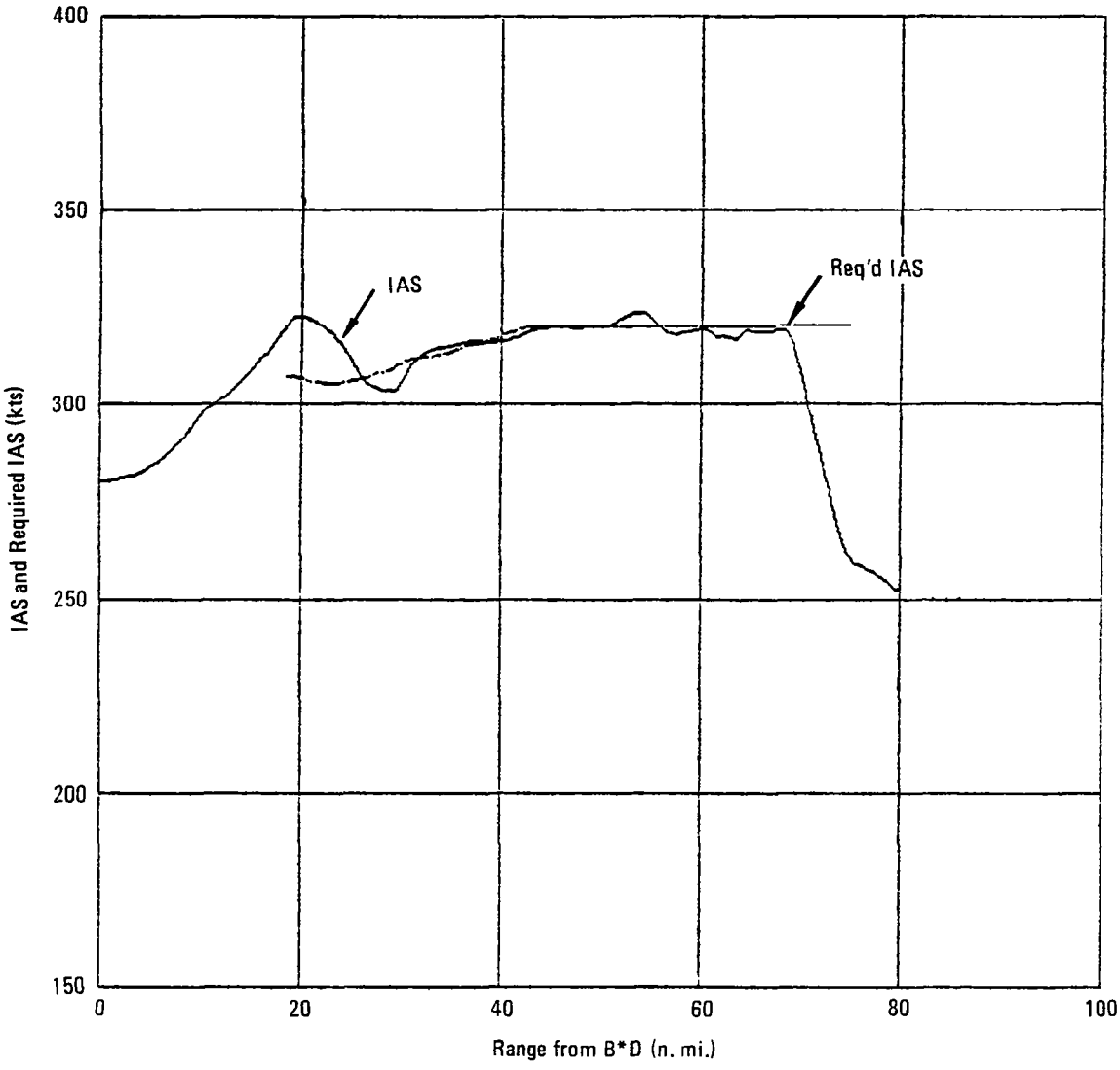

Figure C-7. - IAS and required IAS for figure C-1 descent.

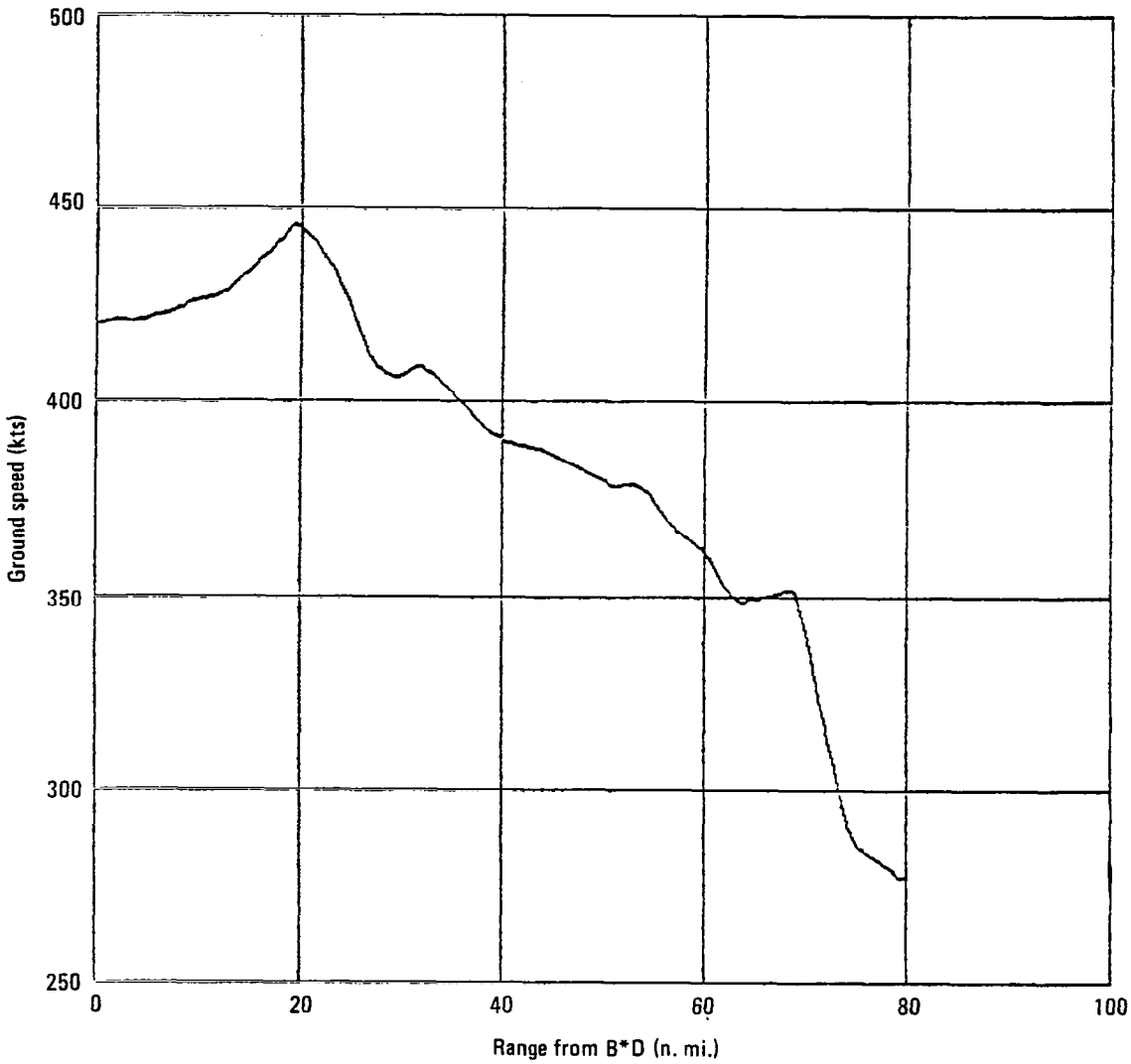

Figure C-8. - Ground speed for figure C-1 descent.

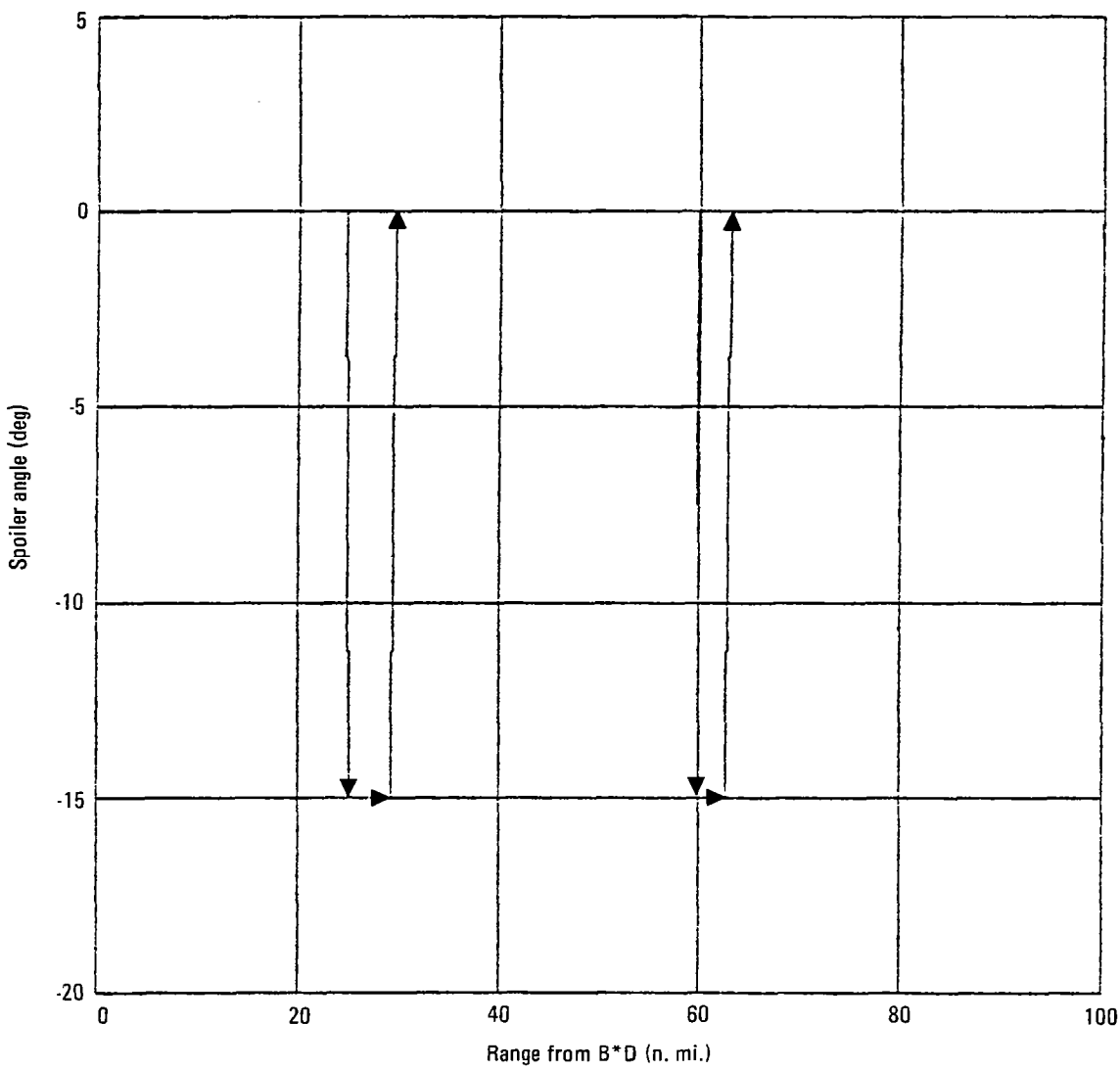

Figure C-9. - Spoiler angle for figure C-1 descent.

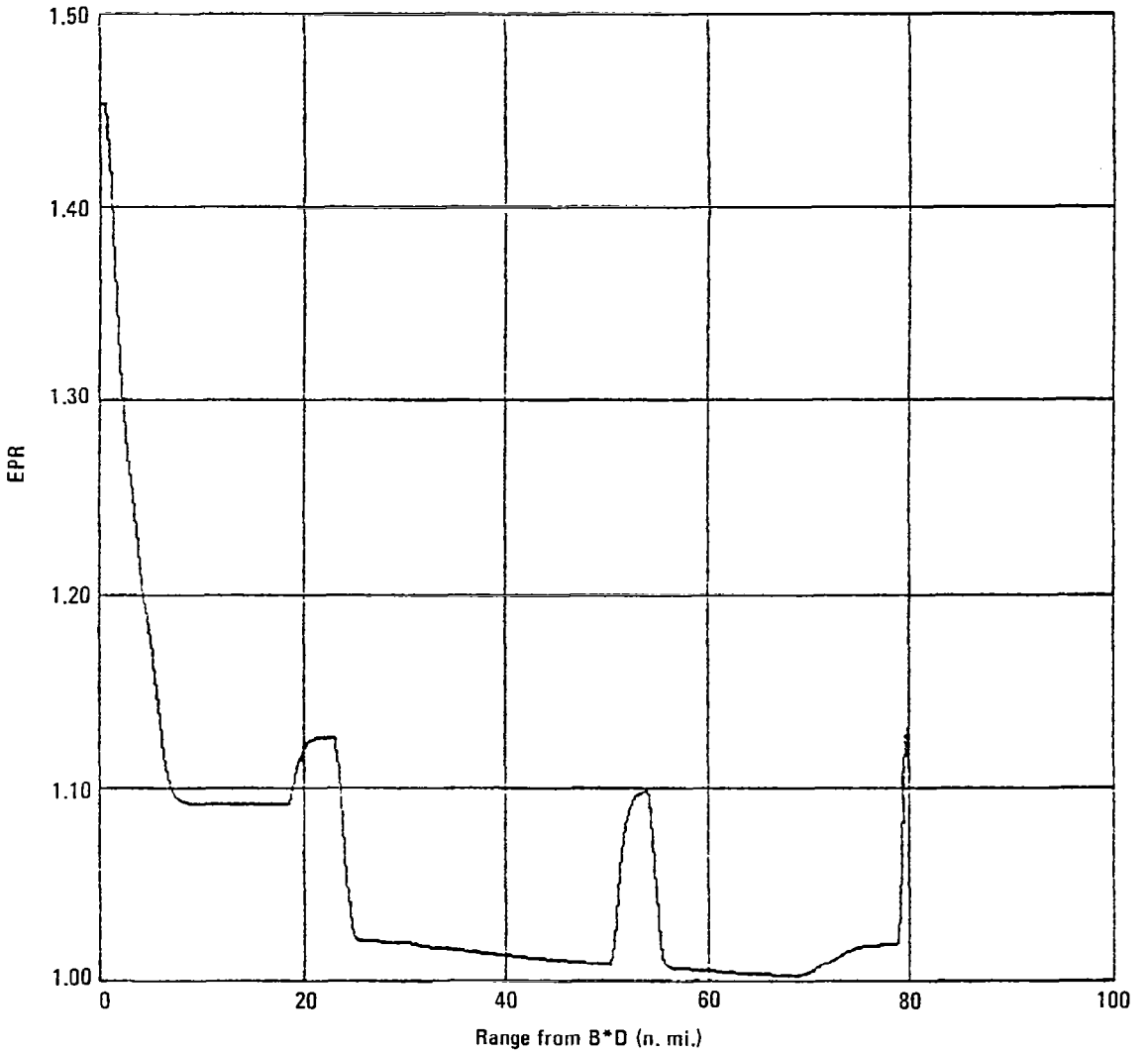

Figure C-10. - Engine pressure ratio for figure C-1 descent.

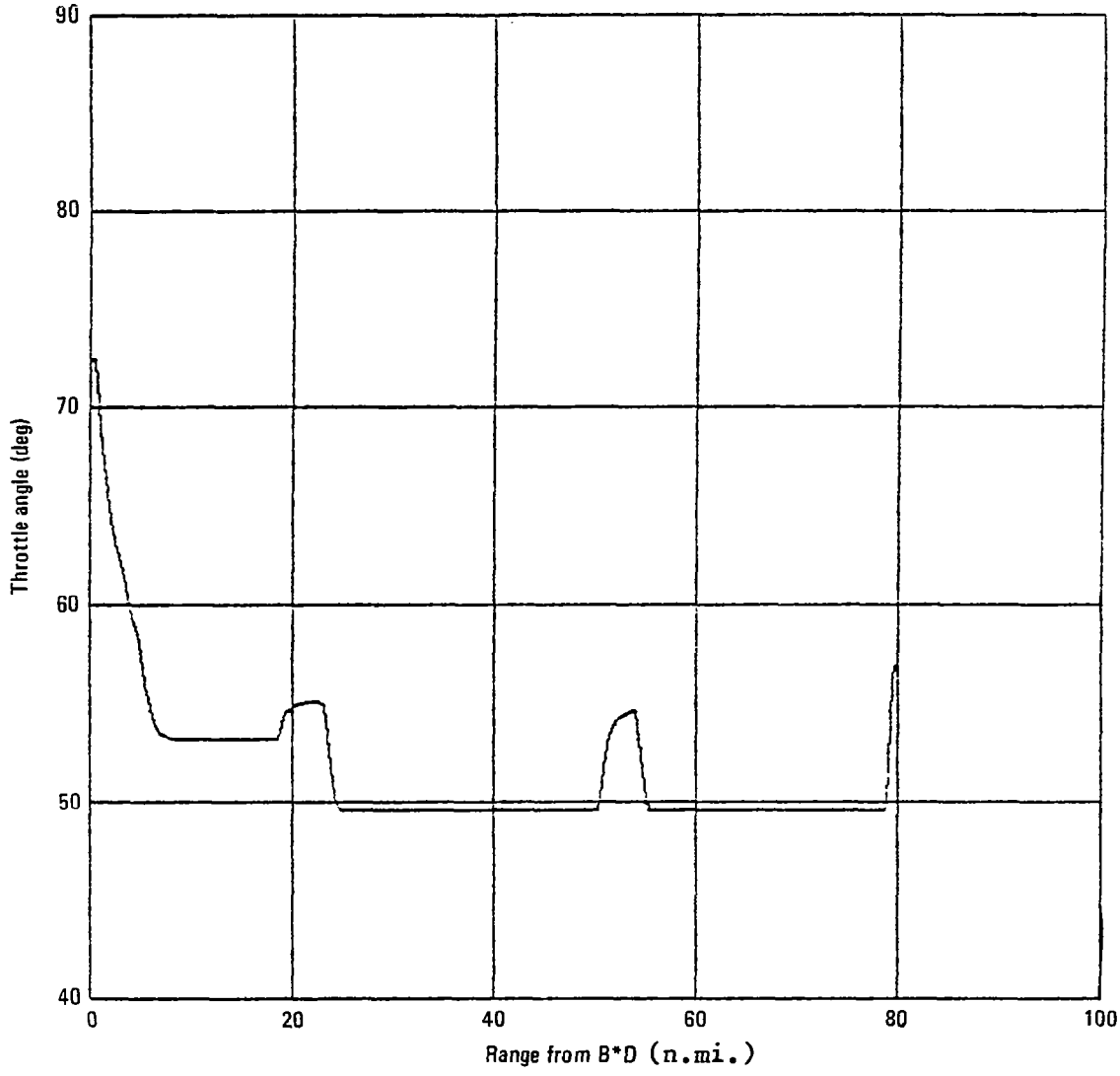

Figure C-11. - Throttle angle for figure C-1 descent.

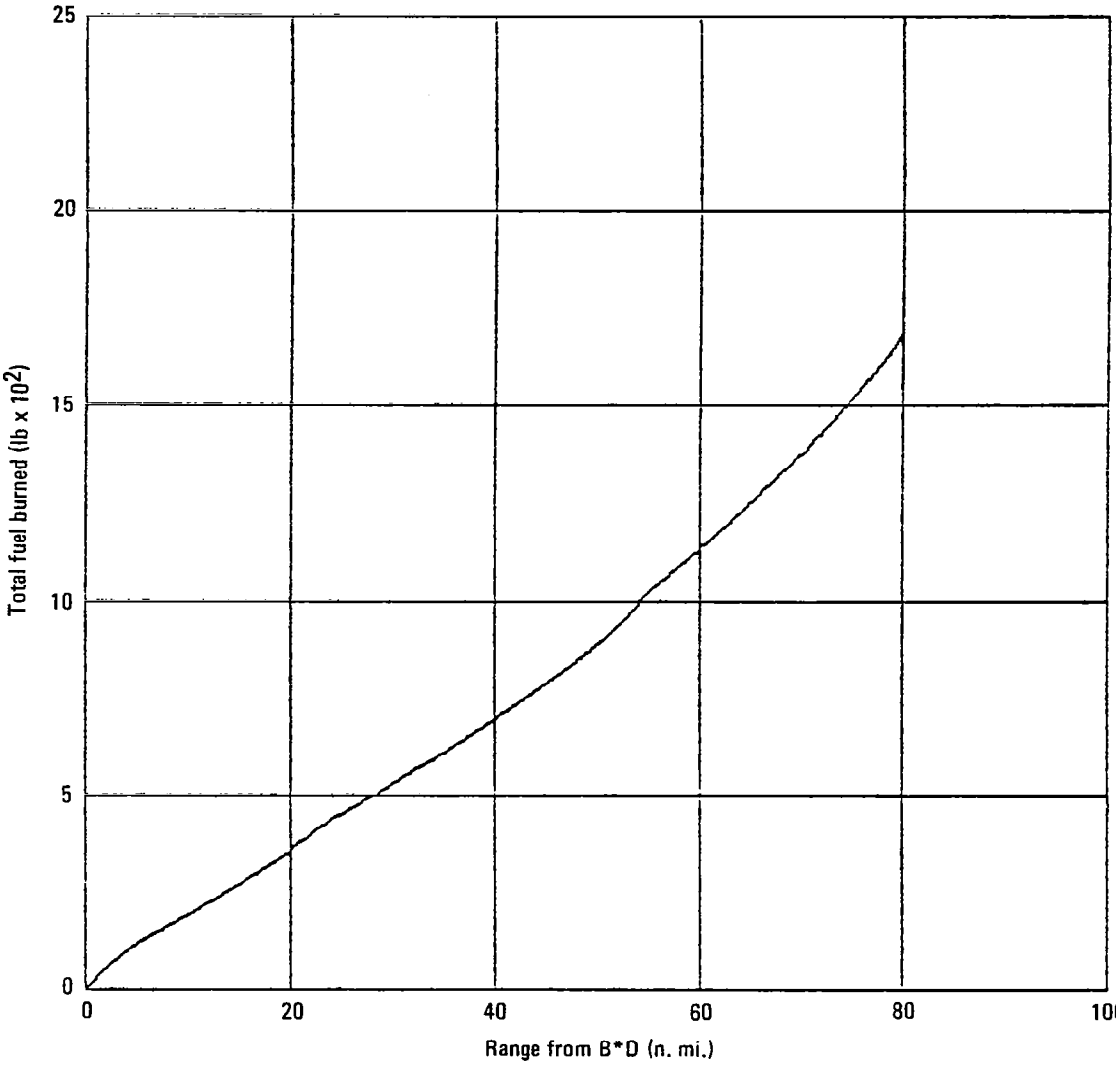

Figure C-12. - Total fuel burned for figure C-1 descent.

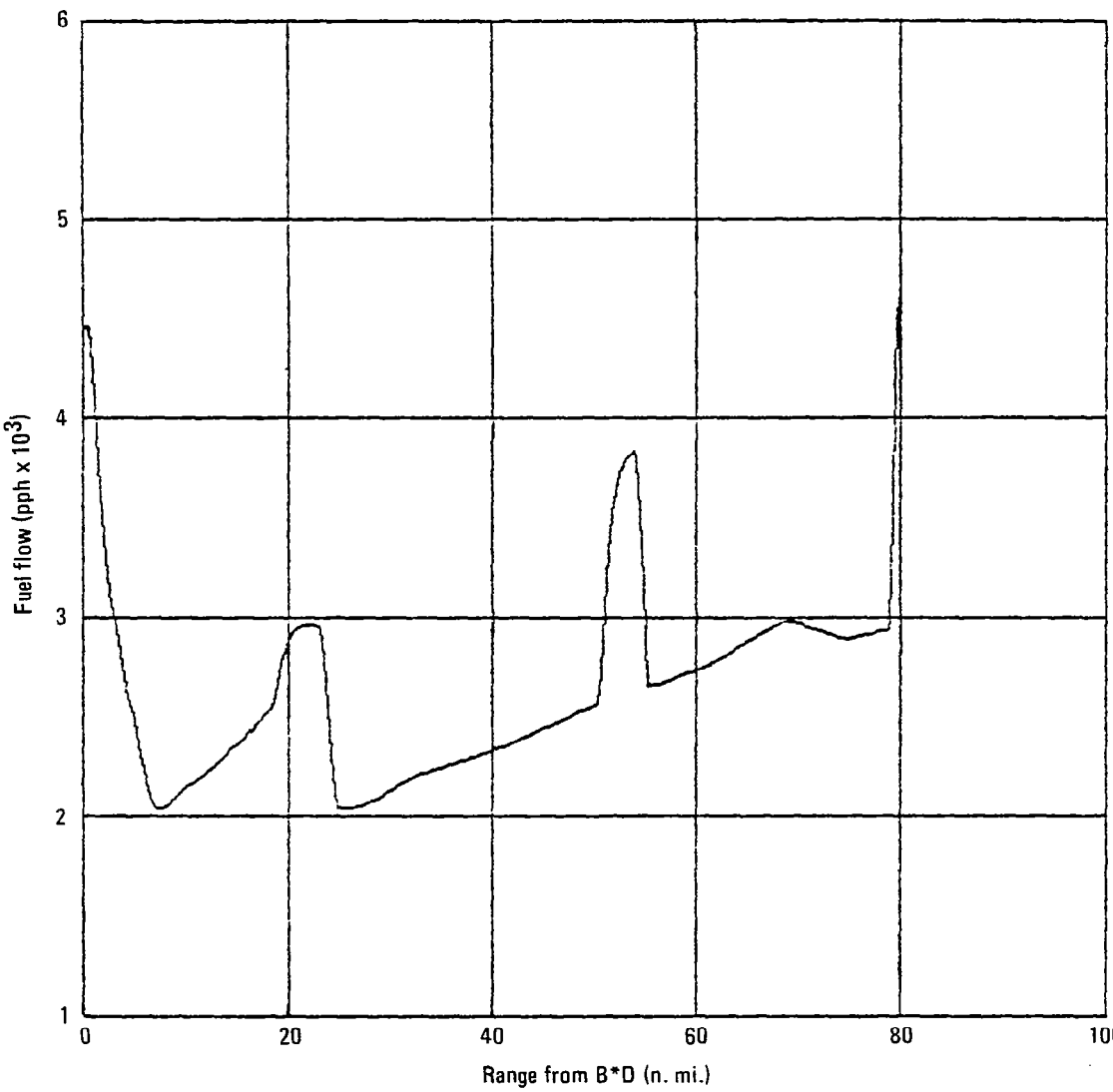

Figure C-13. - Fuel flow for figure C-1 descent.

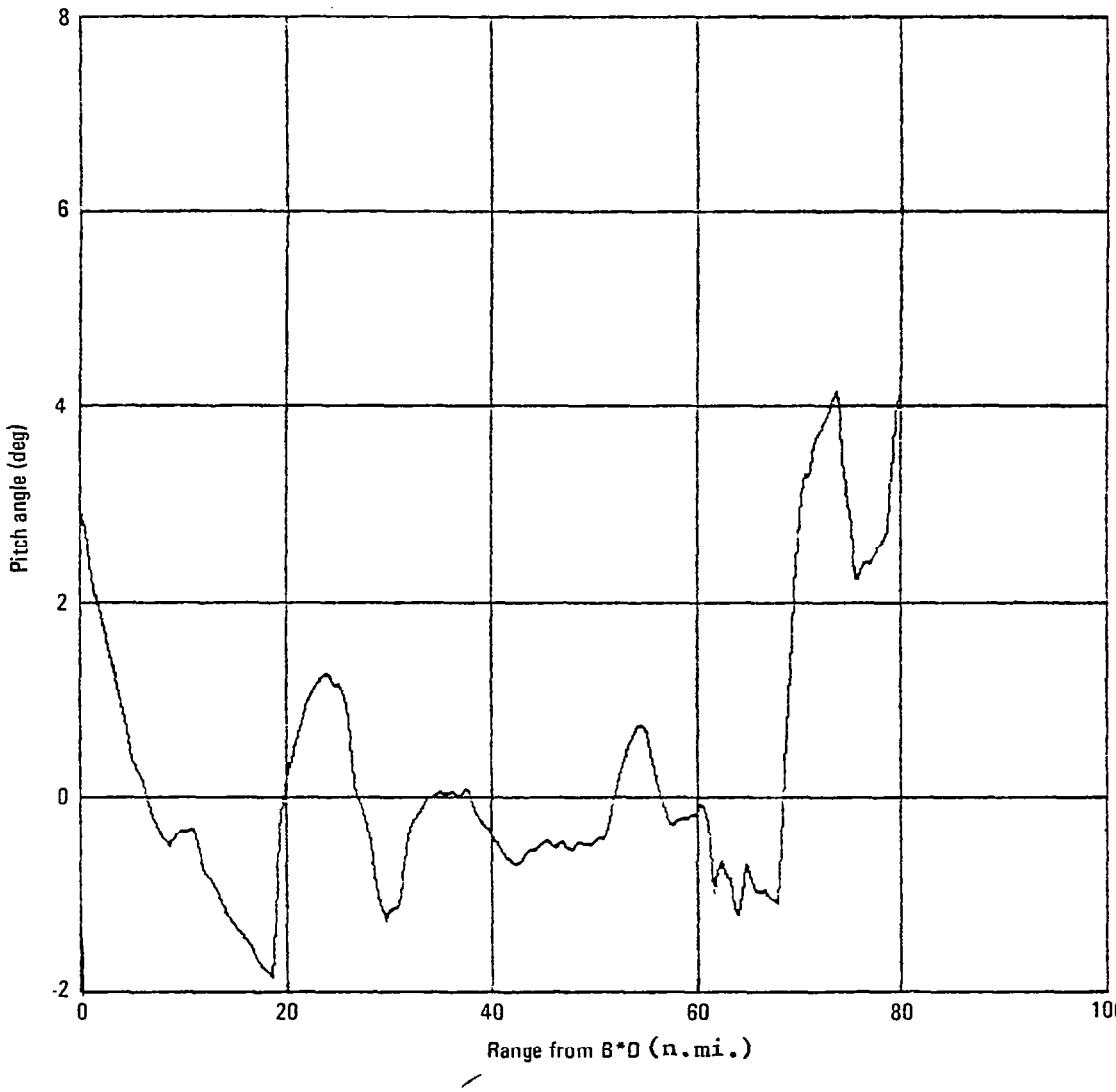

Figure C-14. - Pitch angle for figure C-1 descent.

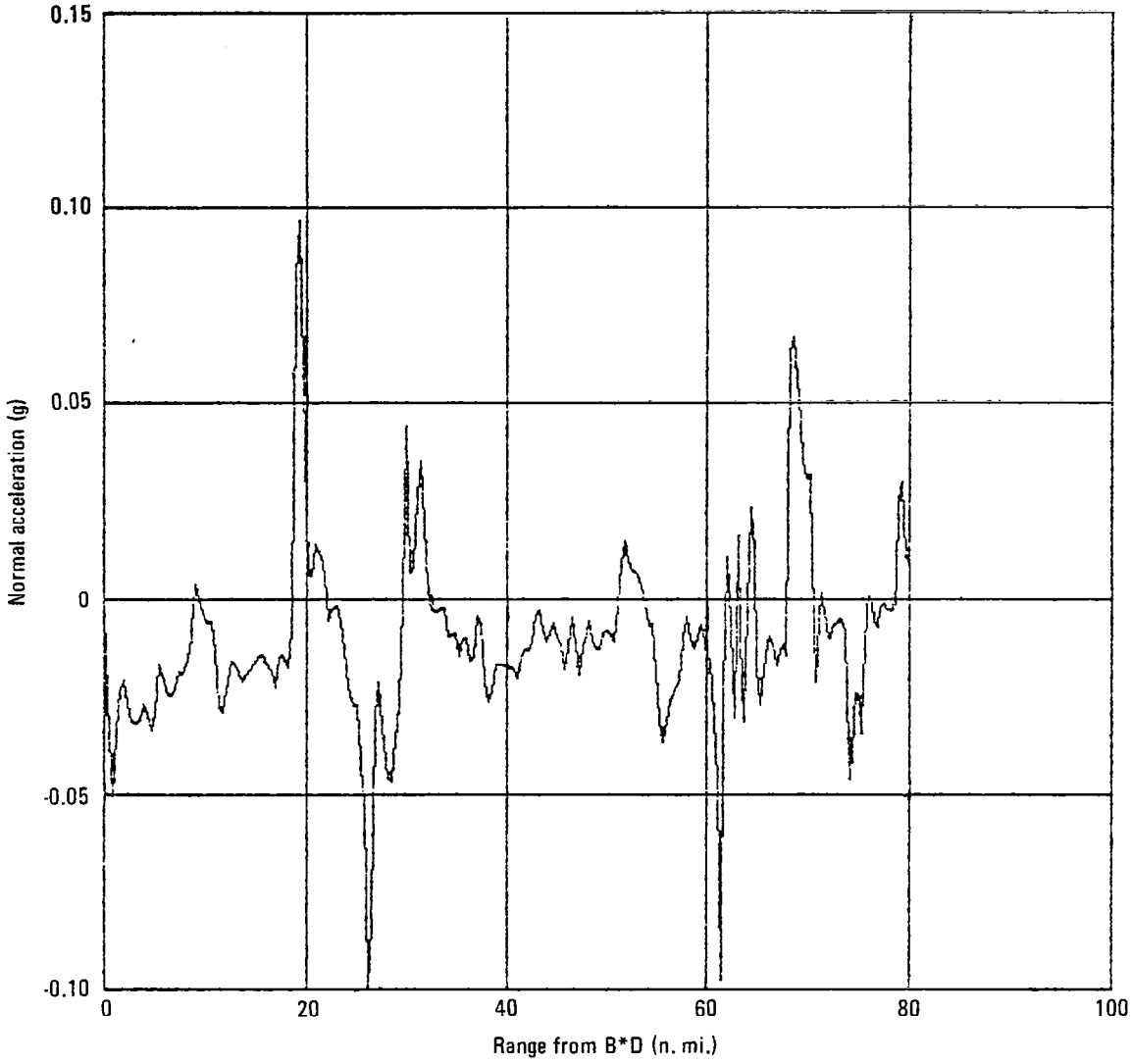

Figure C-15. - Normal acceleration for figure C-1 descent.

APPENDIX D

L-1011 FLIGHT MANAGEMENT SYSTEM DATA BANK INFORMATION FOR THE DALLAS/FT. WORTH DEMONSTRATION FLIGHTS

VORTACS

Name	I.D.	Freq. (MHz)	Latitude	Longitude	MVAR	Hgt (ft)
Acton	AQN	110.6	N32° 26.1'	W097° 39.8'	E9°	848
Ardmore	ADM	116.7	34 12.7	97 10.1	E9	930
Blue Ridge	BUJ	114.9	33 17.0	96 21.9	E8	610
Bridgeport	BPR	116.5	33 14.3	97 46.0	E9	890
Dallas/Ft. Worth	DFW	117.0	32 51.9	97 01.7	E8	557
Gregg County	GGG	112.4	32 25.1	94 45.2	E7	320
McAlester	MLC	112.0	34 51.0	95 46.9	E8	820
Millsap	MQP	117.7	32 43.6	97 59.8	E9	890
Oklahoma City	OKC	115.0	35 26.5	97 46.3	E9	1360
Scurry	SCY	112.9	32 27.9	96 20.2	E8	440
Shreveport	SHV	117.4	32 46.3	93 48.6	E7	190
Texarkana	TXK	116.3	33 30.8	94 04.4	E7	270
Tulsa	TUL	114.4	36 11.8	95 47.3	E8	790
Waco	ACT	115.3	31 39.7	97 16.1	E9	510
Wichita Falls	SPS	112.7	33 59.2	98 35.6	E10	1100
Wink	INK	112.1	31 52.5	103 14.6	E11	2870

WAYPOINTS

I.D.	Latitude	Longitude	
HAZEL	N33° 32.6′	W095° 18.0′	BLUE RIDGE FIVE Arrival
ATLAS	33 25.4	95 48.7	
(BAT)ON	33 09.4	96 36.3	
ALKID	33 05.4	96 43.9	
HAMAK	32 59.8	96 54.4	
YARBB	33 57.7	96 07.0	
RADEX	33 44.4	96 11.8	
HBR	32 41.2	96 54.4	

Note: HBR is a waypoint in between HAMAK and the approach intercept BATCH for north flow approaches to runway 35R. Latitude = same as BATCH; longitude = same as HAMAK

VELMA	N34° 26.6′	W097° 30.7′	BOIDS THREE Arrival
MEDIA	33 35.2	97 39.7	
BOIDS	33 08.4	97 32.3	
PIVIT	33 04.5	97 23.2	
ARINA	32 59.6	97 11.9	
B22	33 32.7	98 00.4	
B62	34 14.5	97 28.0	
AGL	32 41.1	97 11.9	

Note: AGL is a waypoint in between ARINA and GEARS for north approaches to 35L
Latitude = GEARS; longitude = ARINA

DONIE	N31° 37.1′	W095° 43.4′	SCURRY FIVE Arrival
OBITS	32 03.2	96 02.2	
NORMA	32 12.3	95 05.5	
FINES	32 21.3	95 46.9	
SEAGO	32 37.9	96 37.8	
GLADD	32 41.1	96 43.5	
LANED	32 47.3	96 54.5	
LGL	33 06.2	96 54.5	

Note: LGL is a waypoint in between LANED and GARZA for south approaches to 17L.
Latitude = GARZA; longitude = LANED.

EDNAS	N31° 36.7′	W098° 10.1′	ACTON SIX Arrival
GLENN	32 08.0	97 50.6	
GRAMY	32 24.1	98 03.3	
BRYAR	32 31.9	97 31.8	
FLATO	32 40.5	97 20.1	
CREEK	32 46.9	97 11.4	
TQA	32 14.1	99 49.0	
CAR	33 06.1	97 11.4	

Note: CAR is a waypoint in between CREEK and ALIGN for south approaches to 17R.
Latitude = ALIGN; longitude = CREEK.

WAYPOINTS (cont'd)

I.D.	Latitude		Longitude		
GARZA (intercept)	N33°	06.2′	W097°	01.8′	Approach to runway 17L
17L (threshold)	32	54.6	97	01.8	
SL1	32	44.6	97	01.8	
SL2	32	34.6	97	01.8	
ALIGN (intercept)	33	06.1	97	03.0	Approach to runway 17R
17R (threshold)	32	54.6	97	03.0	
SR1	32	44.6	97	03.0	
SR2	32	34.6	97	03.0	
GEARS (intercept)	32	41.1	97	03.0	Approach to runway 35L
35L (threshold)	32	52.7	97	03.0	
NL1	33	02.7	97	03.0	
NL2	33	12.7	97	03.0	
B(ATC)H (intercept)	32	41.2	97	01.8	Approach to runway 35R
35R (threshold)	32	52.7	97	01.8	
NR1	33	02.7	97	01.8	
NR2	33	12.7	97	01.8	

ROUTES

STAR	I.D.	WPTS
ACTON SIX	AQ6	EDNAS
		GLENN
		INK
		TQA
		GRAMY
		AQN
		BRYAR
		FLATO
		CREEK
BLUE RIDGE FIVE	BU5	TUL
		MLC
		YARBB
		RADEX
		TXK
		HAZEL
		ATLAS
		BUJ
		(BAT)ON
		ALKID
		HAMAK
BOIDS THREE	BO3	OKC
		VELMA
		B62
		MEDIA
		SPS
		B22
		BPR
		BOIDS
		PIVIT
		ARINA
SCURRY FIVE	SC5	SHV
		GGG
		NORMA
		FINES
		DONIE
		OBITS
		SCY
		SEAGO
		GLADD
		LANED

ROUTES (cont'd)

Name	I.D.	WPTS
35R, North Flow	RNF	HAMAK HBR B(ATC)H 35R NR1 NR2
35L, North Flow	LNF	ARINA AGL GEARS 35L NL1 NL2
17R, South Flow	RSF	CREEK CAR ALIGN 17R SR1 SR2
17L, South Flow	LSF	LANED LGL GARZA 17L SL1 SL2

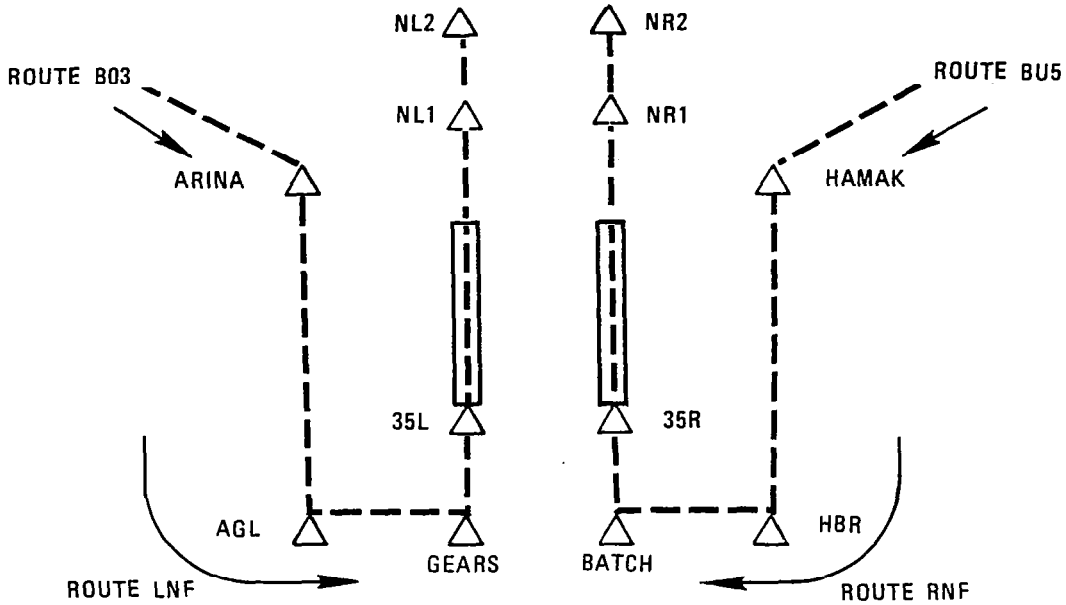

DFW NORTH FLOW

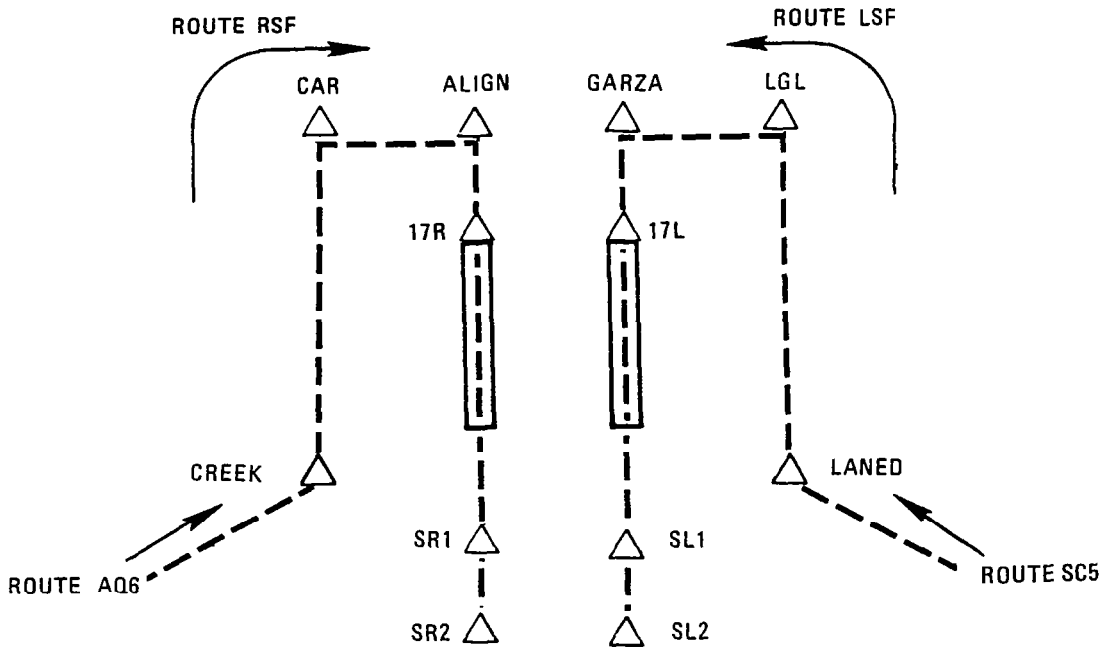

DFW SOUTH FLOW

REFERENCES

1. Sindermann, B. M. and Newman, T. J.; Application of Automatic Guidance and Control for Optimum Cost/Fuel Savings for the Lockheed L-1011 Aircraft. Presented to IEEE 18th Conference on Decision and Control, Fort Lauderdale, Florida, Dec. 13, 1979.

2. Daniels, G. E. and Smith, O.E.; Scalar and Component Wind Correlations between Altitude Levels for Cape Kennedy, Florida, and Santa Monica, California. NASA TN D-3815, 1968.

3. Vaughan, W. W.; Interlevel and Intralevel Correlations of Wind Components for Six Geographical Locations. NASA TN D-561, 1960.

4. Gott, E.; Linear Regression of Interlevel Wind Velocities. IEEE Transaction on Geoscience Electronics, Vol. GE-7, No. 1, January 1969.

5. Charles, B. N., "Lag Correlations of Upper Winds," Journal of Meteorology, Vol. 16, Feb. 1959, pp. 83-86.

6. Knox, C. E. and Cannon, D. G.; Preliminary Test Results of a Flight Management Algorithm for Fuel Conservative Descents in a Time Based Metered Traffic Environment. NASA TM-80194, November, 1979.

7. Stein, Kenneth J.; Advanced Systems Aid Profile Descents. Aviation Week and Space Technology, p. 57-62, Aug. 20, 1979.

8. Stein, Kenneth J.; New Procedures Key to Fuel Savings. Aviation Week and Space Technology, p. 105-111, Aug. 27, 1979.

9. Menga, G. and Erzberger, H., "Time-Controlled Descent Guidance in Uncertain Winds," Journal of Guidance and Control, Vol. 1, No. 2, March-April, 1978, pp. 123-129.

1. Report No.	2. Government Accession No.	3. Recipient's Catalog No.
NASA CR-3280		

4. Title and Subtitle	5. Report Date
DEVELOPMENT OF ADVANCED AVIONICS SYSTEMS APPLICABLE TO TERMINAL-CONFIGURED VEHICLES	September 1980
	6. Performing Organization Code

7. Author(s)	8. Performing Organization Report No.
R. L. Heimbold, H. P. Lee, and M. F. Leffler	LR 29326
	10. Work Unit No.

9. Performing Organization Name and Address	11. Contract or Grant No.
Lockheed-California Company P. O. Box 551 Burbank, California 91520	NAS1-15546
	13. Type of Report and Period Covered
12. Sponsoring Agency Name and Address	Contractor Report October 1978-January 1980
National Aeronautics and Space Administration Washington, D.C. 20546	14. Sponsoring Agency Code

15. Supplementary Notes

Technical Film Supplement L-1269 available on request.
Langley Technical Monitor: Leonard V. Clark
Final Report

16. Abstract

This report documents the analysis performed and flight test results obtained by the Lockheed-California Company in investigating the feasibility of a 4-D (time-controlled) high profile descent.

Work began in October 1978, to develop a technique to add the time constraint to the automatic descent feature of the existing L-1011 aircraft Flight Management System (FMS). Software modifications were incorporated in the FMS computer program and the results checked by lab simulation and on a series of eleven test flights culminating in a demonstration flight to Dallas/Ft. Worth Regional Airport on August 1, 1979. An arrival time dispersion (2σ) of 19 seconds was achieved. Recommended refinements should reduce the dispersion to 8 seconds. The 4-D descent technique can be integrated with the time-based metering method of air traffic control which will be introduced in air route traffic control centers in 1980. This combination promises substantial reductions in delays at today's busy airports.

17. Key Words (Suggested by Author(s))	18. Distribution Statement
4-D Air Traffic Congestion Flight Management Systems High profile descent Automatic flight Advanced avionic systems	Unclassified - Unlimited Subject Category 04

19. Security Classif. (of this report)	20. Security Classif. (of this page)	21. No. of Pages	22. Price
Unclassified	Unclassified	102	A06

For sale by the National Technical Information Service, Springfield, Virginia 22161

NASA-Langley, 1980